

NASA/CR-2008-215345



Constitutive Soil Properties for Cuddeback Lake, California and Carson Sink, Nevada

*Michael A. Thomas, Daniel E. Chitty, Martin L. Gildea, and Casey M. T'Kindt
Applied Research Associates, Inc., Albuquerque, New Mexico*

August 2008

The NASA STI Program Office . . . in Profile

Since its founding, NASA has been dedicated to the advancement of aeronautics and space science. The NASA Scientific and Technical Information (STI) Program Office plays a key part in helping NASA maintain this important role.

The NASA STI Program Office is operated by Langley Research Center, the lead center for NASA's scientific and technical information. The NASA STI Program Office provides access to the NASA STI Database, the largest collection of aeronautical and space science STI in the world. The Program Office is also NASA's institutional mechanism for disseminating the results of its research and development activities. These results are published by NASA in the NASA STI Report Series, which includes the following report types:

- **TECHNICAL PUBLICATION.** Reports of completed research or a major significant phase of research that present the results of NASA programs and include extensive data or theoretical analysis. Includes compilations of significant scientific and technical data and information deemed to be of continuing reference value. NASA counterpart of peer-reviewed formal professional papers, but having less stringent limitations on manuscript length and extent of graphic presentations.
- **TECHNICAL MEMORANDUM.** Scientific and technical findings that are preliminary or of specialized interest, e.g., quick release reports, working papers, and bibliographies that contain minimal annotation. Does not contain extensive analysis.
- **CONTRACTOR REPORT.** Scientific and technical findings by NASA-sponsored contractors and grantees.

- **CONFERENCE PUBLICATION.** Collected papers from scientific and technical conferences, symposia, seminars, or other meetings sponsored or co-sponsored by NASA.
- **SPECIAL PUBLICATION.** Scientific, technical, or historical information from NASA programs, projects, and missions, often concerned with subjects having substantial public interest.
- **TECHNICAL TRANSLATION.** English-language translations of foreign scientific and technical material pertinent to NASA's mission.

Specialized services that complement the STI Program Office's diverse offerings include creating custom thesauri, building customized databases, organizing and publishing research results ... even providing videos.

For more information about the NASA STI Program Office, see the following:

- Access the NASA STI Program Home Page at <http://www.sti.nasa.gov>
- E-mail your question via the Internet to help@sti.nasa.gov
- Fax your question to the NASA STI Help Desk at (301) 621-0134
- Phone the NASA STI Help Desk at (301) 621-0390
- Write to:
NASA STI Help Desk
NASA Center for AeroSpace Information
7115 Standard Drive
Hanover, MD 21076-1320

NASA/CR-2008-215345



Constitutive Soil Properties for Cuddeback Lake, California and Carson Sink, Nevada

*Michael A. Thomas, Daniel E. Chitty, Martin L. Gildea, and Casey M. T'Kindt
Applied Research Associates, Inc., Albuquerque, New Mexico*

National Aeronautics and
Space Administration

Langley Research Center
Hampton, Virginia 23681-2199

Prepared for Langley Research Center
under Contract NNL07AA00B

August 2008

Acknowledgments

Applied Research Associates, Inc (ARA) conducted this soil study under contract to NASA Langley Research Center's (LaRC) prime contractor for engineering support, ATK Space. ATK Space is the TEAMS (Technology Engineering and Aerospace Mission Support) prime contractor. Dr. Ralph Buehrle, LaRC, sponsored the study. The study was conducted for LaRC's Landing Systems ADP group, charged with evaluating Crew Exploration Vehicle (CEV) terrain landing designs. The two sites selected for this study, Cuddeback Lake and Carson Sink, were two of seven candidate sites identified by Mr. George Chi, Johnson Space Center. Mr. Chi's candidate sites were filtered based on flatness, low population density limit, and minimum unobstructed area in the western United States.

LaRC is evaluating airbag landing attenuation systems for the Orion CEV. The current terrain landing design involves parachuting the CEV to a defined landing zone, deploying airbags prior to contact, and releasing the airbag pressures to cushion the capsule during landing. This report provides constitutive soil properties for landing simulations. The primary author is Michael A. Thomas, with contributions from Daniel E. Chitty, Martin L. Gildea, and Casey M. T'Kindt. All are engineers with ARA.

LS-DYNA[®] is a registered trademark of the Livermore Software Technology Corporation.

The use of trademarks or names of manufacturers in this report is for accurate reporting and does not constitute an official endorsement, either expressed or implied, of such products or manufacturers by the National Aeronautics and Space Administration.

Available from:

NASA Center for AeroSpace Information (CASI)
7115 Standard Drive
Hanover, MD 21076-1320
(301) 621-0390

National Technical Information Service (NTIS)
5285 Port Royal Road
Springfield, VA 22161-2171
(703) 605-6000

Table of Contents

1	Introduction.....	3
2	LS-DYNA Material Model 5 Description	4
3	Methodology for Obtaining Constitutive Soil Properties	6
3.1	Geotechnical Laboratory Tests	6
3.1.1	Grain Density	6
3.1.2	Grain size distribution	7
3.1.3	Moisture content.....	7
3.1.4	Atterberg limits	8
3.1.5	Triaxial compression.....	9
3.1.6	Hydrostatic compression.....	16
3.1.7	Uniaxial strain	17
4	Cuddeback Soil A	25
4.1	Location.....	25
4.2	General description.....	28
4.2.1	Man made obstructions observed.....	29
4.2.2	Soil classification	29
4.2.3	Cementation	30
4.3	Selection of Soil A.....	30
4.4	Field observations.....	31
4.4.1	Sampling and sample locations	32
4.4.2	Nuclear density and nuclear moisture content field data.....	34
4.5	Laboratory test data	39
4.5.1	Moisture content and saturation	39
4.5.2	Grain density and size distribution.....	39
4.5.3	Atterberg limits test.....	40
4.5.4	Hydrostatic compression	40
4.5.5	Triaxial compression.....	41
4.5.6	Uniaxial strain	46
4.6	LS-DYNA Material Model 5 inputs.....	54
4.7	Recommended range of model application	54
4.8	Recommended surrogate soil composition.....	55
5	Cuddeback Soil B	56
5.1	Location.....	56
5.2	General description.....	56
5.2.1	Soil classification	57
5.3	Selection of Soil B.....	58
5.4	Field observations.....	58
5.4.1	Sampling and sample sites	58
5.4.2	Nuclear density and moisture data	58
5.5	Laboratory test data	62
5.5.1	Moisture content.....	62
5.5.2	Grain density and grain size analysis	62
5.5.3	Triaxial compression.....	63
5.5.4	Hydrostatic compression	67
5.5.5	Uniaxial strain	68
5.6	LS-DYNA Material Model 5 inputs.....	73
5.7	Recommended range of model application	73

5.8	Recommended surrogate soil composition.....	74
6	Carson Sink Dry Soil	75
6.1	Location.....	75
6.2	General description.....	77
6.2.1	Cementation	78
6.2.2	Soil classification	79
6.3	Field observations.....	79
6.3.1	Sampling and sample locations	80
6.3.2	Nuclear density and moisture data	81
6.4	Laboratory test data	85
6.4.1	Moisture content.....	85
6.4.2	Atterberg limits	85
6.4.3	Grain density and grain size analysis	86
6.4.4	Triaxial compression.....	86
6.4.5	Hydrostatic compression.....	90
6.4.6	Uniaxial strain	91
6.5	LS-DYNA Material Model 5 inputs.....	96
6.6	Recommended range of model application	96
6.7	Recommended surrogate soil composition.....	97
7	Carson Sink Wet Soil.....	98
7.1	General description.....	98
7.2	Laboratory test data	99
7.2.1	Moisture content.....	99
7.2.2	Triaxial compression.....	99
7.2.3	Hydrostatic compression.....	103
7.2.4	Uniaxial strain	104
7.3	LS-DYNA Material Model 5 inputs.....	109
7.4	Recommended range of model application	109
8	Soil to soil comparisons	110
9	Closing Remarks.....	112
	Appendix A: LS-DYNA Theory Manual for Material Model 5	113
	Appendix B: Field Data	115
	Appendix C: Laboratory data.....	134
	Appendix D: Media library on DVD	143

1 Introduction

The Orion Crew Exploration Vehicle (CEV) is the next generation spacecraft being developed by NASA. The early CEV design included the possibility of terrain landings on airbags. Langley Research Center (LaRC) was tasked with the landing design and evaluation. NASA identified two candidate landing sites in the western United States: Carson Sink, NV and Cuddeback Lake, CA. These sites are wide open, mostly flat terrains with varying soil conditions. Both are dry lakebeds for the majority of the year. LaRC is determining soil factors that may affect the landing attenuation system design at the candidate landing sites, and this soil study is part of that effort.

This report quantifies soil variability at each site and provides soil constitutive properties to support LaRC's numerical modeling of the CEV landing. For this modeling, LaRC is using LS-DYNA, a 3-dimensional finite element software program. On field visits to each site, ARA performed in situ measurements and soil sampling. The soil samples were shipped to ARA's geotechnical laboratory for a series of laboratory tests. The tests were designed to yield the required constitutive inputs for LS-DYNA's Material Model 5: Soil and Foam. Each site's range of variation is characterized to the best possible extent with two soil models.

Carson Sink and Cuddeback Lake are terminal lakes in geologic terms. Desert rains create surface runoff that accumulates in the terminal lakebed. There is no water discharge, except for evaporation or ground seepage. Most of the lake water leaves through evaporation until no water remains, thus becoming a dry lake. This seasonal occurrence leads to deposits of fine silt and clay in the lakebed itself due to the fact that smaller particles remain suspended in the water for longer periods of time. Most large particles, such as coarse sand and gravel, fall out before reaching the lakebed. These larger particles form the sandy, gravelly shores observed at both lakebeds. As a result, the soil properties vary depending on the position in the lakebed.

The soil characterization began with field visits to each of the sites. The general field plan consisted of rapidly surveying the area to observe the total number of soil types, then performing in situ measurements and collecting soil samples. After the rapid surveys, the site's most pronounced variability was considered to be the hardest and softest soil. Soil models have been developed for these two materials. Cuddeback Lake's hardest soil was the lakebed itself. The softest was the shoreline soil. In the case of Carson Sink, there was little soil variability but great moisture content variability. The soil was so highly uniform that the first soil model was the in situ surface soil. The second soil was a wetted version of the 1st, simulating high moisture conditions and soft behavior. The increased moisture content is closer to wet season conditions. With two sites, each having two extremes, four total constitutive soil models were developed and are presented in this report.

2 LS-DYNA Material Model 5 Description

LS-DYNA Material Model 5 was identified by NASA LaRC for modeling the soils in preliminary calculations. The constitutive properties derived in this report are tailored for constructing this type of model. This section describes the physical meaning of each of the model inputs. Section 3 addresses how each of the model inputs were obtained from material testing.

Because soil strength is pressure dependent, a pressure dependent material model is necessary for constitutive modeling. In LS-DYNA, Material Model 5: Soil and Foam is the most basic of the pressure dependent strength models available. It is also the oldest LS-DYNA pressure dependent model and therefore has accumulated a considerable amount of user experience and feedback. As a result, the model is quite robust given its simple inputs.

Defining the model requires shear and unloading bulk moduli, three coefficients that define the quadratic shear failure surface, a pressure cutoff value that defines the maximum tension allowed, and 10 points on a pressure-volume strain curve to define compressibility. Table 2-1 defines these inputs. Based on LaRC preference for their numerical modeling, the material model inputs are provided in pounds and inches.

The elastic shear modulus, G , describes shear deformation when the soil is initially loaded. The bulk unloading modulus, BULK, describes the expansion of the soil when the load is reduced. These two parameters are necessary because the loading and unloading behavior of soil is not equal due to permanent deformations.

The a_0 , a_1 , and a_2 inputs define a quadratic fit to a strength curve. The strength curve is defined as a yield surface plotted in J_2' vs. pressure space. Pressure is the mean stress, the average of all the principle stresses on the material. Pressure is positive in compression. J_2' is the second invariant of the stress deviator. Material tests define points on the yield surface, and the quadratic fit is LS-DYNA's approximation of material strength. In the LS-DYNA manual, the second invariant of the stress deviator is denoted J_2 . In this report, the more common notation, J_2' , is used to represent the same quantity.

Volumetric strain behavior is defined by the natural log of the relative volume and is negative in compression. Relative volume is the ratio of the current soil cell volume to the initial volume at the start of the calculation. The volumetric strain is represented as a 10 point curve in pressure vs. volume strain space. Each point on the curve is obtained from material testing at the given pressure.

The LS-DYNA Theory Manual describes Material Model 5 in more detail. Appendix A contains excerpts from the manual.

Table 2-1. LS-DYNA Material Model 5 Inputs.

Input	Obtained from soil test:	Description
MID	N/A	LS-DYNA's material identification number. A unique number identifying an input set of material properties. A number must be assigned.
RO	Nuclear density field test	Mass density. Obtained from dividing weight density (mass/unit volume) by gravity.
G	Uniaxial strain	Elastic shear modulus. The slope of the shear stress vs. shear strain curve. Can be computed from constrained modulus and Poisson's ratio from a uniaxial test.
BULK	Hydrostatic compression	Unloading bulk modulus. It is the slope of the mean stress vs. strain curve when the pressure is reduced (unloaded) from a higher pressure load. Can also be obtained from uniaxial strain unloading.
A0	Triaxial compression	A quadratic fit coefficient. In a J_2' vs. p (second invariant of stress difference vs. pressure) plot, a_0 represents the intersection of the shear failure envelope's (or yield surface) quadratic fit and the J_2' axis. a_0 coefficient is the Y-intercept. The J_2' vs. p plot is derived from stress difference vs. normal stress.
A1	Triaxial compression	a_1 is a quadratic fit coefficient. It is the initial slope coefficient of the shear failure envelope's quadratic fit.
A2	Triaxial compression	a_2 is a quadratic fit coefficient. It is the curvature coefficient of the shear failure envelope's quadratic fit.
PC	Triaxial compression	"Pressure cut-off." Maximum tension stress allowed, representing tensile fracture. It is the mean stress intercept of the shear failure envelope.
VCR	This is a flag variable. VCR=0	VCR=0 turns on volumetric crushing, defined by the 10 points on the pressure-volume curve. VCR=1 turns off. The pressure-volume curve defines the deformation of the material at 10 pressures.
REF	This is a flag variable. REF=0	This option controls the use of reference geometry to initialize the pressure. REF=0 is recommended. This option does not initialize the deviatoric stress state.
EPS1, P1	EPS1=0, P1=0	This is the first point on the pressure volume curve; at zero loading there is zero volume change. EPS is the natural logarithmic volume strain = $(\ln [1 - \epsilon_{\text{volume}}])$, where $\epsilon_{\text{volume}} = (\text{initial volume} - \text{current volume})/\text{initial volume}$
EPS2, P2	Uniaxial strain	2nd pressure-volume point
EPS3, P3	Uniaxial strain	3rd pressure-volume point
EPS4, P4	Uniaxial strain	4th pressure-volume point
EPS5, P5	Uniaxial strain	5th pressure-volume point
EPS6, P6	Uniaxial strain	6th pressure-volume point
EPS7, P7	Uniaxial strain	7th pressure-volume point
EPS8, P8	Uniaxial strain	8th pressure-volume point
EPS9, P9	Uniaxial strain	9th pressure-volume point
EPS10, P10	Uniaxial strain	10th pressure-volume point

3 Methodology for Obtaining Constitutive Soil Properties

This section describes the methodology for deriving LS-DYNA material model inputs from laboratory test data.

3.1 Geotechnical Laboratory Tests

ARA operates a specialized geotechnical laboratory in South Royalton, VT where the soil samples were shipped for testing. The types of tests conducted for this effort are listed and explained below:

- Grain density
- Grain size distribution
- Moisture content
- Atterberg limits
- Hydrostatic compression
- Uniaxial strain
- Triaxial compression

3.1.1 Grain Density

A given volume of soil is comprised of solid particles and void space. The grain density of a soil is the density of the solid particles. Knowing the grain density of a soil allows one to perform accurate saturation and void volume calculations. Soils typically have a grain density of 2.7 +/- 0.1 g/cm³. Although not specifically used in constitutive modeling, the grain density is a basic piece of information useful for characterizing the soil as a whole.

The grain density is measured according to the procedures defined by ASTM D854-83. This test is performed using a pycnometer, a special-purpose glass flask with a drilled ground glass stopper that allows it to be filled with the same volume of water with density ρ_w . First, the weight of a 100-ml pycnometer is determined. Second, the pycnometer is filled with distilled, de-aired water to its fill point and re-weighed, (m_a). Then, the water is dumped, and an oven dried soil sample is placed in the dried pycnometer and weighed to determine the mass of the oven-dried sand sample (m_o). Distilled, de-aired water is added to the pycnometer again to slightly above the soil sample. The air entrapped in the sample soil is removed by vacuum. More de-aired, distilled water is added to the pycnometer until reaching the same fill point, and the mass of pycnometer, soil, and water (m_b) is recorded. Finally, the grain density of the soil is computed, including temperature corrections, which are not shown, by the following:

$$\rho_g = \frac{\rho_w m_o}{[m_o + (m_a - m_b)]} \quad \text{Equation 3-1}$$

3.1.2 Grain size distribution

A given soil contains a variety of particle sizes. The relative proportions of all particle sizes is captured by defining grain size distribution. The distribution is a good indicator of general soil behavior. A soil with mostly fine grains will have poor drainage, retain water for long periods of time, exhibit cohesive strength, and have very low shear strengths at high moisture contents. The low shear strength in fine grained soils is due to pore pressures building up during loading because of the poor drainage. This pore pressure reduces the effective shear stress, carried by grain-to-grain contact in the soil. Grain size distribution is also essential in recommending surrogate soils to replace a soil of interest. Soils with similar grain size distributions tend to have similar behavior. The grain size distribution is not specifically used in LS-DYNA, but it offers great insight into what the soil is comprised of, and how it will behave with varying moisture levels.

Wet or dry sieve analysis can be used to obtain grain size distribution, also a basic test. Dry grain size distribution tests on soils are performed with the material in the oven-dried condition. The sample is broken up and shaken through a stack of sieves that are graduated from coarse at the top to fine at the bottom. The material retained on each sieve is then weighed, and the results are presented in terms of the percent passing (or percent finer than) each sieve size as a function of the logarithm of the grain size. The sieves used for this characterization effort were US standard meshes of No. 5, 10, 20, 30, 40, 70, 100, 140, and 200. Wet sieving flushes the soil with water, further breaking up cohesive particles that would otherwise not pass through a sieve. Once flushed, the retained soil is dried and weighed. Dry sieving is less reliable because cohesive blocks of soil grains can distort the distribution. However, wet sieving is much more time consuming because the retained soil must be completely dried.

3.1.3 Moisture content

The moisture content of a soil is another basic test and key property. It is the gravimetric ratio of water to dry soil material. Although not a direct input to LS-DYNA's Material Model 5, water plays an important role in soil strength and knowing the moisture content in conjunction with grain density allows one to compute saturation and air void volumes in the soil. Soils have an optimum moisture content, at which soil strength is maximized. Any moisture content lower or above this optimum value will reduce the soil strength. At lower values, removing water also removes some cohesion strength. At higher values, the extra water causes pore pressures to build up in the soil, reducing its effective strength. Approximate moisture content (w%) can be obtained through field testing with a nuclear density gage, and verified through laboratory testing.

Laboratory testing to obtain moisture content is performed by first weighing a set of soil samples. Then the samples are oven dried and weighed again to measure the difference caused by the loss of water. The difference in weight is m_w . The oven dried weight is m_s . Individual moisture content is calculated for each sample, and the results are averaged. The formula for calculating water content is:

$$w\% = \frac{m_w}{m_s} \qquad \text{Equation 3-2}$$

3.1.4 Atterberg limits

The Atterberg limits test defines the degree to which a soil behaves plastically, and is used to classify silts and clays. Fine grained soils can exist in any of several states depending on the amount of water in the soil. As water is added to a dry soil, each particle is covered with a film of adsorbed water. As more water is added, the thickness of the water film covering the particle increases, permitting the particles to slide past one another more easily, thus affecting the engineering properties, e.g., shear strength of the soil. The Atterberg limits test defines the boundaries of four states in terms of limits as follows:

- Liquid Limit – the boundary between the liquid and plastic states.
- Plastic Limit – the boundary between the plastic and semi-solid states.
- Shrinkage Limit – the boundary between the semi-solid and solid states.

These limits are further refined in terms of the water content associated with these boundaries. The water contents at which different clays pass from one state to another vary considerably, and thus can be used for identification and comparison of different clays.

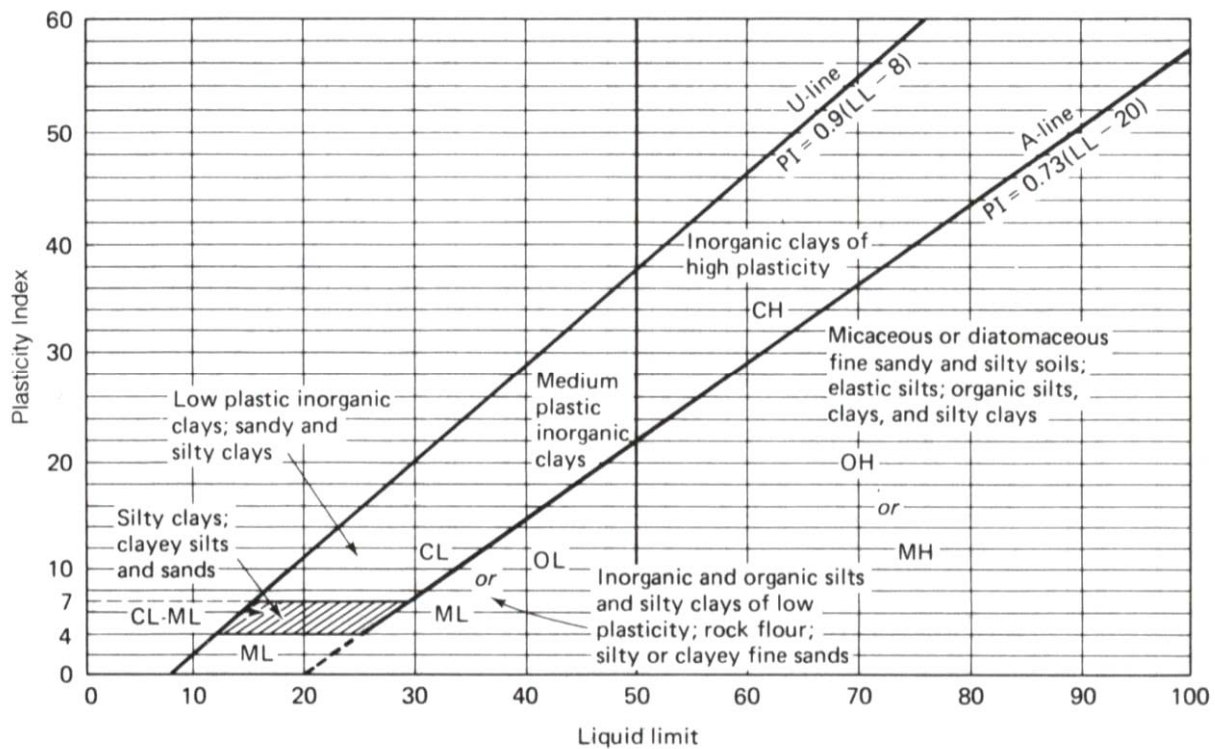


Figure 3-1: Cassagrande's plasticity chart, showing several representative soil types. (Developed from Cassagrande, 1948, and Howard, 1977.)

In order to determine these limits for each soil, we followed ASTM Method D4318-05, which prescribes the current standard test methodology. Based on the results of these tests, standard soil classifications were determined based on Cassagrande's plasticity chart shown in Figure 3-1.

The A-line (lower line in Figure 3.1) generally separates the more claylike materials from silty materials, and the organics from the inorganics. The U-line indicates the upper bound for general clays. Only special clays, such as quick clays, plot above the U-line.

3.1.5 Triaxial compression

The results of triaxial compression tests are used to define the strength envelope, or yield surface as it's referred to in LS-DYNA, of the soil. The following paragraphs describe the triaxial testing machine, how the sample is tested, and how the coefficients of the shear failure surface, a_0 , a_1 , and a_2 are derived from laboratory test data.

3.1.5.1. Triaxial test apparatus

All of the mechanical property tests were performed in a triaxial compression test apparatus, which is illustrated schematically in Figure 3-2. For each test, a cylindrical specimen of soil is first prepared inside a fluid-tight membrane to prevent infiltration of the confining fluid (air). In the triaxial apparatus, it is possible to apply two independently controlled components of load to the test specimen, as appropriate to each individual test. Pressurized fluid (air) in the vessel is used to impose a hydrostatic stress, simulating the effect of adjacent soil in the field. The other component of load is derived from a piston, which extends through a seal in the top of the pressure vessel, loading the cylindrical specimen in the axial direction. Electronic instrumentation is used to measure both the applied loads and the resulting deformations of the soil specimens. The following paragraphs describe in more detail how the test specimens were prepared, instrumented, and tested.

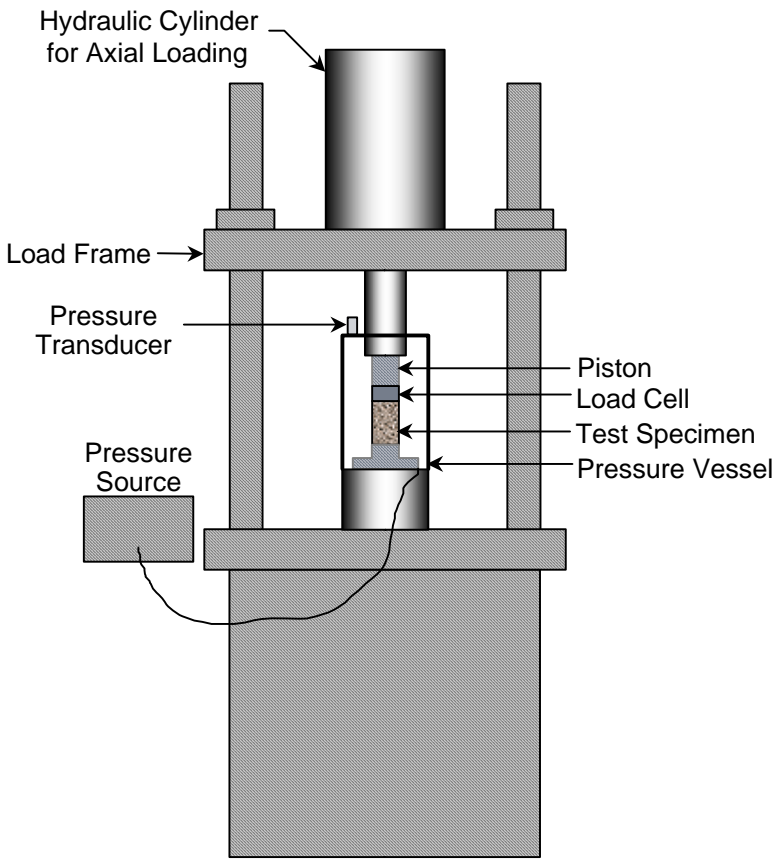
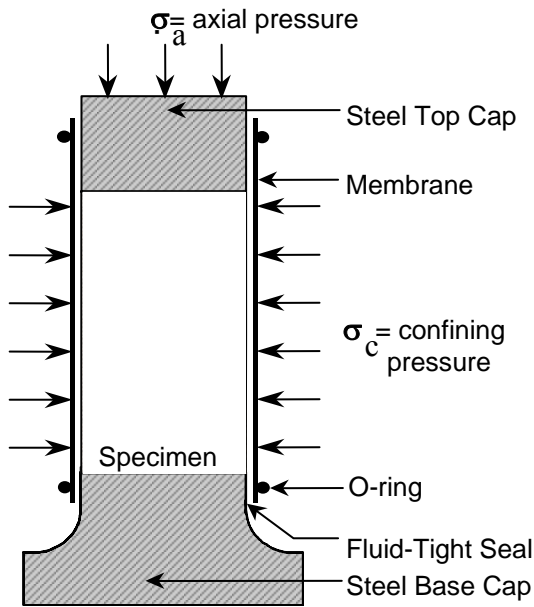


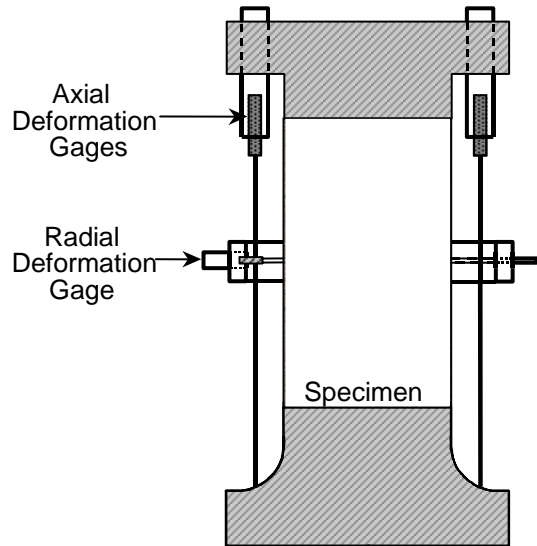
Figure 3-2: Schematic and photograph of a triaxial compression test apparatus.

3.1.5.2. Soil specimen preparation

The first step in the test process is to pack the soil to the measured field density inside the latex rubber membrane that separates the specimen material from the confining fluid. The membrane lines the inside of a steel cylinder mold, which can be removed by splitting in half. The soil is placed in the mold in measured lifts and compacted to the field density. The soil sample reconstitution is described in more detail in the individual material chapters. Once the mold is filled, the top cap is installed in the same manner as the bottom cap, and final measurements of the specimen dimensions and mass are made. The sample is then placed in the triaxial apparatus. Figure 3-3 illustrates how the membranes are sealed on each end to hardened steel endcaps through which the axial load was applied. The membrane was then sealed to the bottom cap using sealant and O-rings. Figure 3-4 is a “ready to test” photograph.



Specimen Preparation and Loading



Instrumentation

Figure 3-3: Schematic of an instrumented soil specimen.

Electronic instruments were used to monitor the applied loads and specimen responses during the tests. Three linear variable differential transformer (LVDT) type displacement transducers were installed as illustrated in Figure 3-3 to provide measurements of specimen deformations under load. A pressure transducer was used to monitor the confining pressure, which is equal to the radial stress on the specimen, and a load cell measured the axial load. The load cell was located inside the pressure vessel to eliminate errors that would result from seal friction if it were outside the vessel. The necessary corrections were made to eliminate the effects of confining pressure on the load cell output. All of the instruments were calibrated against standards traceable to the National Institute of Standards Technology (NIST) and adjusted to provide the necessary measurement resolution over the expected range of each test. A microcomputer based digital data acquisition system was used to record the transducer output at equally-spaced discrete intervals in time.



Figure 3-4: Specimen photo.

3.1.5.3. Deriving constitutive parameters from triaxial test results

In the triaxial compression, or strength test, the specimen is loaded hydrostatically to a pre-selected confining pressure. The confining pressure is then held constant while a compressive axial strain is imposed. The imposed axial strain induces an increment of axial stress above the confining pressure level, and that stress difference results in shear stresses on all planes except the principal directions parallel and perpendicular to the specimen axis. The shear strength of

earth materials is strongly dependent on the normal stress level. By performing strength tests at a range of confining pressure levels, the strength envelope (yield surface) of the material can be defined. The measured specimen deformations provide additional information on the material's volumetric response to shear loading. For this effort, confining pressures of 2, 5, 10, 20, and 50 psi were selected. Each test corresponds to a point on the strength (yield surface) curve, and the maximum shear stresses achieved at these pressures define the strength of the materials over the stress range of interest. The lower confining pressures simulate the near surface soil conditions.

Two components of load are measured in the triaxial compression test. The measured confining pressure is equal to the radial stress on the specimen. Force is also measured in the axial direction, from which the axial stress is determined. The strength data in this report are presented in terms of true axial stress, σ_a . True axial stress is computed at each evenly spaced time interval. It is defined as the total axial load divided by the current cross sectional area of the specimen as derived from the radial deformation measurement. True stress difference, σ_Δ , is the difference between the true axial stress and the confining pressure. Because the confining pressure is always applied to the current area, it is naturally a measure of true radial stress, σ_c . For presentation of strength results, the true stress difference is plotted against true mean stress, $\bar{\sigma}$, which is the average of the stresses in three perpendicular directions. True mean stress is equal to pressure p in LS-DYNA, as explained in the following derivation. The triaxial test outputs are:

$$\sigma_\Delta = \sigma_a - \sigma_c = \text{true stress difference} \quad \text{Equation 3-3}$$

$$\bar{\sigma} = (\sigma_a + 2\sigma_c) / 3 = \text{true mean stress} \quad \text{Equation 3-4}$$

where:

σ_a = true axial stress

σ_c = true radial stress = confining pressure

$\bar{\sigma} = p$ = pressure, as explained in the following derivation

To relate the triaxial test data to LS-DYNA's yield surface, one must use Equation 19.5.1 in LS-DYNA's user manual (see Appendix A) to describe the shear failure surface in Material Model 5 format:

$$\frac{1}{2} s_{ij} s_{ij} = a_0 + a_1 p + a_2 p^2 \quad \text{Equation 3-5}$$

LS-DYNA Equation 2.10 specifies s_{ij} as the deviatoric stress tensor defined by:

$$s_{ij} = \sigma_{ij} + (p + q) \delta_{ij} \quad \text{Equation 3-6}$$

Where p is the pressure and q is the bulk viscosity. Because viscosity is not used in Material Model 5, $q = 0$. LS-DYNA Equation 2.11 defines p as:

$$p = -\frac{1}{3} \sigma_{ij} \delta_{ij} = -\frac{1}{3} \sigma_{kk} \quad \text{Equation 3-7}$$

where: σ_{ij} = the stress tensor
 δ_{ij} = the Kronecker delta, which is one if the subscripts are the same and zero otherwise

Equation 3-5 and Equation 3-7 are written using indicial notation, in which summation over the repeated subscripts in each term is implied. Thus, p is simply the mean (average) of the three diagonal components of the stress tensor, shown in Equation 3-4.

In the special case of the triaxial compression test, the measured stresses are principal stresses and the intermediate principal stress is equal to the minimum principal stress. Specifically, the axial stress, σ_a , is the maximum principal stress and the other two principal stresses are equal to the confining pressure, σ_c . In triaxial testing, one of the most important data outputs is principal stress difference, σ_Δ , given in Equation 3-2. σ_Δ is also referred to as the stress deviator.

Because the stresses measured with respect to the axial and radial directions on the test specimen are principal stresses, the stress tensor expressed relative to those axes has no off-diagonal components, and is given by:

$$\sigma = \begin{bmatrix} \sigma_a & 0 & 0 \\ 0 & \sigma_c & 0 \\ 0 & 0 & \sigma_c \end{bmatrix} \quad \text{Equation 3-8}$$

Returning to Equation 3-6, the expanded version of the stress deviator tensor, s , is given by:

$$s = \begin{bmatrix} \sigma_a - p & 0 & 0 \\ 0 & \sigma_c - p & 0 \\ 0 & 0 & \sigma_c - p \end{bmatrix} \quad \text{Equation 3-9}$$

In a triaxial compression test, p is given by:

$$p = \frac{\sigma_a + 2\sigma_c}{3} \quad \text{Equation 3-10}$$

and:

$$\sigma_a - p = \frac{3\sigma_a - \sigma_a - 2\sigma_c}{3} = \frac{2(\sigma_a - \sigma_c)}{3} = \frac{2\sigma_\Delta}{3} \quad \text{Equation 3-11}$$

$$\sigma_c - p = \frac{3\sigma_c - \sigma_a - 2\sigma_c}{3} = \frac{\sigma_c - \sigma_a}{3} = \frac{-\sigma_\Delta}{3} \quad \text{Equation 3-12}$$

Thus, Equation 3-9, still for the special case of triaxial compression loading, can be re-written:

$$s = \begin{bmatrix} \frac{2\sigma_\Delta}{3} & 0 & 0 \\ 0 & \frac{-\sigma_\Delta}{3} & 0 \\ 0 & 0 & \frac{-\sigma_\Delta}{3} \end{bmatrix} \quad \text{Equation 3-13}$$

The left hand side of Equation 3-5 is the second invariant of the stress deviator tensor, defined as J_2' :

$$J_2' = \frac{1}{2} s_{ij} s_{ij} \quad \text{Equation 3-14}$$

When the stress tensor is a diagonal, the indicial notation of Equation 3-14 expands to:

$$J_2' = \frac{1}{2} \left[(s_{11})^2 + (s_{22})^2 + (s_{33})^2 \right] \quad \text{Equation 3-15}$$

Further, for the triaxial compression deviator stress tensor given by Equation 3-13, we have:

$$J_2' = \frac{1}{2} \left(\frac{\sigma_\Delta}{3} \right)^2 \left(2^2 + (-1)^2 + (-1)^2 \right) = \frac{\sigma_\Delta^2}{3} \quad \text{Equation 3-16}$$

The foregoing development details the methods for computing J_2' (the LHS of Equation 3-5) and p from the stresses measured in the triaxial compression tests at the strength limit (or elastic limit). Once triaxial data are converted to J_2' and p , one can plot the resulting values of J_2' against p and perform a quadratic fit to define the required Material Model 5 coefficients, a_0 , a_1 , and a_2 .

An example strength envelope based on triaxial compression tests is presented in terms of mean stress and stress difference in Figure 3-5. Also shown is the linear fit to the triaxial compression test data that corresponds to reasonable values of cohesion and friction angle. To derive the coefficients for input to LS-DYNA, it is necessary to fit the square of the stress difference, as defined by Equation 3-21. The strength data is re-plotted in terms of J_2' vs. pressure p , and is shown in Figure 3-6. Material Model 5 uses a quadratic fit to describe this yield surface, given in Equation 3-17.

$$J_2 = 0.490 + 1.386p + 0.979p^2 \quad \text{Equation 3-17}$$

Therefore, the Material Model 5 strength coefficients are:

$$A0 = 0.490$$

$$A1 = 1.386$$

$$A2 = 0.979$$

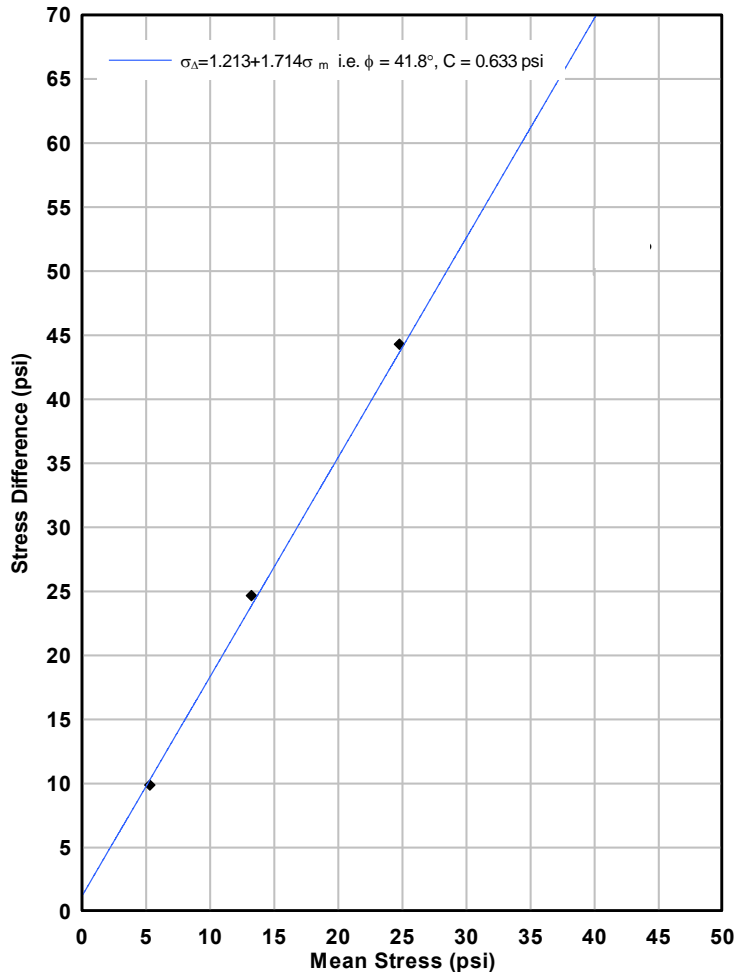


Figure 3-5: Example strength envelope. Black points represent peak strengths from triaxial tests. Blue line is a strength fit.

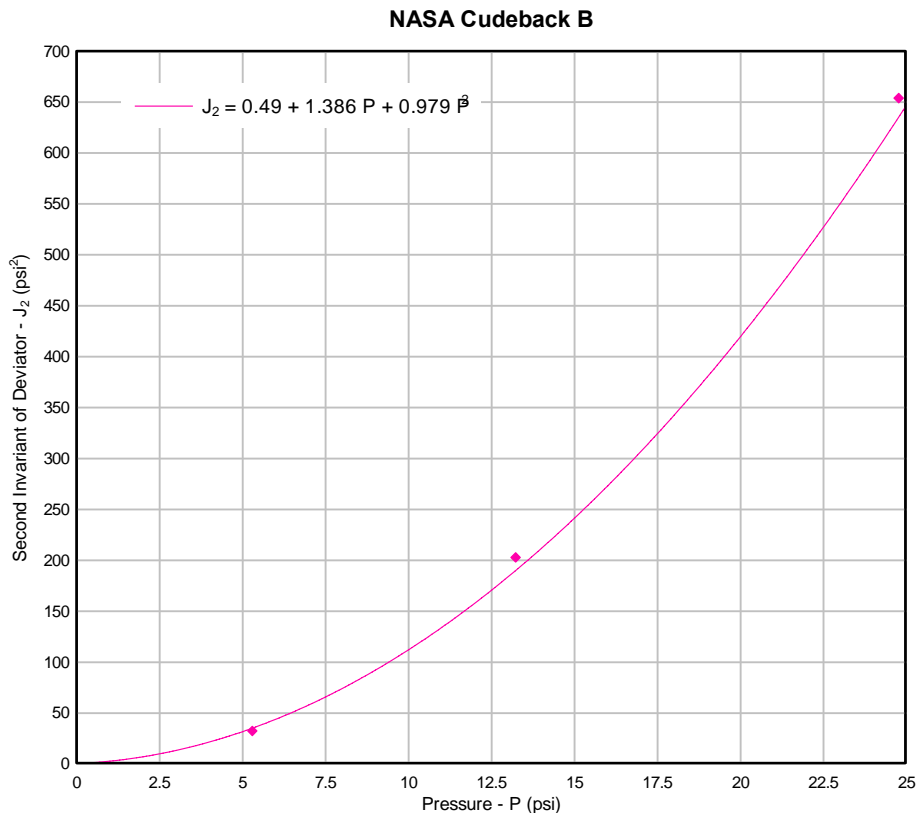


Figure 3-6: Strength envelope in terms of LS-DYNA's yield surface, J_2' vs. p . Black points from Figure 3-5 are converted to J_2' and plotted as pink points.

3.1.6 Hydrostatic compression

Hydrostatic compression tests are also conducted using the triaxial device. In the hydrostatic compression test, the cylindrical soil specimens are loaded only by fluid (air) pressure, without any piston loading. The stresses on the specimen are the same in all directions and there is no shear stress on any plane. This is referred to as the hydrostatic state of compression. Material Model 5's pressure p is equal to the fluid pressure. The results of these tests are used to define the volumetric deformation behavior of the material for modeling. The stress state is completely defined by the confining pressure. When confining pressure is reduced, the soil expands at a different rate than compression. This expanding rate yields the bulk unload modulus (BULK, see Table 2-1).

In the laboratory, LVDT measurements are used to define axial and radial deformations which, in turn, are used to compute the current volume of the specimen at each time step. The volumetric strain, ε_v , can be computed using the following equation:

$$\varepsilon_v = \frac{V_o - V_d}{V_o} \quad \text{Equation 3-18}$$

Where V_d = current (deformed) volume of the specimen

and V_o = initial specimen volume (including grains and void space)

3.1.6.1. Deriving constitutive parameters from hydrostatic compression

The axial and radial specimen strains are recorded as the fluid pressure increases inside the vessel. The recorded data forms a pressure vs. volumetric strain curve. The test typically starts with an initial rate of compression, denoted as I in Figure 3-7.

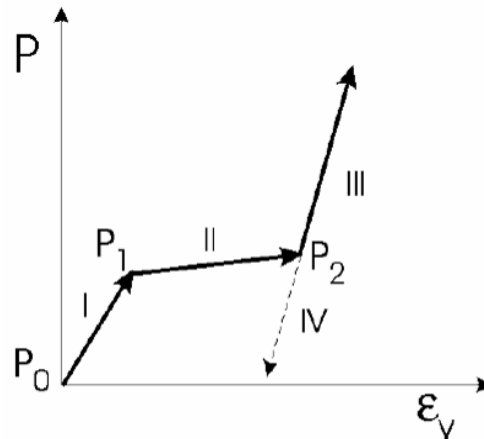


Figure 3-7: Theoretical hydrostatic compression curve. Pressure p vs. volumetric strain ϵ_v . The slope of Segment IV, the unloading portion, corresponds to the bulk unloading modulus.

3.1.7 Uniaxial strain

The uniaxial strain test also utilizes the triaxial device, albeit differently. In a uniaxial strain test, the axial stress and confining pressure are applied in such a way that the specimen undergoes compressive axial strain with no strain in the radial direction. The uniaxial strain loading is accomplished with an automated loading control system using the radial deformation measurement as feedback in the control loop. If the radial strain increases, the confining pressure is increased to return the radial strain to zero. Because no radial strain is allowed in a uniaxial strain test, the axial strain is equal to the volumetric strain in the specimen. There is a difference between axial and radial stress, and hence shear stresses exist in the specimen. However, the uniaxial strain constraint typically prevents the stress state from reaching the strength envelope, and failure of the specimen does not occur. The Material Model 5 shear modulus G and the pressure-volume curve can be derived from uniaxial strain data, as described in the following section.

3.1.7.1. Deriving constitutive parameters from uniaxial strain

The elastic constants to calculate shear modulus G are derived from a uniaxial strain test. First, Poisson's ratio can be obtained from an axial stress vs. confining pressure plot, a uniaxial test output. There are two independent components of loading applied, confining pressure and axial load. Other linear combinations of these two independent components can yield other properties.

For example, the mean stress and stress difference are invariants of the stress tensor and deviatoric stress tensor, respectively. To assure consistency, two different derivations of Poisson's ratio are presented below. As an aid, example plots are provided.

The first derivation is based on a relationship between axial stress and confining pressure. The elastic Poisson's ratio value can be derived from the initial portion of the axial stress vs. confining pressure curve. A fitted line is drawn over the initial curve portion. The inverse slope of the fitted line is commonly called lateral earth pressure, k_0 . Poisson's ratio, ν , is related to k_0 by:

$$\nu = \frac{k_0}{1 + k_0} \quad \text{Equation 3-19}$$

Figure 3-8 is an example application of the first method of obtaining ν from uniaxial test results. Commonly, there is a very small region at the beginning of the test where the data look somewhat incoherent because the loading piston is just making contact with the specimen. Usually, uniaxial strain control cannot be maintained in this region because of sample "seating," when the loading piston closes the tiny gaps between test hardware contact points. Because it occurs at very low stress only, it is ignored for this analysis. The Poisson ratio ν is derived from the initial linear portion of the test. In Figure 3-8, the initial linear portion reaches 35 psi axial stress. By fitting a line to that region, we find that it has a slope of 4.406. So $k_0 = 1/4.406$. From Equation 3-19, $k_0 = 0.227$ and $\nu = 0.185$.

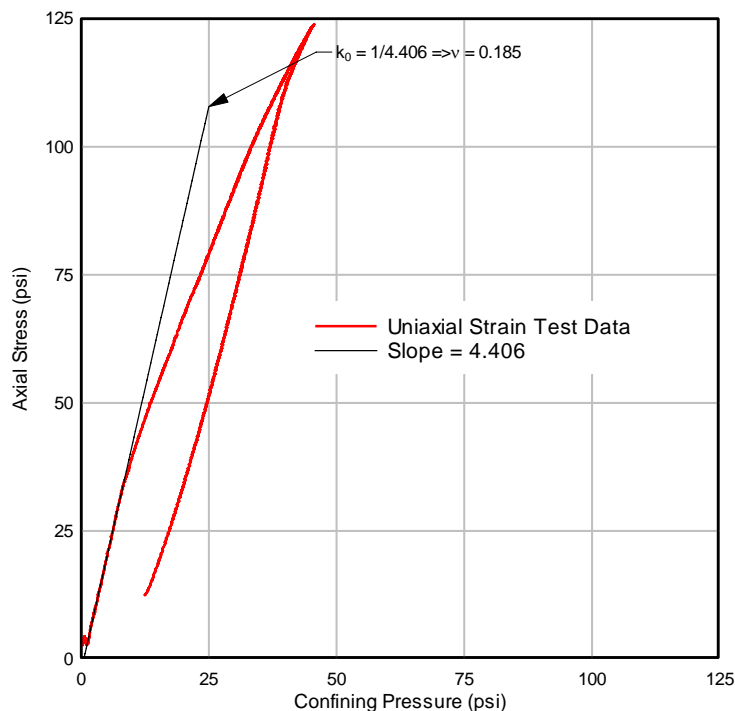


Figure 3-8: Example of axial stress vs. confining pressure plot from uniaxial test.

The second method of deriving ν is to examine the stress path in terms of mean stress and stress difference. Uniaxial test data can be used to plot mean stress vs. stress difference, as shown in Figure 3-9. The definitions of mean stress and stress difference are shown in Equation 3-2 and Equation 3-4. The slope of this different curve can also be used to calculate ν .

In Figure 3-9, the slope does not have a commonly used name or symbol. For convenience, call the slope of the line k^* . It is seen that $k^* = 1.598$. Poisson's ratio is related to k^* by:

$$\nu = \frac{3 - k^*}{6 + k^*} \quad \text{Equation 3-20}$$

Thus, $\nu = 0.185$, which agrees with the first derivation.

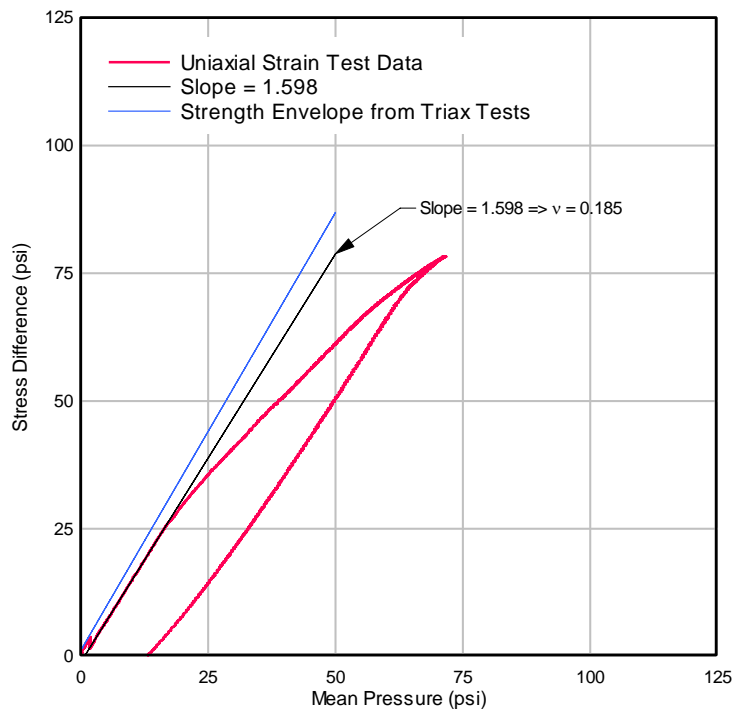


Figure 3-9: Example of stress difference vs. mean stress plot from uniaxial test.

The preceding paragraphs present two approaches to defining Poisson's ratio, which is one elastic constant. It is necessary to have one more elastic constant for a complete set. Consider the stress-strain curves plotted in Figure 3-10. In a uniaxial strain test, the radial strain is constrained to be zero, and the axial strain is the same as the volume strain. In Figure 3-10, axial strain is plotted against both axial stress and mean stress. As with the definition of Poisson's ratio, for the purpose of defining elastic constants, attention is confined to the initial linear regions of the curves. First, consider the axial stress curve in Figure 3-10. The initial slope of the axial stress curve is the constrained modulus, M , of the material. It is defined as the ratio of

axial stress to axial strain under uniaxial strain conditions. From Figure 3-10, it is seen that $M = 6950$ psi.

Similarly, the slope of the mean stress-volume strain curve is defined as the bulk *loading* modulus, K . Actually, bulk modulus is defined as the ratio of pressure to volumetric strain under hydrostatic loading, but as long as the material behaves elastically, this definition is equivalent. From Figure 3-10, $K = 3370$ psi. It is of interest to know how these values relate to other elastic constants. Recall that Young's modulus, E , is the ratio of axial stress to axial strain under unconfined compression (or tensile) loading. The relations between E and the constrained and bulk moduli are:

$$M = \frac{E(1-\nu)}{(1+\nu)(1-2\nu)} \quad \text{Equation 3-21}$$

$$K = \frac{E}{3(1-2\nu)} \quad \text{Equation 3-22}$$

From those two equations, it is straightforward to find the relationship between M and K :

$$\frac{M}{K} = \frac{3(1-\nu)}{(1+\nu)} \quad \text{Equation 3-23}$$

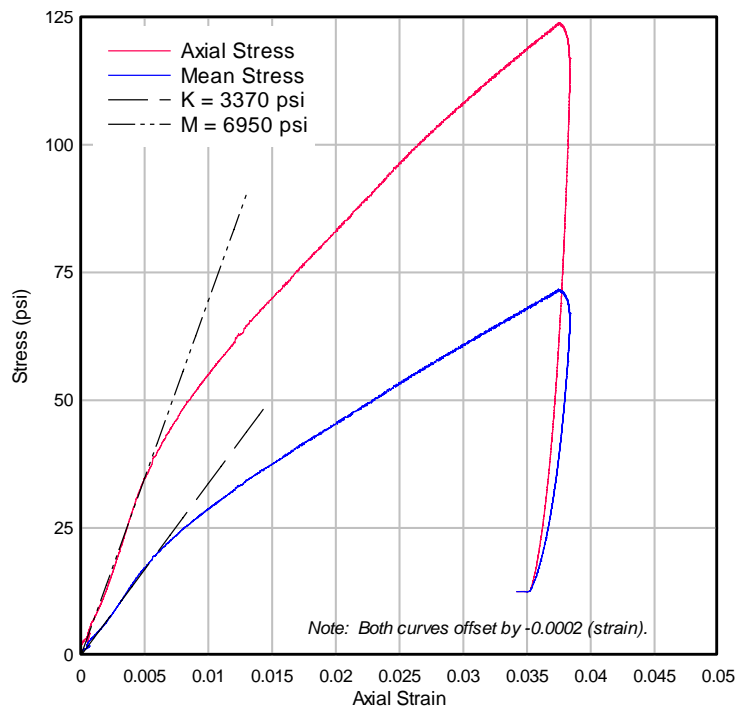


Figure 3-10: Example stress vs. strain curves from uniaxial test.

If the right hand side (RHS) of Equation 3-23 is computed from the values of M and K determined above and the left hand side (LHS) is computed from ν , it is found that both are equal to 2.06. Thus, we have a consistent set of elastic constants. During Material Model 5 input derivation, slight fit adjustments for constrained and bulk moduli were made to ensure Equation 3-23's consistency. The final elastic constant of interest is the shear modulus, G , which is related to E and ν by:

$$G = \frac{E}{2(1+\nu)} \quad \text{Equation 3-24}$$

In summary, for the initial linear loading phase, the elastic constants for the example case are:

Table 3-1: Example summary of elastic constants from uniaxial strain testing

Young's Modulus E	6370	psi
Poisson's Ratio ν	0.185	
Shear Modulus G	2690	psi
Bulk Loading Modulus K	3370	psi
Constrained Modulus M	6950	psi

The unload bulk modulus is derived from the same uniaxial strain test data as shown in Figure 3-10. Because bulk modulus is required, attention is restricted to the mean stress vs. volume strain curve. Figure 3-11 is an expanded view of the unload region. As the unloading behavior is not very linear, geotechnical expertise is used to approximate the curve with a single line. The portion shown as a heavy blue line was considered in the linear fit. The resulting value of unload modulus is $K_u = 17,000$ psi.

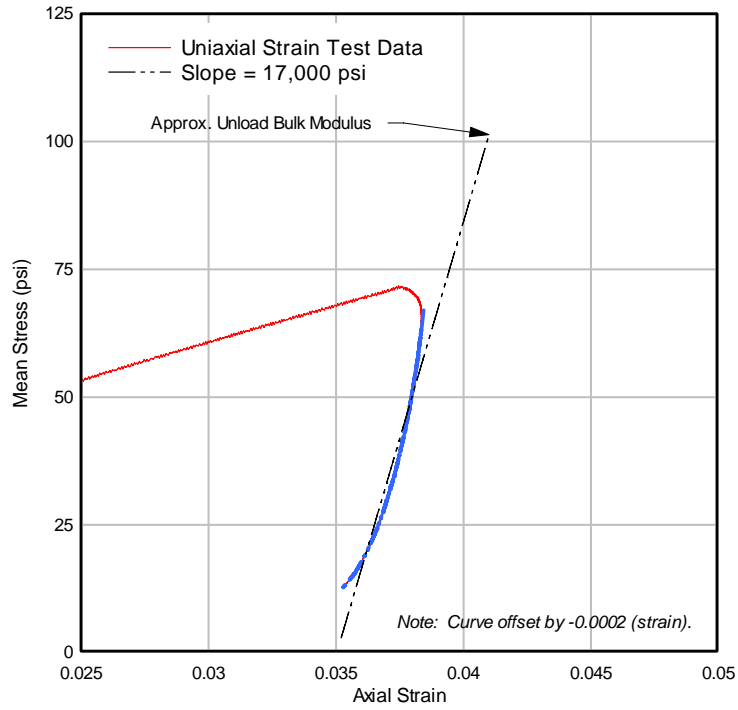


Figure 3-11: Expanded view of the unload region of the uniaxial strain test.

According to the LS-DYNA documentation, the compressibility curve used for Material Mode 5 is defined in terms of logarithmic strain, which is defined as:

$$\varepsilon_{\log} = \ln\left(\frac{V}{V_0}\right) \quad \text{Equation 3-25}$$

where: V = current volume
 V_0 = initial unstressed volume

Because there is no radial strain in the uniaxial strain test, the cross sectional area remains constant and the logarithmic strain can be computed from the initial length and change in length of the specimen as:

$$\varepsilon_{\log} = \ln\left(\frac{L_0 - \Delta L}{L_0}\right) \quad \text{Equation 3-26}$$

where: L_0 = initial specimen length
 ΔL = change in length (positive in compression)

The logarithmic strain is negative in compression. The pressure-logarithmic strain curve from the uniaxial strain test is presented in Figure 3-12 along with the ten-point idealization for input to LS-DYNA. The tabulated points are:

Table 3-2: Example pressure-volume points from uniaxial strain test.

Pressure (psi)	Logarithmic Strain
0	0.0000
16.39	-0.0050
18.24	-0.0056
20.44	-0.0064
22.48	-0.0072
24.31	-0.0080
28.42	-0.0100
36.81	-0.0149
52.42	-0.0250
70.6	-0.0378

The ten points are chosen in such a way to best characterize the shape of the compressibility curve.

NASA Cuddeback (B)
D6B07

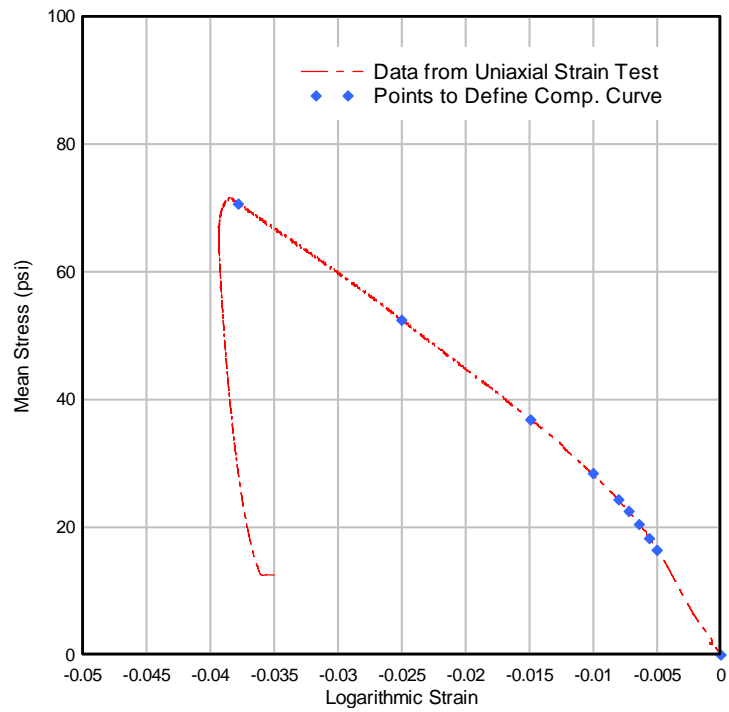


Figure 3-12: Ten points on the pressure-volume compressibility curve in terms of logarithmic strain.

4 Cuddeback Soil A

The general description, field observations, test data, and Material Model 5 inputs for Cuddeback Soil A are discussed in this chapter. Cuddeback Soil A is the interior lakebed of Cuddeback Lake during *dry* conditions. Deriving a wet soil model for Cuddeback Lake was outside the scope of this effort; in lieu of a wet soil model derived from laboratory testing, the closest representative model for wet simulation at Cuddeback Lake is the Carson Sink Wet Soil Model described in Chapter 7.

Chapter 4 is written with additional explanations of general soil behavior, site observations, and laboratory testing details that are applicable to the other soil model chapters. It is recommended that one read the entirety of this chapter before proceeding to the other soil model chapters.

4.1 Location

Cuddeback Lake is located approximately 30 miles northeast from Edwards Air Force Base, CA. Figure 4-1 shows the lake in relation to nearby points of interest. The light tan color is Soil A. The land is under Bureau of Land Management (BLM) jurisdiction, and the airspace is controlled by Edwards. An abandoned airstrip and Air Force bombing range lie immediately to the east.

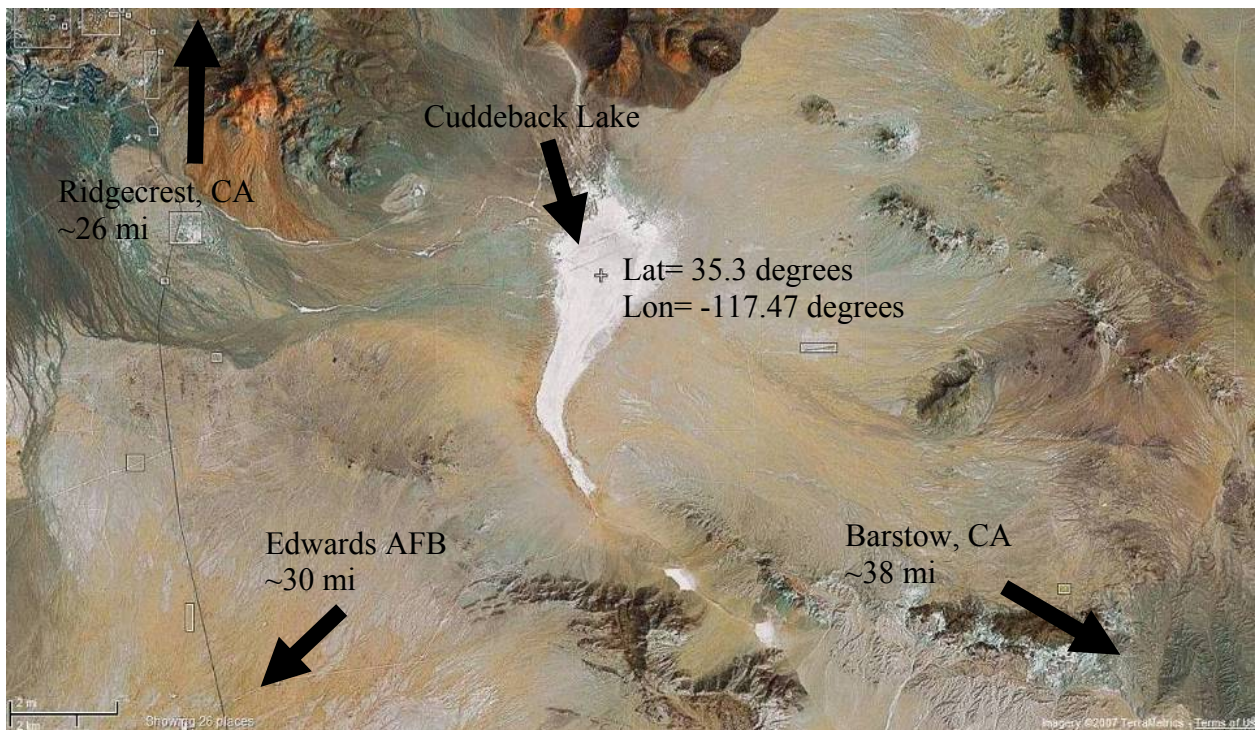


Figure 4-1: Cuddeback Lake aerial photo.

The circular landing zone defined by NASA does not entirely fit on Cuddeback Lake. It is centered at latitude 35.3° and longitude -117.47°. The zone is 10 km in diameter (Figure 4-2) and the lakebed itself is an elongated shape of approximately 4 km by 8 km and covers approximately 40 percent of the area of the zone. The remaining areas are alluvium soil, which comprise the largest area inside the circle.

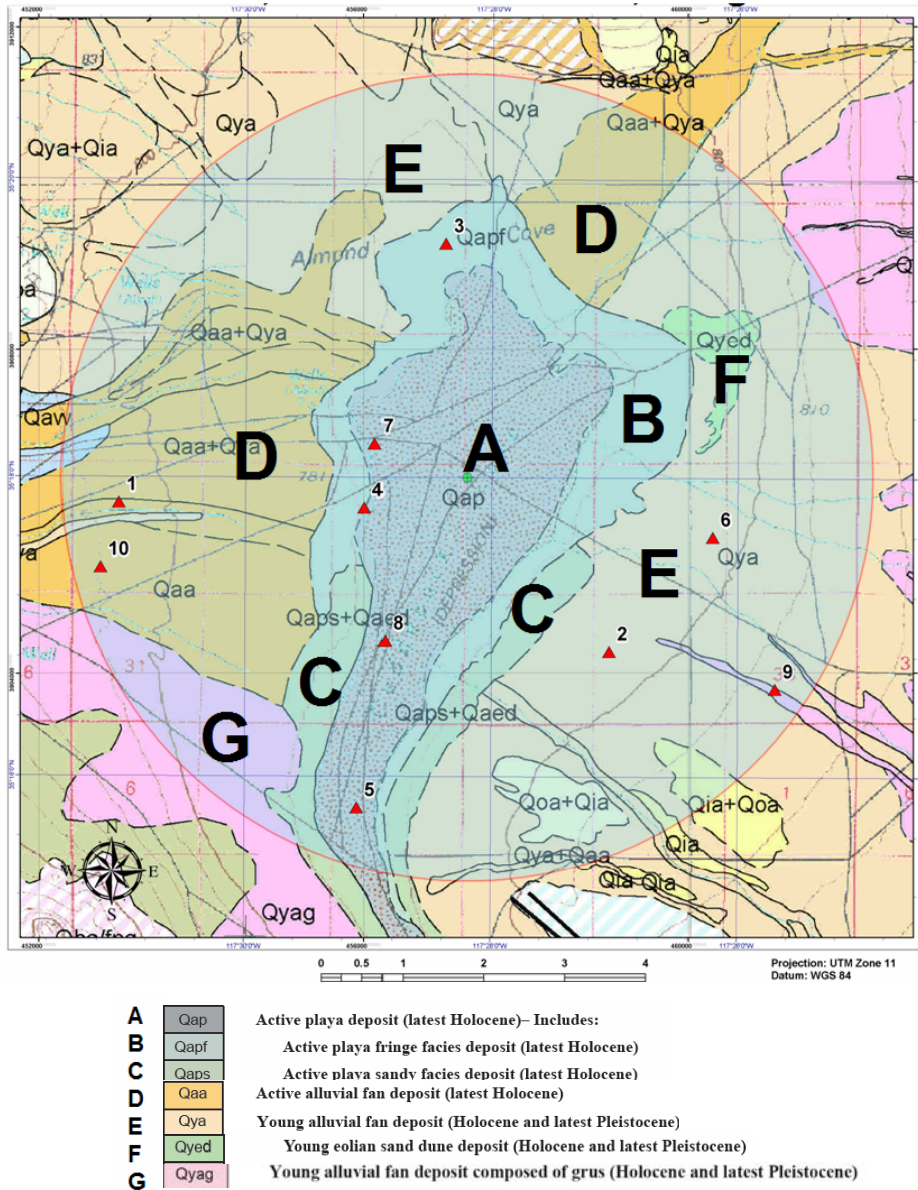


Figure 4-2: USGS Cuddeback Lake map identifying 6 major soil types within landing zone. The zone is a 10 km diameter circle centered at latitude 35.3° and longitude -117.47°.

Table 4-1: Figure 4-2 soil type descriptions.

- A** Hard, sun-baked clay lakebed where fines have accumulated
- B** Soft, dry shorelines where clayey silts have accumulated
- C** Soft, dry shorelines very similar to Soil B, but with more sand
- D** Open plain, sand and fines, light vegetation, and shallow stream beds
- E** Open plain, silty sands, light vegetation, some surface gravel
- F** Sand dunes with short vegetation growing on them
- G** Open plain, mostly sands from granite mountain source

4.2 General description

Cuddeback Lake is a playa, a dry barren area in the lowest part of an undrained desert basin located in the Mojave Desert of southern California. The playa is dry most of the year. However, according to Bureau of Land Management local staff, the playa could be submerged for up to a month during a single desert rainstorm. This submergence usually happens in the winter season. Soil A's dry cracked surface (Figure 4-3) is mostly clay with lesser amounts of silt and occasional sand. It is a very hard surface when dry, and contains very little moisture (<1%) within a few inches of the surface. Within Soil A's footprint (Figure 4-2), there are some wind deposited dunes. These dunes are rare and represent a tiny fraction of the lakebed's area. Though most of the dunes are less than three feet high, there are a few in the northwest part of the lakebed that are in excess of 12 feet (Figure 4-4). The dunes can grow, shrink, or move from year to year due to northeasterly winds.

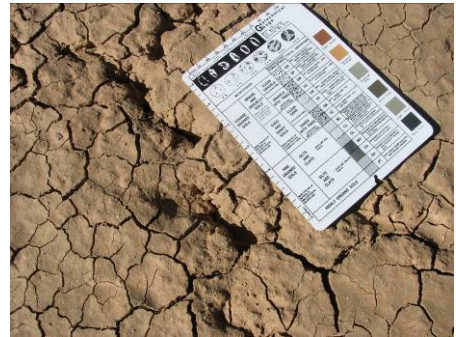


Figure 4-3: Soil A's cracked surface with 6 inch card for scale.

Around the lakebed are alluvial fans originating from the surrounding mountains. The most immediate alluvial deposit is the shoreline, surrounding the lakebed. The shoreline is Cuddeback Soil B, described in the next chapter. The alluvium is graded and finer near the lakebed; however, there are a few dry stream channels that show indications of periodic fast moving floods. These floods deposit gravel, cobble, and boulder sized rocks near the lakeshore, particularly along the eastern side of Soil A's footprint. These rocks seem mostly confined to Soil B's surface, and up to 8 inch diameter rocks were observed (Figure 4-4). Other obstructions include fences, signs, and other man made objects. These obstructions may be important considerations in the landing simulations, but modeling obstructions is beyond the current scope of this task.



Figure 4-4: Observed obstructions including ~12 ft vegetated sand dunes in the northeast shore (left) and rock deposits on the eastern shore (right).

The alluvial fans surrounding the lakebed contain stiff vegetation in the form of sage brush and small desert trees. This vegetation may be capable of puncturing airbag material, and therefore should also be considered by the landing engineer. The density of vegetation is readily

observable from close-in aerial photography. The vegetation commonly reached a height of about 2 to 4 ft.

Soil A can vary from very hard when it is dry to slimy, sticky, and soft when wet. Though wet soil was not encountered during the October 2007 field visit, seasonal flooding could make Soil A the softest soil at the site. During sample excavation, water was added to handfuls of Soil A, and it quickly became a very cohesive material with low shear strength. Other soils, such as silts and sands, are not as sensitive to changes in moisture content.

4.2.1 Man made obstructions observed

Of particular interest to the landing engineer are the various man made obstacles on or around the lakebed. One major disturbance is a 15 ft diameter, over 30 ft deep shaft on the northern edge of the lakebed. Another major obstacle is a 25 ft tall wooden tower situated in the rocky areas of the eastern shore. Figure 4-5 shows the tower on the left, and the shaft on the right. There are also many ~4 ft tall barb wire fences stretching over the 10 km landing circle. A 2x2x4 ft concrete block also lies in the middle of the lakebed. During the field visit, Global



Figure 4-5: Man made obstructions.

Positioning System (GPS) coordinates of most encountered obstacles were recorded by photographing the GPS device along with the object. This report does not include a compiled list of the obstructions; however, a complete photographic record of each obstruction and GPS coordinate is available on DVD and has been provided to the NASA Program Manager, Dr. Ralph Buehrle. Before the CEV could use Cuddeback for landing, there are significant obstacles that will need to be cleared.

4.2.2 Soil classification

Cuddeback Soil A is classified as CL/CH under the Unified Soil Classification System. CL is inorganic clay of low to medium plasticity, including clay mixed with sand and silt. CH is inorganic clay of high plasticity, predominately clay content and extremely sticky. The clay content of Soil A varied from area to area, but the soil was almost always >50% clay.

Soil A's cracked surface can be explained by clay's volumetric relationship with water content. When submerged, water seeps into Soil A and causes slight expansion. Swelling is a very common property of clay. When the clay dries out, the clay shrinks, leaving tensile fractures on the surface. These fractures are typically very shallow with an average depth of about ¼ inch.

Another defining attribute of Soil A is the presence of cohesive strength. Clays exhibit cohesion, and allow the soil to withstand small tensile stresses. Water content generally increases below the surface, and so does cohesion. Granular soils, such as the silts and sands that surround Soil A, have very little or no cohesion. Figure 4-6 exemplifies Soil A's cohesive strength. It was relatively easy to dig large intact chunks of Soil A with a shovel. This cohesion is the primary reason why Soil A is stiffer than all the surrounding soils, because cohesion increases the shear resistance of the soil.



Figure 4-6: Soil A cohesion.

4.2.3 Cementation

Soil A displayed cementation, which is a strengthening phenomenon when the soil is dried out. Cementation differs from cohesion because it is caused by lack of water. When the lakebed dries out, the dissolved minerals form bonds between particles. These bonds are very brittle, and once broken, they are not recovered until wetted and dried out again. Cementation is typically manifested on the surface. Nearly all Cuddeback soils exhibited cementation within one inch of the surface, but it added very little to the overall strength. Figure 4-7 illustrates the effect of cementation on the surface. Although held together by cementation, the soil plates shown are very thin and fragile. The Material Model 5 properties contained herein do not account for cementation because the effects of cementation are considered negligible. It is also very difficult to collect intact sample of lightly cemented soil.



Figure 4-7: Soil cementation.

4.3 Selection of Soil A

Cuddeback Soil A represents the dry conditions of the interior lakebed at Cuddeback Lake. It is mostly clay soil. It is the product of fine sediment deposits in Cuddeback Lake from seasonal rains. The field visit was conducted during dry conditions, and Soil A exhibited a hard, sun-baked clay behavior. After surveying all the major soil types, Soil A was quickly determined to be the hardest soil present by a significant margin. It was also much more difficult to dig than any other soil.



Figure 4-8: Airbag drag on Soil A. Note the lack of deformation behind the bag.

The field visit began with soil investigations from west to east across the site (Figure 4-11), at designated points CD-1 thru CD-8 in Appendix B. Soil descriptions, shear vane, dynamic cone penetrometer (DCP), and nuclear densitometer measurements were taken at consistent depths in each soil zone. After all six soil zones were inspected, the hardest and softest soils present were selected by observation and DCP strength. Soil A was the hardest by far, and Soil B was the softest due to its wind deposited nature.

Two soil types were chosen to represent the extremes regarding their response to landing. Soil A was selected because its hard condition is likely to maximize peak accelerations during impact. This was considered a key factor because landing design uses a peak acceleration limit for astronaut safety. Another major factor in choosing Soil A was its large central area in the landing zone. Statistically speaking, Soil A represents the most likely landing spot. Soil B was the second selected soil, and is discussed in Chapter 5.

4.4 Field observations

The field testing yielded the soil densities recommended for modeling. The water contents obtained in the field established the variability of the moisture. The laboratory moisture contents, however, are still considered more accurate when tied to specific properties.

Field conditions were extremely dry during the visit. The field visit began after arrival with a visual assessment of the soil across Cuddeback Road, the road heading northeast across the lake (Figure 4-11). The scan began with western point CD-1 (see Appendix B) and continued to CD-5 on the eastern side. The visual assessment confirmed the accuracy of the USGS surface geology map (Figure 4-2). CD-1 and CD-2 were in Soil D, primarily sand mixed with silt. CD-3 and CD-5 was in Soil B. CD-4 was in Soil A. CD-6 was in Soil G at the highest elevation on site, CD-7 was in the sand dunes (Soil F) and CD-8 was in Soil E. It is worth noting that vegetation grew larger as one progressed farther east into Soil E territory. Soil G was visited last, and determined to be very similar to D.

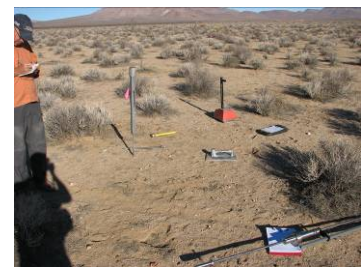


Figure 4-9: Soil D.

The hardness of Soils C, D, E, F, and G were all in between Soil A and B. Nearly all possessed a thin layer of surface cementation. The common theme was a significant sand content, although from different sources. Soil E was derived from a rhyolite rock source east of the site, and the Soil G was derived from a granite source. The alluvium around the rest of the site was a mix varying from mostly for rhyolitic constituents to alluvium with mostly granitic constituents.



Figure 4-10: Field observations. (left) Soil A with mounds, a rare occurrence. (center) Example of Soil B's sparse vegetation coverage. (right) Example of Soil E's tall vegetation.

4.4.1 Sampling and sample locations

After establishing the relative uniformity of Soil A across the site, three source locations were chosen for sampling. The circle center was chosen as the first sample source. The second source was approximately 2 km to the south, and the third was another 2 km south beyond the second. At each source location eight samples were taken from consistent depths. Figure 4-11 shows the sampling sites.

The sampling procedure involved segregating the soil by depth, 6 inches at a time. For one sample hole, the 0-6 inch deep soil was placed in one sample bag. The next 6-12 inches were placed in another bag. And so on, until reaching 24 inches. Sampling was terminated at 24 inches because further excavation revealed the same soil. It also became unnecessary to sample deeper because most of the significant soil deformation would occur within the top 24 inches. Only density and moisture content increased with depth. At each of the sample locations, multiple sample holes were dug to reduce dependency on a single excavation.

Sampling by depth is the best way to characterize playa soil because it tends to be deposited uniformly. Differences are mainly due to depth, not area.

Although effort was made to explore the entire 10 km circle outside of the lakebed, field access was mainly limited to dirt roads because the desert brush and small trees are stiff enough to cause damage to automobiles, and dense enough to prevent free passage. For future reference, at least one sample was taken from all six major soil types (Figure 4-2), and they are stored at ARA's laboratory. No laboratory tests were performed on Soils C, D, E, F, or G.

NASA Crew Exploration Vehicle (CEV) Landing Area
 Sample Collection for Soil Model Development

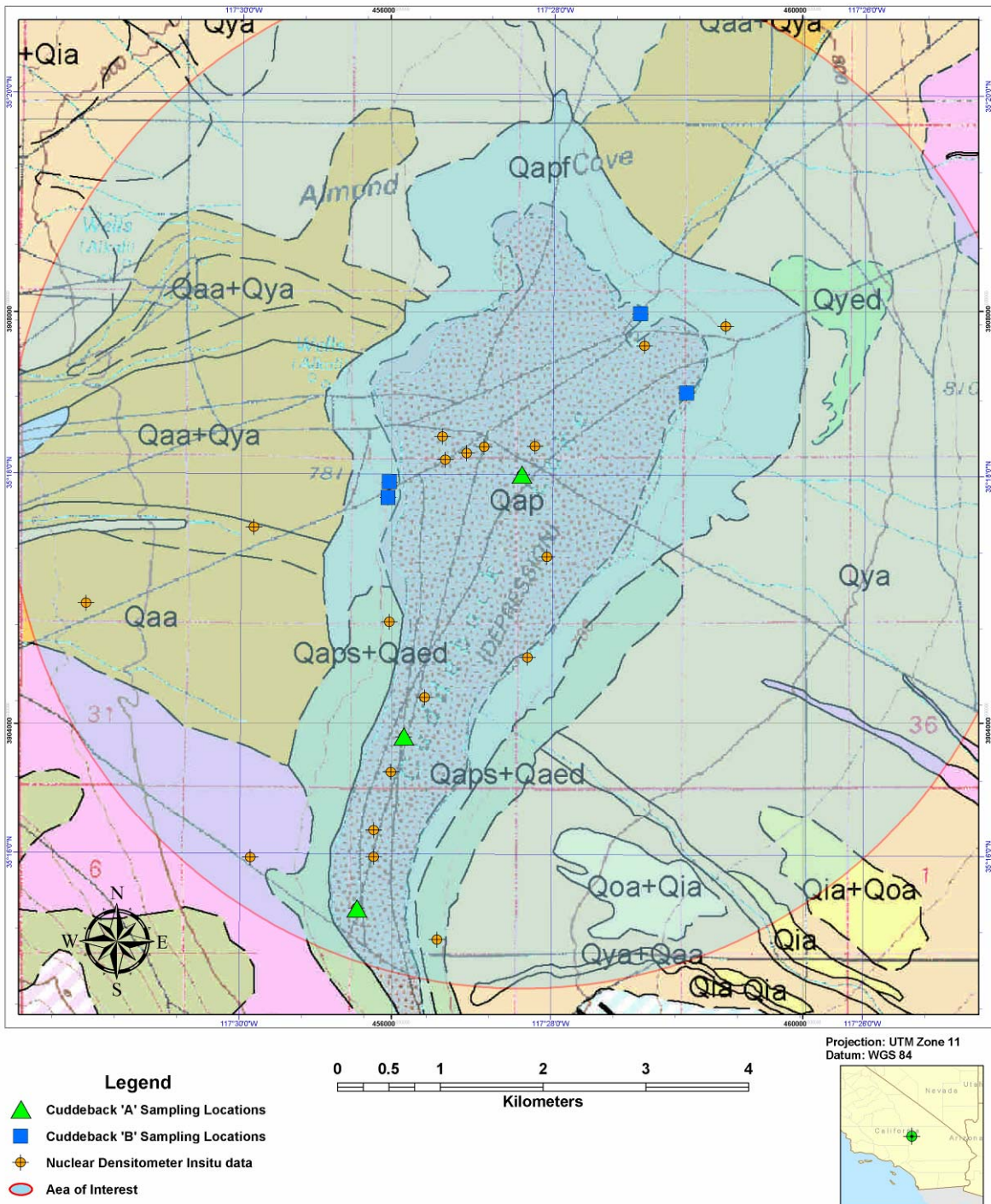


Figure 4-11: Soil sampling locations for Cuddeback Soil A and Soil B. Area of interest is 10 km landing circle. (USGS map.)

4.4.2 Nuclear density and nuclear moisture content field data

Merrell-Johnson Engineering of Barstow, CA was subcontracted to perform nuclear density and nuclear moisture content testing according to the ASTM Standard D6938. A CPN MC-3 Portaprobe device was used. It was calibrated every morning before use against a standard block of known density material.

The nuclear density gage is capable of estimating the in situ density and moisture with minimal disturbance. It is used to conduct a one minute test that involves inserting a probe into the ground. Nuclear density gauges are commonly used in the construction industry, especially for determining pavement densities and soil densities for shallow foundations. The probe contains tiny amounts of Americium-241 or Cesium-137 radioactive elements. Regulations associated with the nuclear sources require a locally licensed operator to perform these tests. A detector measures the amount of radiation emitted from the inserted probe. When calibrated against a standard block of known density, the gage can measure the average soil density between the probe and the detector. The density gage's probe can extend up to 12 inches into the soil, and can be set to any one inch increment of depth.

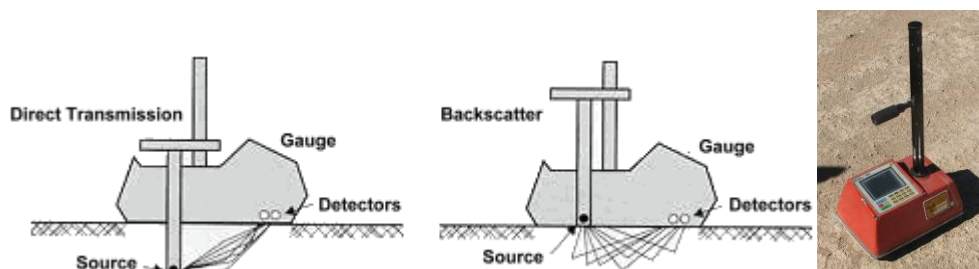


Figure 4-12: Nuclear density gage.

Nuclear density tests were conducted in conjunction with all sampling. Density tests were conducted in all major soil types, with 122 total tests. 53 tests were conducted in Soil A, and 35 in Soil B. The density test involves driving a spike into the soil to make room for the insertion of the source probe. The efforts were taken to test in 6 inch increments, but sometimes soil caved in during the insertion of the probe and altered the depth by filling the hole. As a result, the density data is presented in the common depth ranges recorded during the field visit.

The nuclear density gage measures wet density, i.e., the bulk density including water. It also measures water content based on hydrogen atom content in the soil. Water contains hydrogen, and a calibration factor is used to relate radiation count with water content. Based on the detected water content, a dry density value is calculated from subtracting the weight of water. Summaries of Soil A's measured field data are provided in the following tables. N is the number of tests taken in the specified depth range. SE is the standard error; StDev is the standard deviation. Q1 and Q3 are 25th and 75th percentiles.

Table 4-2: Wet Density (lbs/ft³) descriptive statistics by depth in Soil A.

Depth (in)	N	Mean	SE Mean	StDev	Minimum	Q1	Median	Q3	Maximum
0-4	3	89.467	0.584	1.012	88.3	88.3	90	90.1	90.1
0-6	20	92.11	0.655	2.929	88.1	89.625	92.35	93.45	100.3
0-11	6	92.38	1.32	3.23	88.5	88.8	92.9	95.13	96.4
6-16	20	93.85	1.12	5.02	78.3	92.58	94.55	96.35	101.9
12-23	4	102.23	2.11	4.23	96.4	97.78	103.3	105.6	105.9

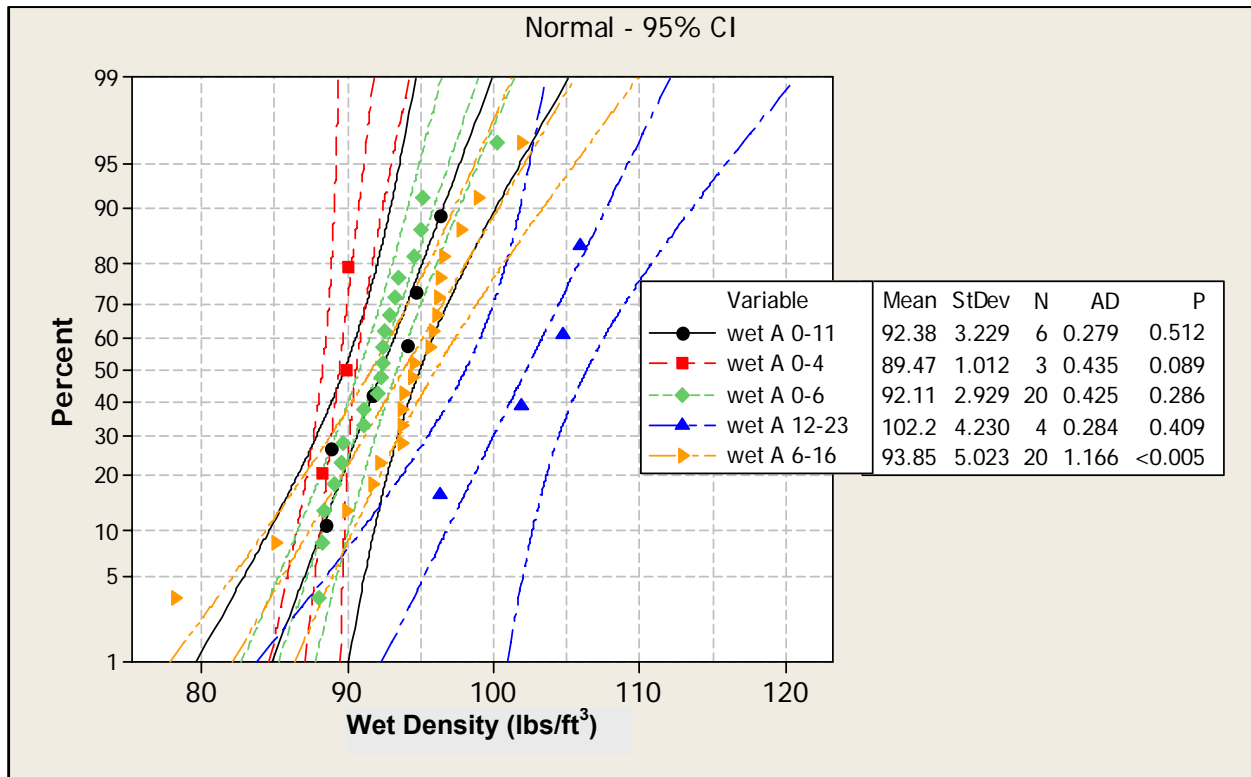


Figure 4-13: Probability plot of Soil A's wet densities (lbs/ft³) by depth (inches).

Figure 4-13 is a normal probability plot of Soil A's wet densities from Table 4-2. It displays an increasing density trend with depth, typical for soils. The curved dotted lines represent the 95% confidence interval, assuming normal distribution of data. If another nuclear density test was conducted in that depth range, there is a 95% chance the result would lie within these bounds. The wider the bounds, the greater the uncertainty. Overall, the near surface soil density had rather consistent density, attributed to the uniform nature of the lakebed soil. The deeper soil, 12-23 inches, were much higher density but also more variable. The 0-6 inch wet density average, $\rho_{wet} = 92 \text{ lbs/ft}^3$, was chosen as the laboratory specimen density because this was the most representative of the depths that would experience the most deformation. The formula for calculating RO, the LS-DYNA Material Model 5 mass density, is:

$$RO = \frac{\rho_{wet}}{g}$$

Equation 4-1

Using Equation 4-1 in the following example computation, we find that the mass density $RO = 0.000138$. To be consistent with the units used in the laboratory tests (psi), the mass density is presented in units of $lb\ s^2/in^4$:

$$RO = \frac{\rho_{wet}}{g} = \frac{\frac{92\ lbs}{ft^3} \frac{1\ ft^3}{12^3\ in^3}}{\frac{32.2\ ft}{s^2} \frac{12\ in}{ft}} = 0.000138\ lb\ s^2 / in^4$$

Table 4-3: Water content (%) descriptive statistics by depth in Soil A.

Depth (in)	N	Mean	SE Mean	StDev	Minimum	Q1	Median	Q3	Maximum
0-4	3	3.927	0.263	0.456	3.52	3.52	3.84	4.42	4.42
0-6	20	3.811	0.0943	0.4215	3.22	3.5125	3.77	4.1125	4.81
0-11	6	3.932	0.115	0.282	3.5	3.71	3.925	4.205	4.28
6-16	20	7.18	0.224	1.001	5.75	6.48	6.845	7.885	9.81
12-23	4	10.403	0.663	1.327	9.09	9.19	10.325	11.693	11.87

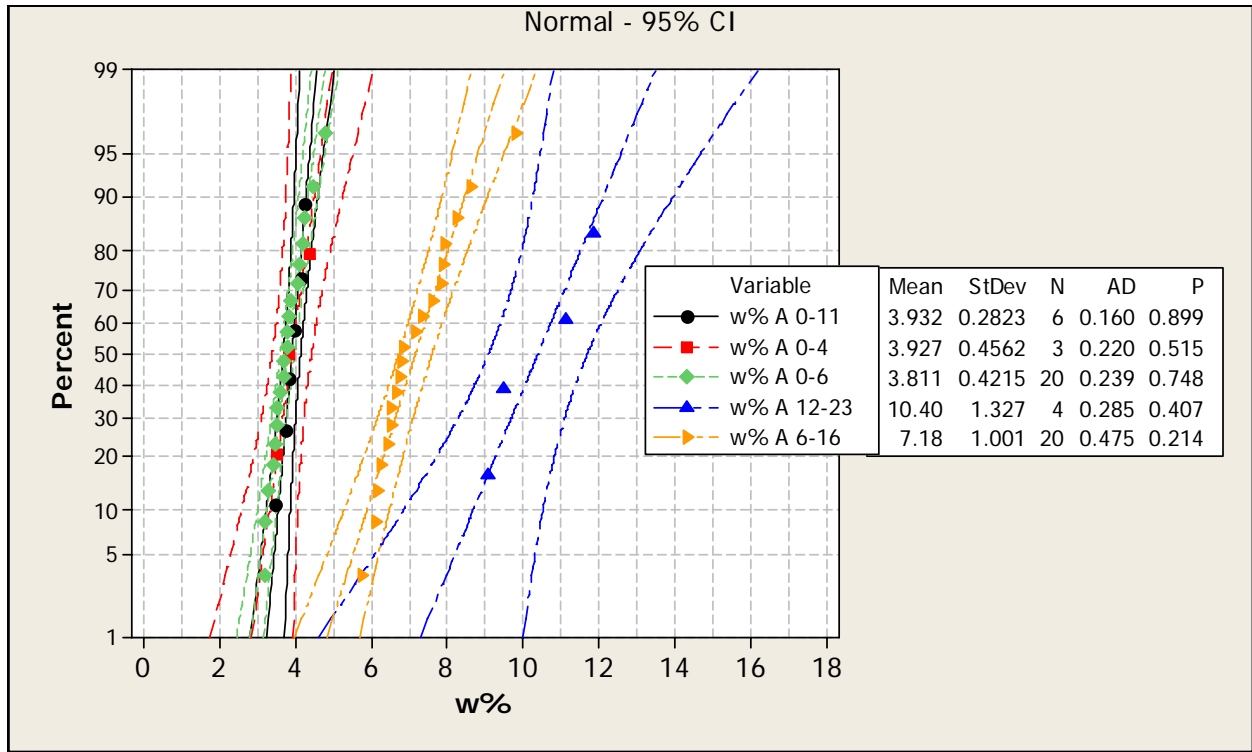


Figure 4-14: Probability plot of Soil A's field measured water contents (%) by depth (in).

Water content also tends to increase with depth. Table 4-3 and Figure 4-14 indicate that the 0-6 inch soil is very dry with almost no exceptions. No wet spots of any kind were observed at the site. A few nuclear moisture tests were conducted at 1-2 inches deep and revealed water contents <1%. This low moisture content leaves the fine surface grains subject to wind erosion. The rare vegetation on the Soil A accumulated these fines into mounds. The average detected moisture content was 4% for 0-6 inch soil. Significant gains in moisture content do not occur until 12 inches deep. To represent water contents in the laboratory, samples from 0-12 inches were combined to obtain 8 inch tall specimens for testing.

All Cuddeback soil was much drier than its Carson Sink counterpart. The water table at Cuddeback is much deeper than Carson Sink's. It is hypothesized that Cuddeback Lake would dry out faster than Carson Sink if subjected to equal flooding. However, no seasonal data was available to confirm this hypothesis.

Table 4-4: Dry density (lbs/ft³) descriptive statistics by depth in Soil A.

Depth (in)	N	Mean	SE Mean	StDev	Minimum	Q1	Median	Q3	Maximum
0-4	3	86.1	0.529	0.917	85.1	85.1	86.3	86.9	86.9
0-6	20	88.735	0.659	2.949	84.6	86.3	88.6	90.4	97.1
0-11	6	88.88	1.27	3.11	85.3	85.45	89.3	91.58	92.7
6-16	20	87.63	1.12	5.02	72.5	85.5	88.45	90.8	96.4
12-23	4	92.58	1.55	3.09	88.1	89.43	93.5	94.8	95.2

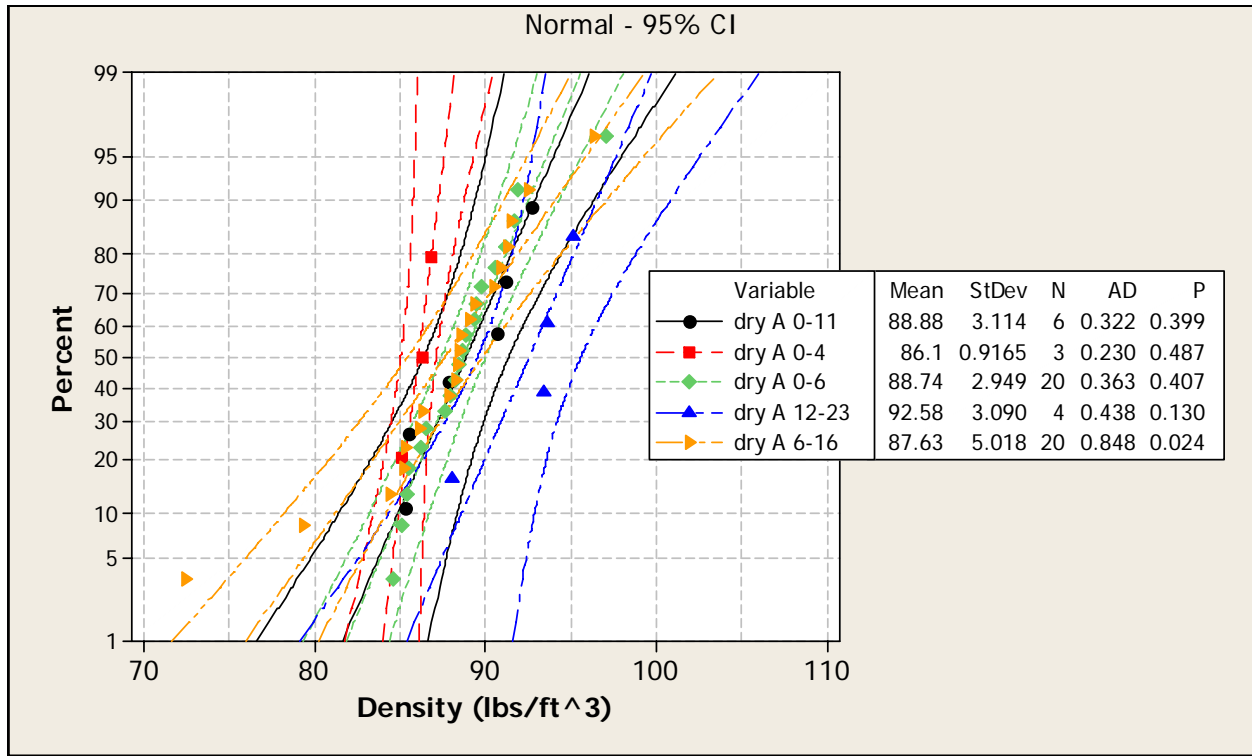


Figure 4-15: Probability plot of Soil A's dry densities (lbs/ft³) by depth (in).

Table 4-4 and Figure 4-15 show the calculated dry density based on the estimated water content from the nuclear density gage. The dry density is a more reliable soil property, and Soil A has a relatively consistent dry density down to 23 inches. Higher dry densities are associated with higher shear strengths. The 6-16 depth category has one outlier at 73 lbs/ft³. This outlier could be due to the presence of a fracture void. When dry density is known, one can compute porosity. The relationship is given as:

$$n = 1 - \frac{\rho_{dry}}{G_s} \quad \text{Equation 4-2}$$

The dry density, ρ_{dry} , averaged 90 lbs/ft³ (1.44 g/cm³). The specific gravity of the grains, G_s , was 2.76 g/cm³. Using Equation 4-2, the average porosity n is 48%. This means 48% of Soil A's bulk volume is comprised of void space filled by air or water. It is typical for clays to contain

large void space. These voids are characterized by tiny air pockets and do not collapse easily when Soil A is dry. Soil A easily carried the weight of vehicles with very little deformation.

When the soil is submerged, the dry density essentially remains the same. A significant portion of air voids are replaced by water, and the shear strength of the soil drops dramatically. With high saturation, these voids are easily collapsed and deformations increase. Although a wet Cuddeback Lake model was not developed, the method for constituting one would be to add water to a sample while still maintaining the same dry density. This approach would be consistent with the approach used for developing the Carson Sink wet model.

4.5 Laboratory test data

This section contains the results of laboratory tests on Soil A. The fits to obtain elastic constants for Material Model 5 are included with the test result figures. The test log in Table 4-5 summarizes the tests using the triaxial apparatus.

Table 4-5: Test log for Cuddeback Soil A tests

Test ID	Sample ID	Type	Confining Pressure (psi)	Moisture content	Dry Density (lbs/ft ³)	Grain Density G_s (g/cm ³)	Porosity n
J8B08	CDL	Triax	2	6.29%	86.56	2.76	49.8%
J8D08	CDL	Triax	5	6.33%	86.52	2.76	49.8%
J9B08	CDL	Triax	10	7.14%	86.14	2.76	50.0%
J10B08	CDL	Triax	20	6.28%	86.84	2.76	49.6%
J30D08	CDL	Triax	50	6.39%	86.47	2.76	49.8%
J21A08	CDL	Uniax	50	6.16%	86.66	2.76	49.7%
J21A08	CDL	Hydrostat	50	6.16%	86.66	2.76	49.7%

4.5.1 Moisture content and saturation

After each specimen was tested, a portion of the sample was used for moisture content testing. Eight moisture tests were conducted. The average moisture content was 6% for all Soil A tests, which corresponds to a saturation level of 17%. This saturation level is low in general terms of soils. Saturation is defined as the volume of water divided by the total volume of voids; an equivalent expression is 17% of the voids are filled with water.

The significance of the laboratory moisture content is that the saturation is so low that the soil will behave as an unsaturated soil. The mechanical significance means that essentially no pore pressures will develop because the moisture can flow to remaining air voids without holding pressure. Pore pressures develop when a soil is compressed and the water has no where to go.

4.5.2 Grain density and size distribution

The grain density of Soil A was determined to be 2.76 g/cm³ by pycnometer. Figure 4-16 displays the dry sieve results for Soil A. As discussed in 3.1.2, there are two forms of sieve analysis. We believe the dry sieve analysis is misleading because the percent passing the #200 sieve is too low. We believe that many particles remain cemented together after being dried, and the dry sieve results are skewed toward the coarser side. Wet sieve analysis reflects a 95% fines content. The very high clay content contributed to Soil A's higher strength because it could withstand a small amount of tensile stress due to clay cohesion. However, when wet, the clay will turn against Soil A's strength, and shear strength will dramatically decrease.

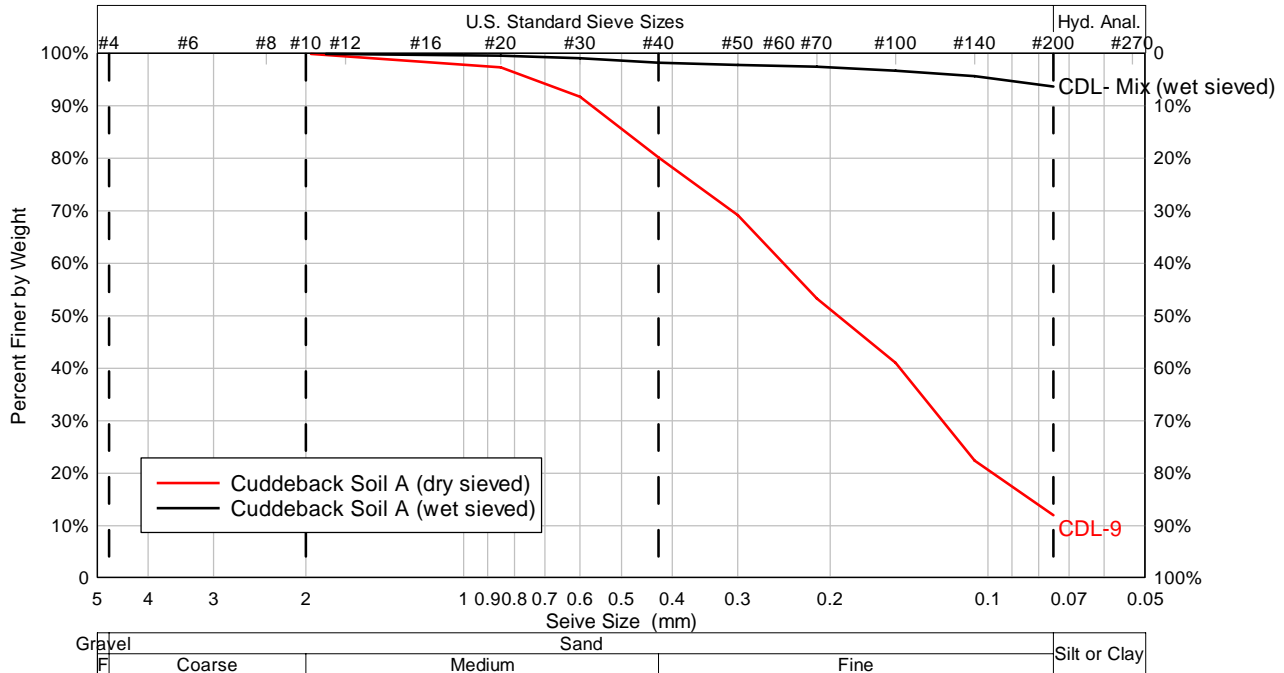


Figure 4-16: Soil A grain size distribution.

4.5.3 Atterberg limits test

The results of the Atterberg limit tests, described in Section 3.1.4, are presented in Table 4-6. Soil A was classified as a clay with low to medium plasticity. Soil B was classified as primarily a silt with some clay with low plasticity.

Table 4-6. Results from Atterberg limits test on soils from Cuddeback Lake.

Soil ID	Liquid Limit	Plastic Limit	Plasticity Index	Soil Classification
Soil A	42	27	15	CL
Soil B	33	24	9	ML

4.5.4 Hydrostatic compression

A hydrostatic compression test was run for each soil. A hydrostatic compression test subjects the soil specimen to equal pressure on all principle axes by applying confining pressure only. It is a

two segment test. First, the confining pressure starts at zero and increases to a pressure of interest, 50 psi. Second, the pressure reduces to a much lower pressure, 10 or 20 psi, to capture the unloading strain as the soil expands from a compressed state.

The modeling significance of hydrostatic compression is primarily the unloading portion of the test. Soils unload at a different rate than loading, and this effect is described by the bulk unloading modulus. To completely model a soil, the behavior of the soil after load has been reduced or removed needs to be accounted for.

The hydrostatic compression test and uniaxial strain test provide a means of obtaining the bulk unloading modulus. The volumetric strain results from both are plotted here for comparison. Note the similar slopes on both test curves.

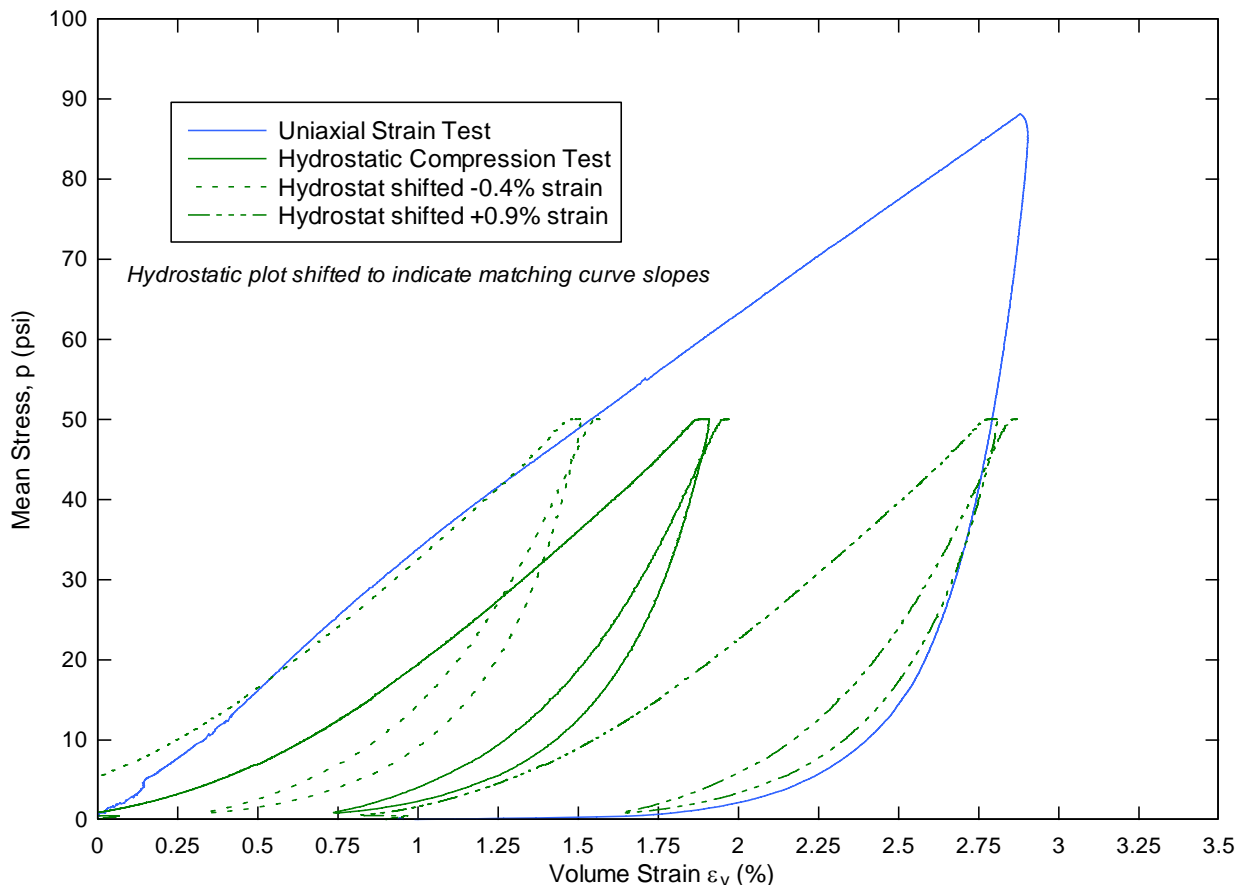


Figure 4-17: Soil A hydrostatic compression test. Uniaxial strain data plotted for comparison.

4.5.5 Triaxial compression

A suite of five triaxial compression tests were run on each of the soils. In a triaxial compression test, a confining pressure is maintained on the specimen’s sides while axial load is applied. The

confining pressure is held constant throughout the test. The five confining pressures used for this study were 2, 5, 10, 20, and 50 psi, which should cover the range of modeling interest. The bias toward low confining pressures reflects the low stress design of the airbag landing systems. LaRC Landing Systems ADP presented two airbag designs with design pressures between 2 and 6 psi. The target wet density for sample specimens was 92 lbs/ft³.

Figure 4-18 shows the results of all five triaxial compression tests in terms of stress difference vs. strain. Both radial and axial strain are shown. Radial strain, the lateral expansion of the cylindrical specimen, is on the left. Axial strain, the vertical compression, is shown on the right. Throughout this report, 2 psi tests are shown in red, 5 psi in blue, 10 psi in green, 20 psi in purple, and 50 psi in orange. Stress difference is defined in Equation 3-3. The layout of the plot allows one to track both radial and axial strain at the same loading. A point on the stress difference axis represents a single load on the specimen. The strain axis represents the two separate strains associated with that loading. The peak of the curve represents the strength of the specimen. The peak stress difference value for each test is then used to derive the constitutive material properties as described in Chapter 3.

In Figure 4-19, the peaks from Figure 4-19 are plotted as a strength envelope. The strength envelope space is stress difference vs. mean stress. Mean stress is equivalent to pressure p in Material Model 5. It is defined in Equation 3-4. The five triaxial tests generate five points on the strength envelope plot. A fitted line is drawn through the five points, and is referred to as the failure envelope. An element of soil whose stress path encounters this line would experience shear failure.

The slope of the line is correlated to ϕ , the internal angle of friction, which is 38.6°. The angle ϕ describes the friction between the grains of the soil. The physical meaning is the maximum angle at which the soil can support itself. To aid in understanding, imagine the granular soil falling from the top of an hourglass into the bottom. The soil forms a conical accumulation shape, and the slope of the cone is the angle of internal friction. If subjected to a greater slope, the soil collapses and returns to the internal friction slope. The angle ϕ is a shear strength property of the soil commonly used in geotechnical engineering. The cohesion c , is correlated to the intersection of the failure envelope and the stress difference axis, which is equal to half of the stress difference. Cohesion represents the tensile strength of the soil, which is 6.75 psi. Most soils have some small amount of cohesion, influenced by water, and clays have the highest amount. Dry sands have zero cohesion.

Figure 4-20 shows the laboratory test derived LS-DYNA's Material Model 5 yield surface. The points from Figure 4-19 are equated to J_2' and plotted as a function of pressure p . The method of equating stress difference to the second invariant J_2' is described in Chapter 3.1.5.3. A quadratic fit to the five triaxial strength points is made, and the fit coefficients are the a_0 , a_1 , and a_2 inputs for Material Model 5.

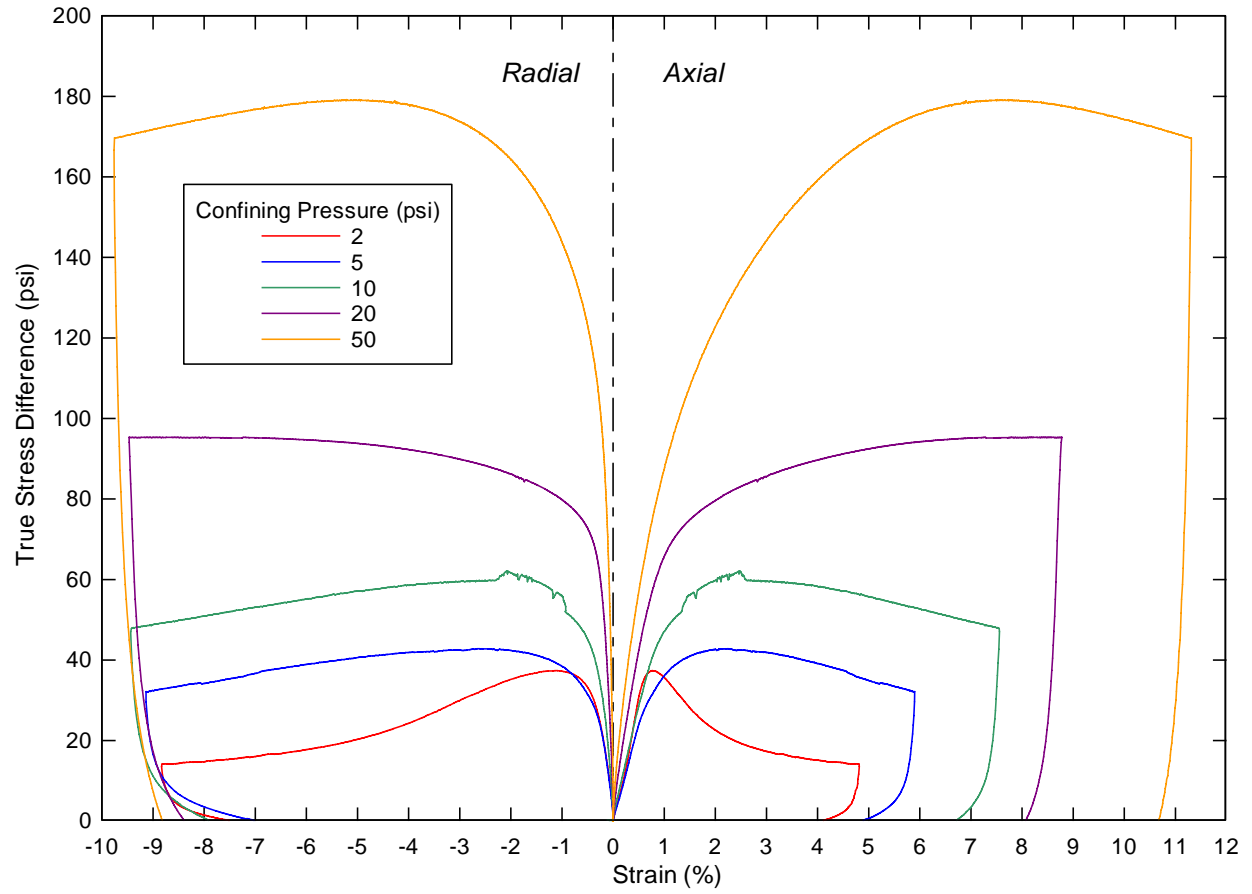


Figure 4-18: Soil A triaxial test results for 2, 5, 10, and 20 psi confining pressures.

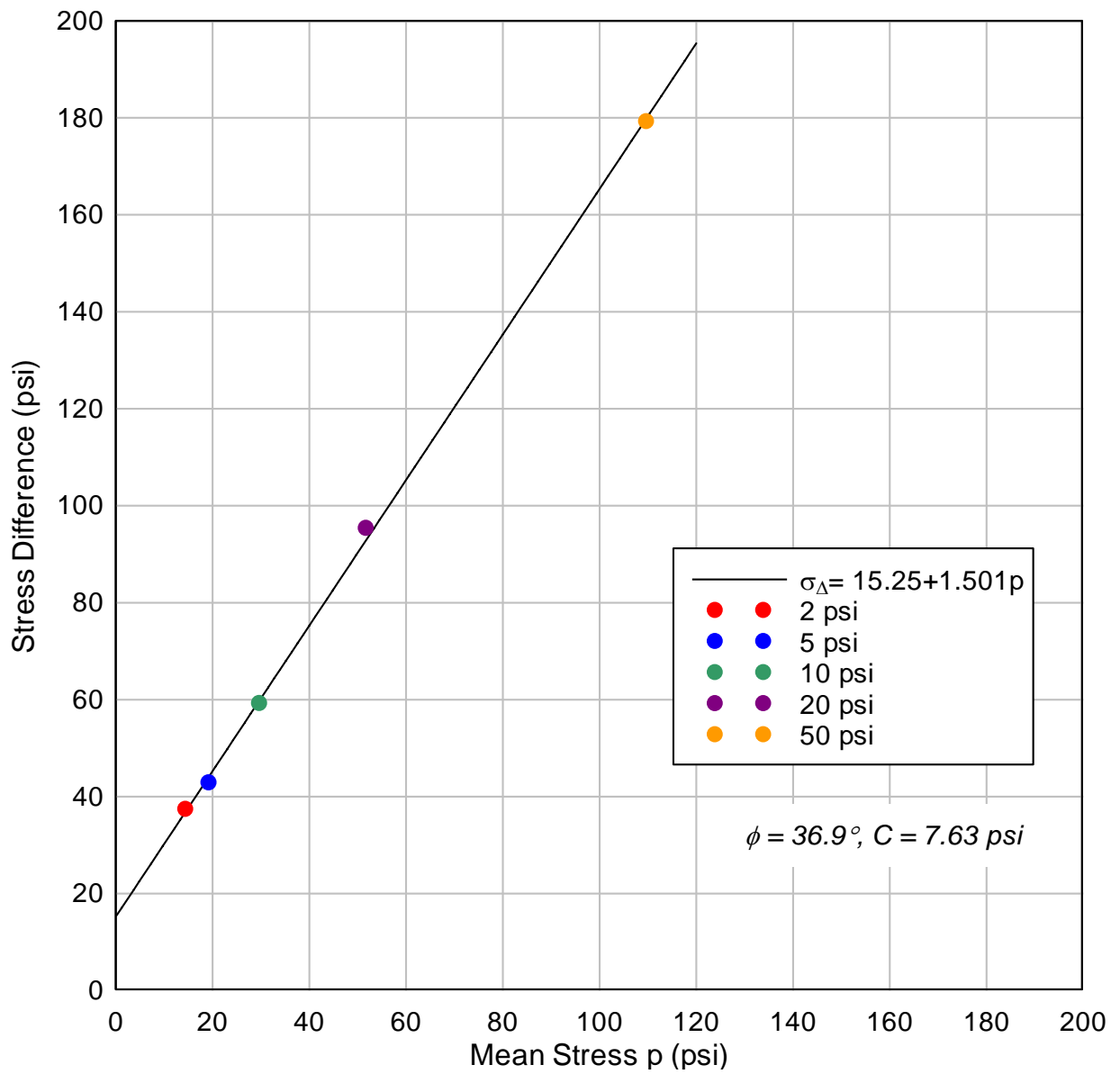


Figure 4-19: Soil A strength envelope results.

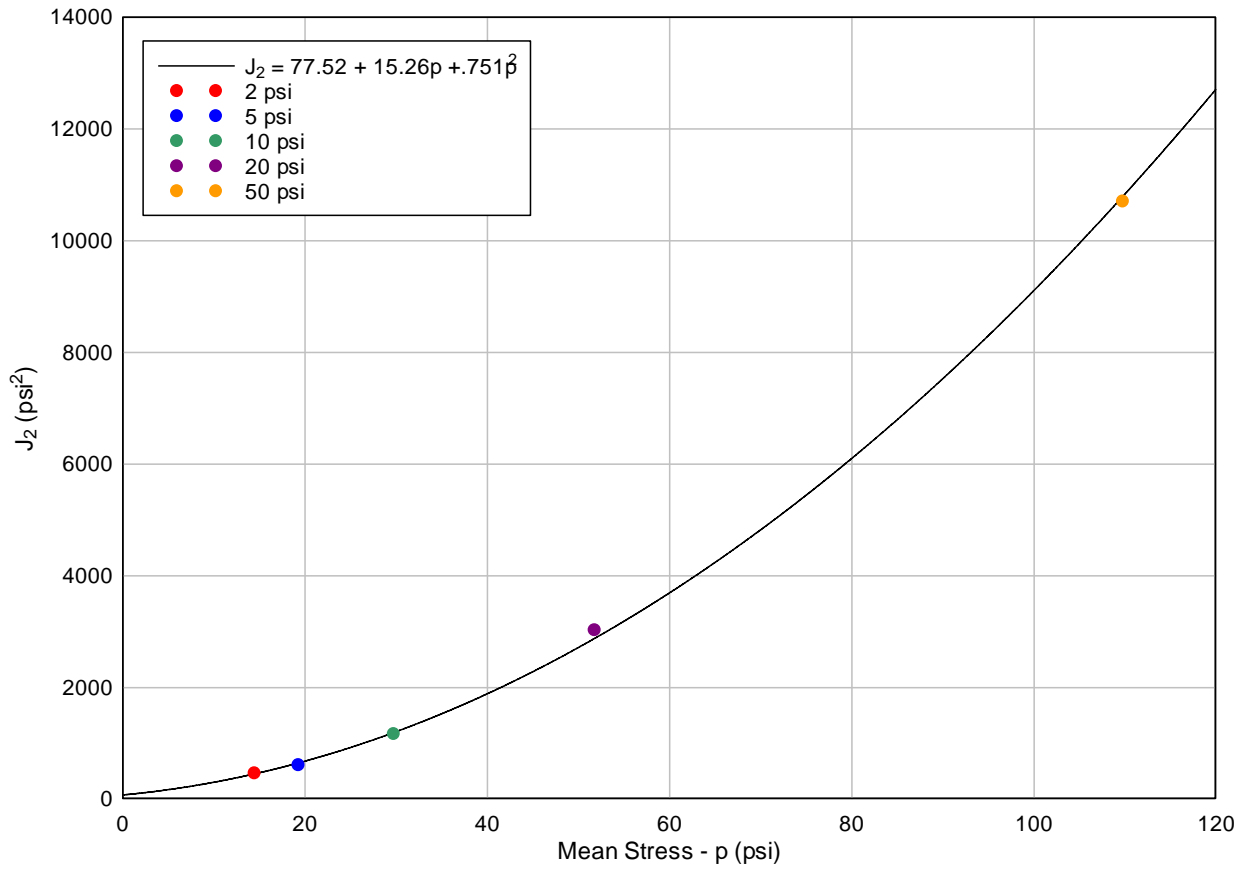


Figure 4-20: Soil A Material Model 5 yield surface fit from triaxial test data.

4.5.6 Uniaxial strain

One uniaxial strain test was run on Soil A. The uniaxial strain test prevents radial strain from occurring by means of a radial confining pressure control algorithm. As load is applied, a radial LVDT measures the strain, and the data feed is used to control the amount of confining pressure applied to the specimen. As a result, the uniaxial confining pressure is always increasing to maintain zero radial strain during the test.

The uniaxial strain tests typically have three segments: an initial loading portion, a stiffer closed void portion, and an unload portion. The three segments can be idealized by three slopes. The initial loading portion represents the constrained modulus used in constitutive model construction. The second portion always has a lower slope (lower modulus) than the first because the soil is stiffening up as the voids close. The third portion represents the expansion of the soil when unloaded, similar to the hydrostatic compression.

Figure 4-21 shows the three segments of the uniaxial test in terms of stress difference vs. mean stress. Figure 4-23 is a plot of only the unloading portion of the test in terms of mean stress vs. volumetric strain. The unloading portion can also be used to compute the bulk unloading modulus (BULK) input for Material Model 5. It provides an additional method to confirm the bulk unloading rate.

The shear modulus G can be obtained from either the slopes drawn in Figure 4-24, or the Poisson ratio calculation in Figure 4-26. The method for calculation G from uniaxial strain is outlined in Chapter 3. Figure 4-27 is the uniaxial test data plotted in terms of mean stress vs. logarithmic strain. Because mean stress is equal to pressure p and logarithmic strain is the logarithmic change in axial strain (no radial strain allowed, $\varepsilon_c = 0$), Figure 4-27 represents the pressure-volume behavior of Soil A in the axial direction. Because the soil is assumed to be isotropic, the same curve also represents pressure-volume deformation in the radial direction.

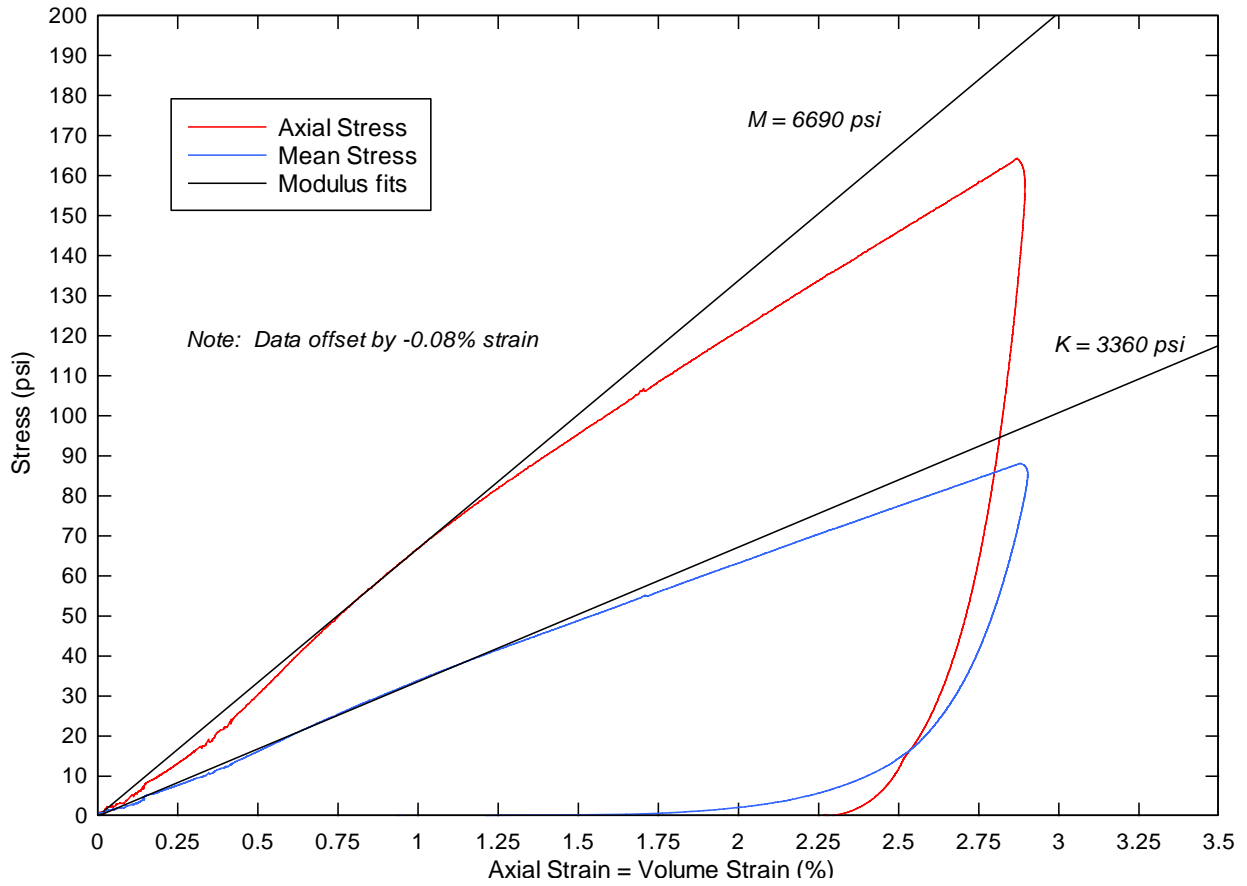


Figure 4-21: Soil A uniaxial strain test results. Constrained and bulk moduli fits shown.

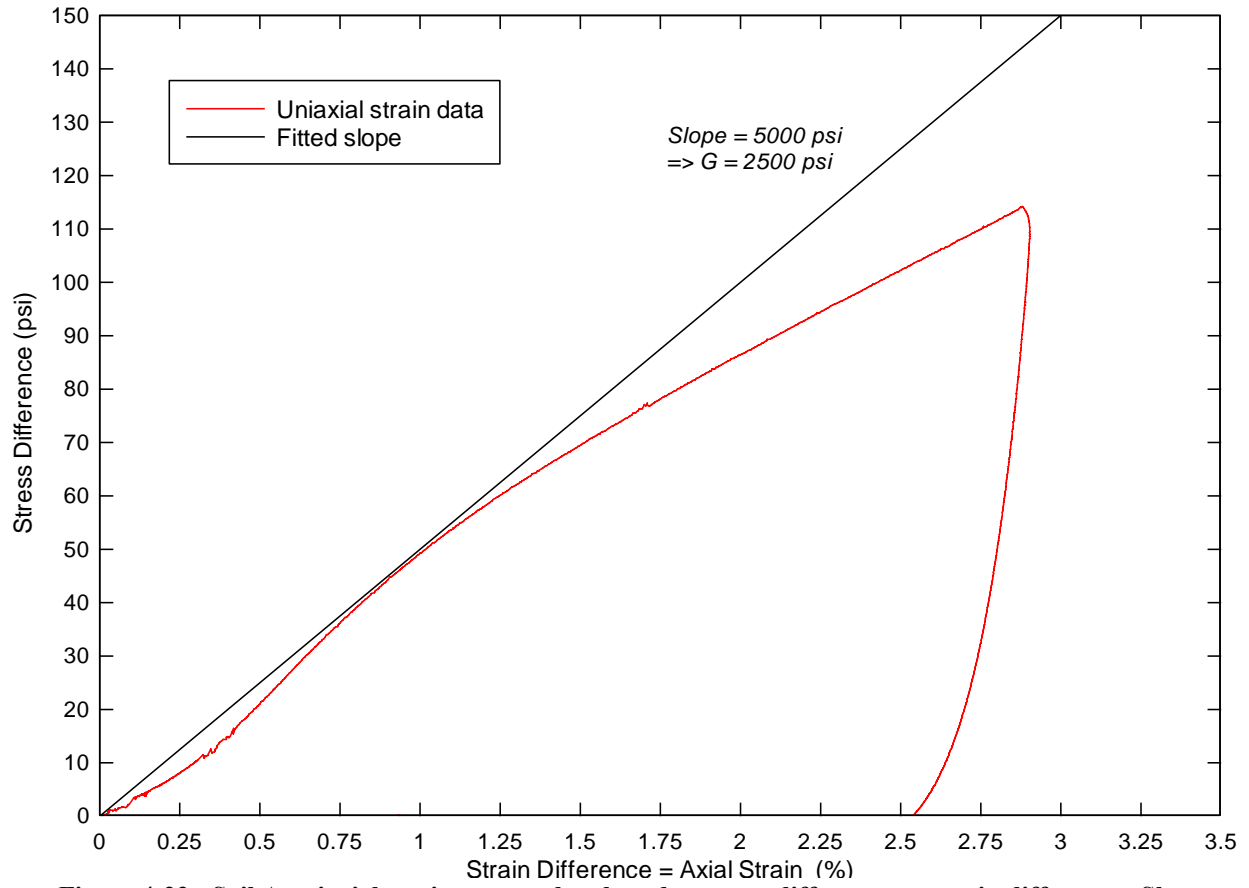


Figure 4-22: Soil A uniaxial strain test results plotted as stress difference vs. strain difference. Shear modulus G fit shown.

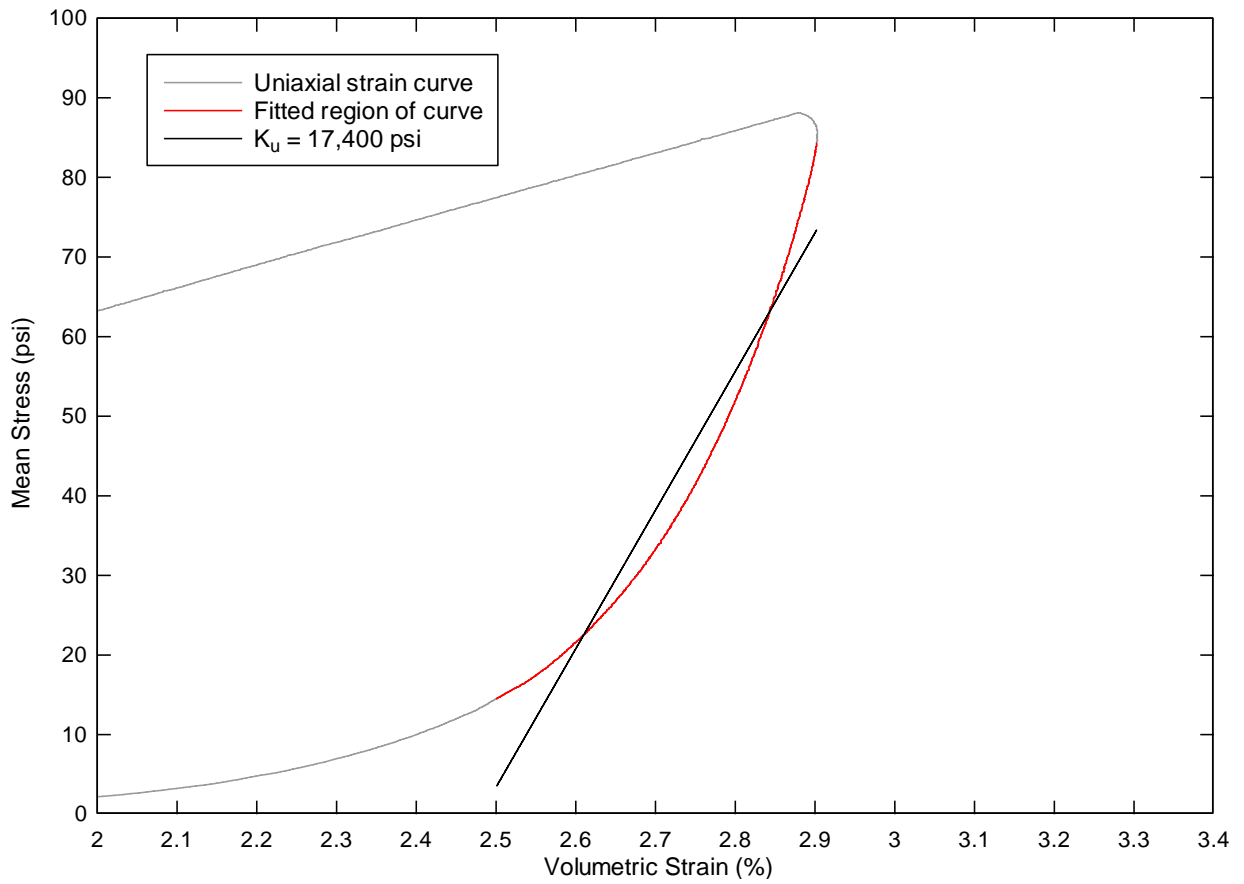


Figure 4-23: Soil A uniaxial strain unloading portion. Determination of bulk unloading modulus K_u (BULK) by linear fit.

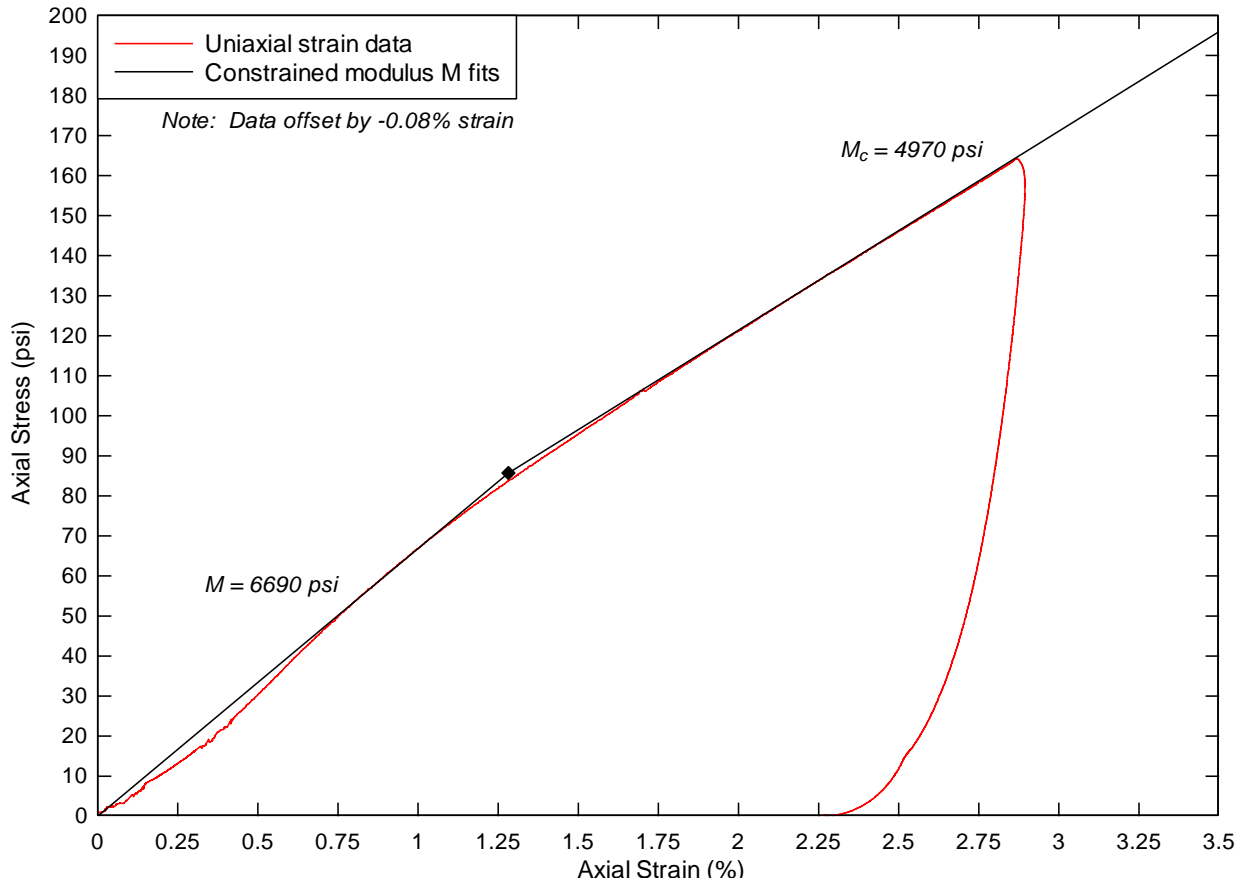


Figure 4-24: Soil A uniaxial strain test results plotted as stress vs. axial strain. Constrained modulus M fit to stress-strain slopes.

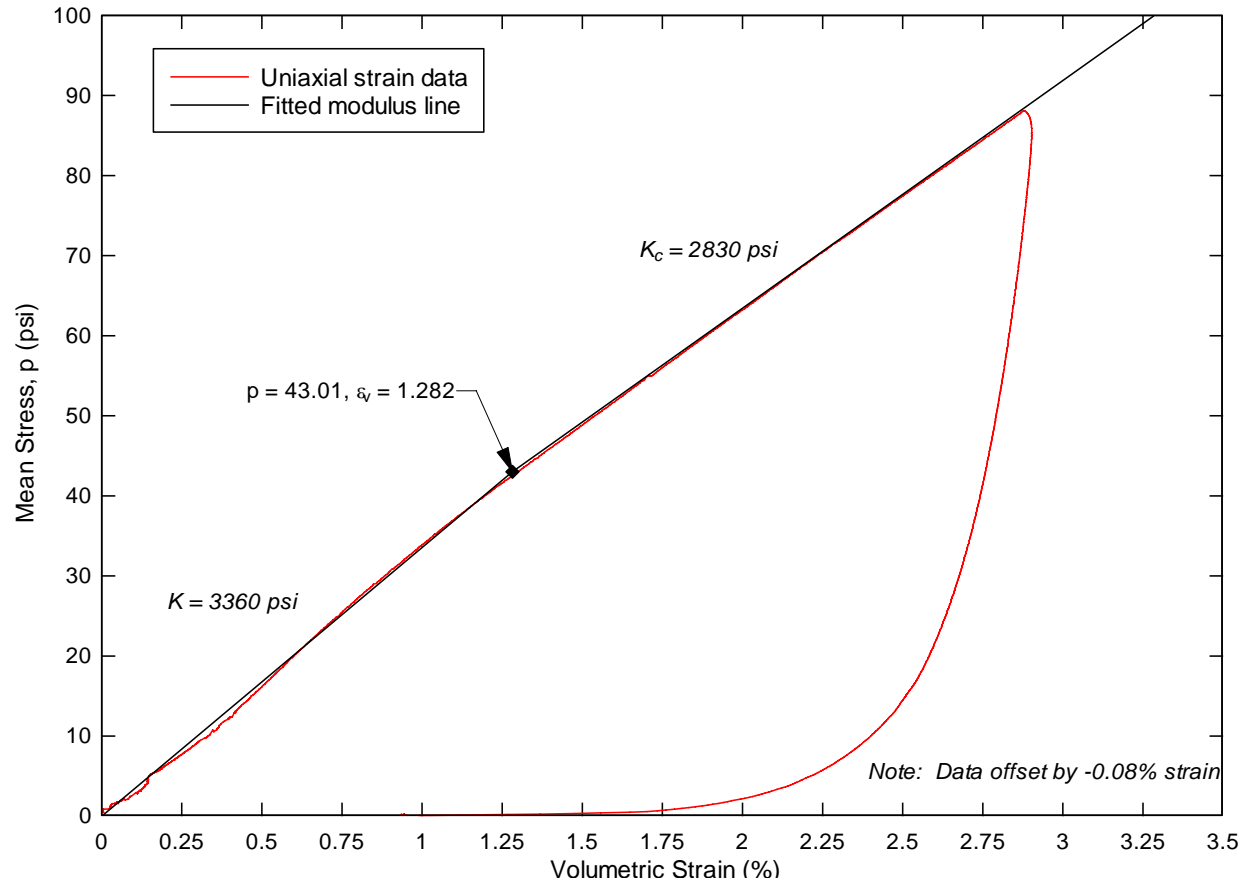


Figure 4-25: Soil A uniaxial strain results plotted as mean stress vs. volume strain. Determination of bulk modulus K shown as linear fit.

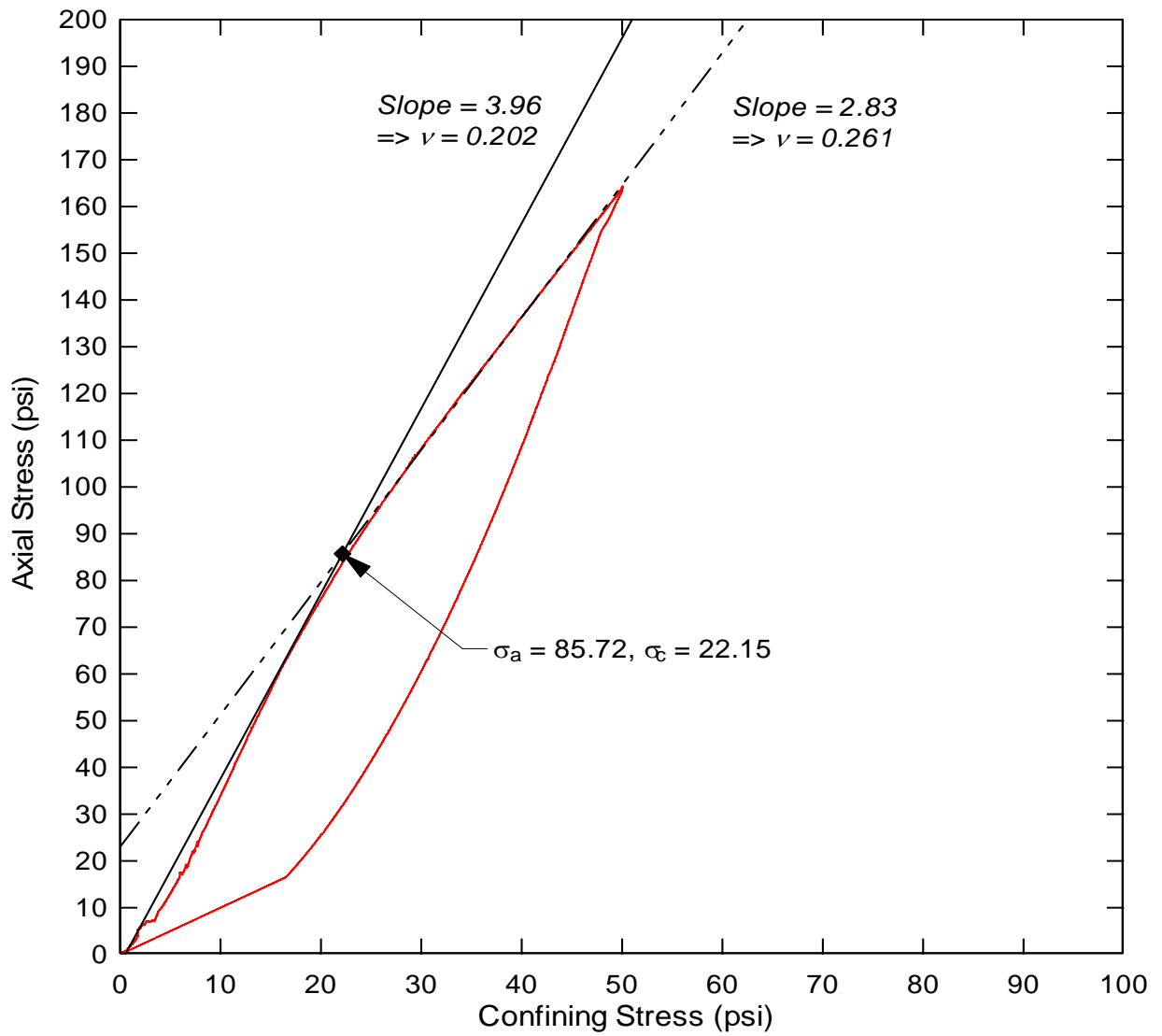


Figure 4-26: Soil A uniaxial strain test. Determination of Poisson's ratio.

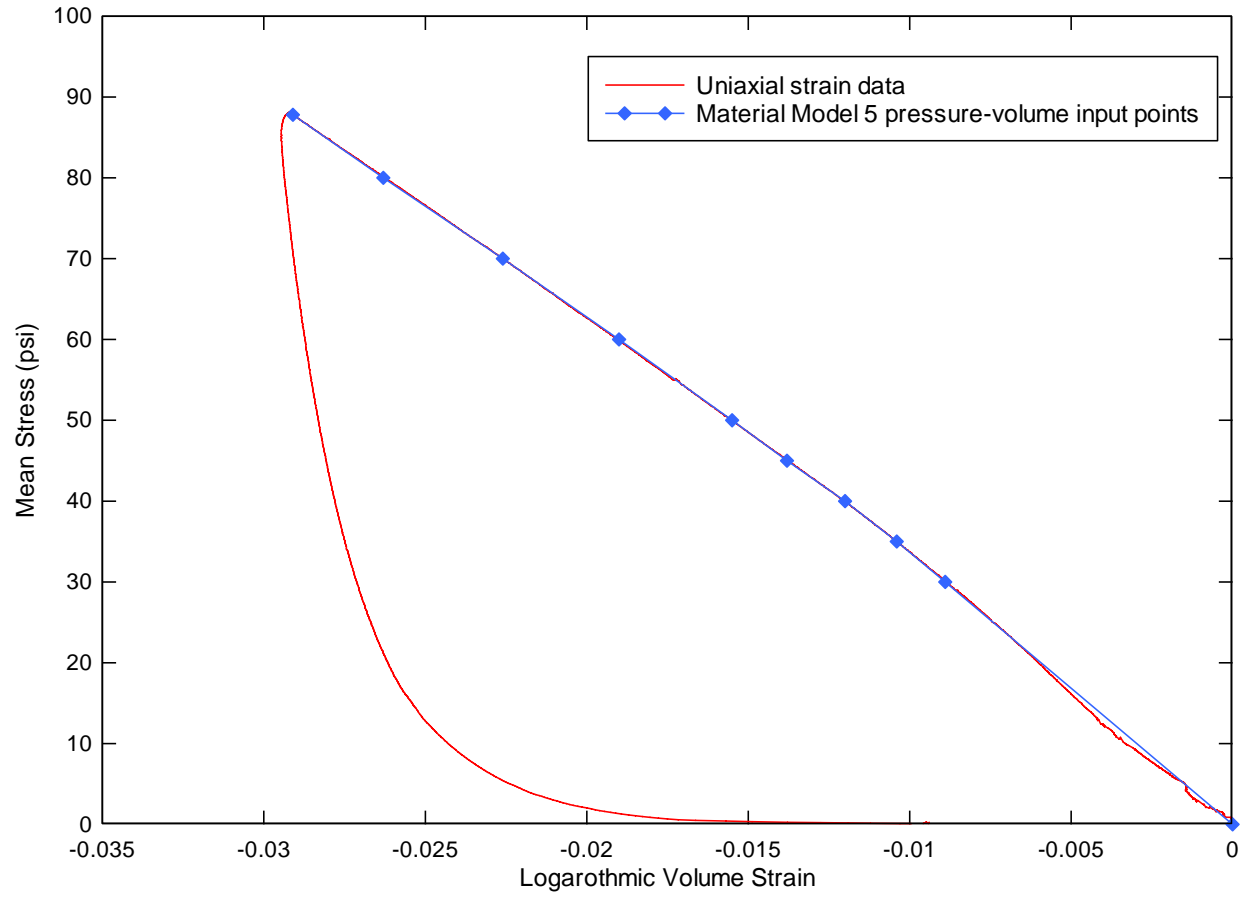


Figure 4-27: Soil A Material Model 5 pressure-logarithmic volume curve with 10 input points. Obtained from uniaxial strain test.

4.6 LS-DYNA Material Model 5 inputs

The recommended set of inputs for modeling Soil A in LS-DYNA Material Model 5: Soil and Foam is shown in the table below. It is assembled from field wet density, triaxial compression, hydrostatic compression, and uniaxial strain test data.

Table 4-7: Material Model 5 inputs for Soil A

	<u>Input</u>	<u>Value</u>	<u>Units</u>			
Mass density	RO	0.000136	lb s ² /in ⁴			
Shear modulus	G	2500	psi			
Bulk unloading modulus	K	17400	psi			
Yield surface coefficient	A0	77.520	psi ²			
Yield surface coefficient	A1	15.26	psi			
Yield surface coefficient	A2	0.751	-			
Pressure cutoff	PC	-2	psi			
	<u>Input</u>	<u>Value</u>	<u>Input</u>	<u>Value</u>	<u>Units</u>	
Pressure-volume point	EPS1	0.0000	P1	0	psi	
Pressure-volume point	EPS2	-0.0089	P2	30	psi	
Pressure-volume point	EPS3	-0.0104	P3	35	psi	
Pressure-volume point	EPS4	-0.0120	P4	40	psi	
Pressure-volume point	EPS5	-0.0138	P5	45	psi	
Pressure-volume point	EPS6	-0.0155	P6	50	psi	
Pressure-volume point	EPS7	-0.0190	P7	60	psi	
Pressure-volume point	EPS8	-0.0226	P8	70	psi	
Pressure-volume point	EPS9	-0.0263	P9	80	psi	
Pressure-volume point	EPS10	-0.0291	P10	87.8	psi	

Table 4-8: Summary of elastic constants

Young's Modulus E	6010	psi
Poisson's Ratio v	0.202	
Shear Modulus G	2500	psi
Bulk Modulus K	3360	psi
Constrained Modulus M	6690	psi

4.7 Recommended range of model application

The Soil A material model is only recommended for use simulating the dry season at Cuddeback Lake. Soil A is expected to produce higher peak accelerations during impacts than other, softer soil models. Soil A can also be used to estimate relatively hard soils.

4.8 Recommended surrogate soil composition

It is possible to estimate the field soil behavior in landing experiments by using a surrogate soil. For full scale landing drops, if the composition and mechanical behavior of surrogate soil is similar to the field soil, a significant savings can be obtained by performing the tests on a surrogate soil. Full scale drops in the field and transporting a large quantity of the field soil to the experiment facility can be expensive alternatives.

Determining a surrogate soil depends on several factors. One very important matching parameter is the grain size distribution. Soils with the same distribution tend to behave in similar ways. They are similar because much of the global soil behavior is governed by the nature of the grain-to-grain contacts. Another parameter important to match is water content. For clay soils such as Carson Sink and Cuddeback, ensuring similar water content is key because clay strength is very sensitive to water content, especially at higher levels. Matching the grain density is desirable for reconstituting the same wet density with equal void space. Soil A's wet density averaged 48% void space. If Soil A's grains were less dense ($< 2.76 \text{ g/cm}_3$), the volume of voids would be less. The Atterberg limits test provides a method of comparing a surrogate soil's plasticity to the field soil. A clay with similar Atterberg limits should be used as a surrogate.

In addition to matching physical properties, surrogate soil composition should be calibrated by laboratory testing to compare to the field soil. Very general soil behavior can usually be mimicked by matching grain size distribution and clay/sand/silt contents, but specific behavior requires trial-and-error compositions tested until strength and deformation behavior is similar to the field soil. Even then, an exact match is not likely to be found due to the inherent variability of soils. The best one can hope for is similar behavior across a window of interest.

The surrogate soil recommendation presented here is a first-order engineering estimate based on physical properties. Determining a high fidelity surrogate soil through laboratory testing was beyond the scope of this project. Wet sieve analysis revealed a 95% fines content as the recommended surrogate soil composition for Soil A. These fines are mostly clay with lesser silt. A 60% clay, 35% silt, and 5% sand mixture is a recommending starting point.

5 Cuddeback Soil B

The general description, field observations, test data, and Material Model 5 inputs for Cuddeback Soil B is discussed in this chapter. Cuddeback Soil B comprises the soft shoreline soils that surround Soil A. It is the polar opposite of Soil A in terms of softness. Soil B is a dry soil model. A wet version of the Soil B model was not within the two-model scope of the current effort.

5.1 Location

Soil B surrounds the northern half of the Soil A area, and can be up to one km wide. Figure 4-2 illustrates the lading zone coverage of Soil B. It represents the second most likely soil to be encountered upon landing based on distance from the desired landing point in the center of zone.

5.2 General description

Soil B was the softest soil observed at Cuddeback Lake. The soil is deposited by particle precipitation just before entering the lakebed (Soil A), and by wind. The combined methods of deposition add very little compactive effort to the soil. As a result, the soil is very loose when the surface is broken. Soil B is not as flat as Soil A. Slight surface undulations were observed. Some stream beds cut into the soil, but were no deeper than a few inches than the adjacent surface soil. Soil B's surface is dotted with small vegetation, characterized as desert sage brush or similar bristly plants. The eastern side of Soil B contains many acres of rocks on the surface. This "rock garden" is shown in Figure 5-1, with rocks up to 8 inches in diameter.



Figure 5-1: Surface rock deposits on Soil B in the eastern shore.

Soil B is mostly free of man-made objects. The only significant obstacles were cattle fences and gate crossings on the eastern side.

Soil B has more void space than Soil A, and the void spaces are much more easily collapsible. Soil B is so soft that SUV tires caused significant depressions of 1-3 inches beyond the surface. Walking on Soil B gives the impression of walking on stiff snow, as shown in Figure 5-2 (d). It is comprised of very fine silts, shown close up in Figure 5-2 (b). In some areas Soil B's surface was coated with a thin layer of pebbles, shown in Figure 5-2 (c). In Figure 5-2 (a), an example

of the small vegetation is shown. Small mounds, accumulated by wind, surround these small bushes, and a ¼-½ inch weakly cemented surface covers the entirety of Soil B. Upon breaking the surface, Soil B exhibited very low densities, confirmed by nuclear density testing.

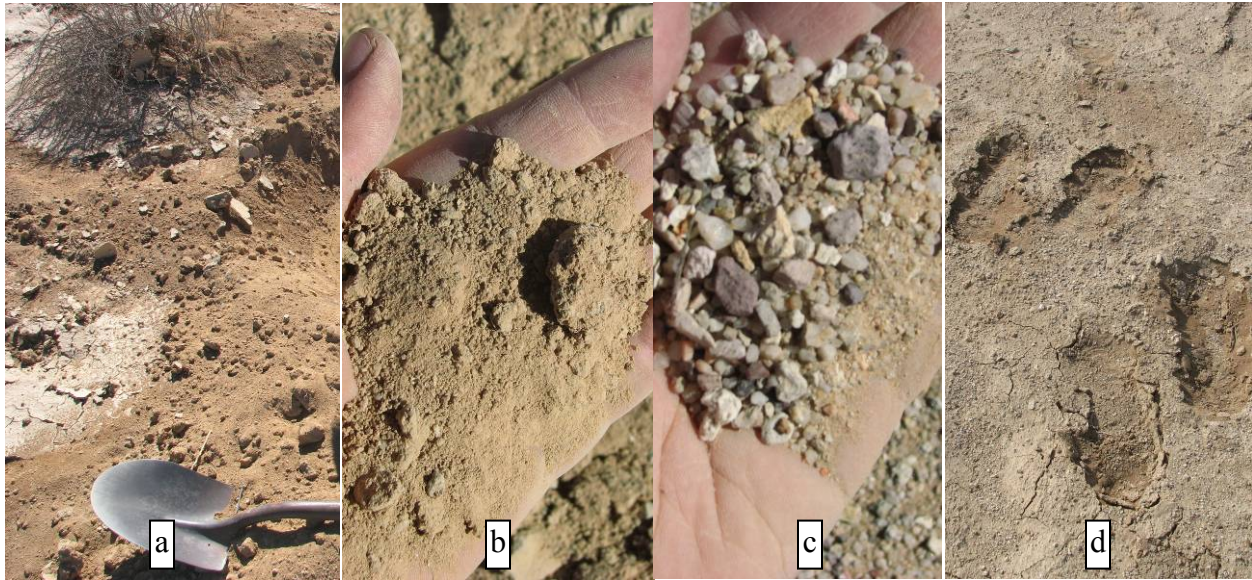


Figure 5-2: (a) Soil B excavation reveals powdery fine grains (reddish brown) underneath the cemented surface (tan). (b) Close-up of Soil B grains. (c) Close –up of small pebbles coating Soil B’s surface on the western shore. (d) ~1 inch footprint depressions of 190-lb man, size 13 shoe in Soil B.

Soil B’s ability to highly compress is due to the less cohesive, more granular nature of silt when it is very dry. Unlike Soil A, there is not enough clay content to create cohesion in dry conditions. In the lack of moisture, there is little cohesive force to resist shear stress, and the low density soil responds by compressing to a stronger density to support load.

5.2.1 Soil classification

Soil B is classified as ML in the Unified Soil Classification System, a primarily silt soil with some clay. The surface coatings of rocks are not included in this classification because they weren’t present in the subsurface composition of Soil B.

5.3 Selection of Soil B

Soil B was selected because it was the most compressible soil on the site. One of the perceived risks of the CEV landing is excessive deformation of the soil leading to tipping of the capsule during landing. Designed horizontal landing speeds of up to 27 mph and vertical speeds of 17 mph lead to concerns regarding highly deformable soil effects. If the soil compresses too much upon impact, the capsule's airbags may plow the soil in front and eventually tip over, harming the astronauts. Soils C, D, E, F, and G were not as soft as Soil B, and presented less of an overturning risk. During the field visit, the NASA Program Manager conducted an airbag drag test to measure frictional resistance. Figure 5-3 illustrates soil deforming 1-3 inches as an airbag was dragged across the surface of Soil B. Approximately 280 lbs of sand was loaded on the airbag. The resulting deformation caused a small amount of plowing in front of the bag. This data can be obtained from Dr. Buehrle, and video is available on DVD.



Figure 5-3: ~280 lb loaded airbag drag causes some plowing

illustrates soil deforming 1-3 inches as an airbag was dragged across the surface of Soil B. Approximately 280 lbs of sand was loaded on the airbag. The resulting deformation caused a small amount of plowing in front of the bag. This data can be obtained from Dr. Buehrle, and video is available on DVD.

5.4 Field observations

This section deals with sample collection and field testing.

5.4.1 Sampling and sample sites

Soil B is essentially silty soil along the shoreline. It was rather consistent across the western, northern, and eastern sides. It was relatively dry and soft and was found in a slightly undulated surface sometimes topped with sand and gravel. The sand and gravel was very thin and sometimes non-existent. The soil sampled here was described as only having rare gravel content and behavior can be modeled as silty soil without any gravel. When Soil B was sampled, the surface rocks and sand were excluded.

Four sample sites were chosen to represent Soil B (see Figure 4-11). Two sources were near the access road in the west, the second came from the northern shore, and the third came from the near the rocky deposits in the east. The northern sample was in close proximity to dunes. The third sample site was in close proximity to the rocky areas, but no rocks were present at the sample site.

5.4.2 Nuclear density and moisture data

The nuclear density and moisture data for Soil B, as well as the descriptive statistics and probability distributions, are shown on the following pages.

Table 5-1: Wet density (lbs/ft³) descriptive statistics by depth in Soil B.

Depth (in)	N	Mean	SE Mean	StDev	Minimum	Q1	Median	Q3	Maximum
0-6	15	82.77	2.7	10.45	68	71.8	84.6	91.6	99.7
6-12	16	97.42	1.73	6.94	84.5	93.73	98.3	102.13	109
12-24	4	102.83	0.427	0.854	101.6	101.93	103.1	103.45	103.5

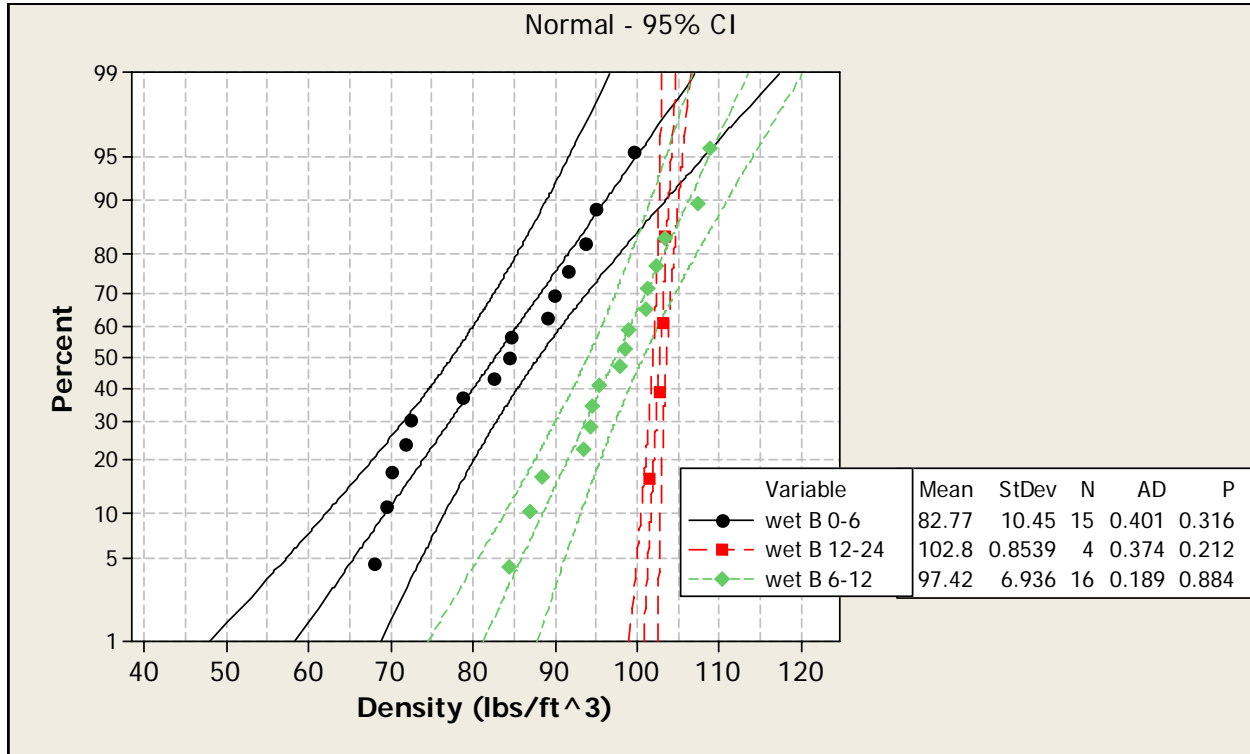


Figure 5-4: Probability plot of Soil B's wet densities (lbs/ft³) by depth range (in).

Soil B starts with a very low wet density on the surface, and rapidly increases with depth. The density variability on the surface is also fairly wide, with a standard deviation of 10.5 lbs/ft³. As one goes deeper into Soil B, the density approaches 100 lbs/ft³ beyond 12 inches. This increased density is indicative of Soil B's tendency to compress to sustain load. The 0-6 inch depth range density averaged 82 lbs/ft³. This was the target density for reconstituting laboratory specimens for testing, and is much lower than the 6-12 inch depth range of 97 lbs/ft³. The lower density was chosen because the Soil B model emphasizes the soft soil behavior.

Table 5-2: Water content (%) descriptive statistics by depth in Soil B.

Depth (in)	N	Mean	SE Mean	StDev	Minimum	Q1	Median	Q3	Maximum
0-6	15	1.783	0.211	0.818	0.61	1.37	1.73	2.17	4.07
6-12	16	6.362	0.551	2.205	2.81	4.218	7.055	8.098	10.26
12-24	4	9.24	1.36	2.73	6.5	6.7	9.33	11.69	11.8

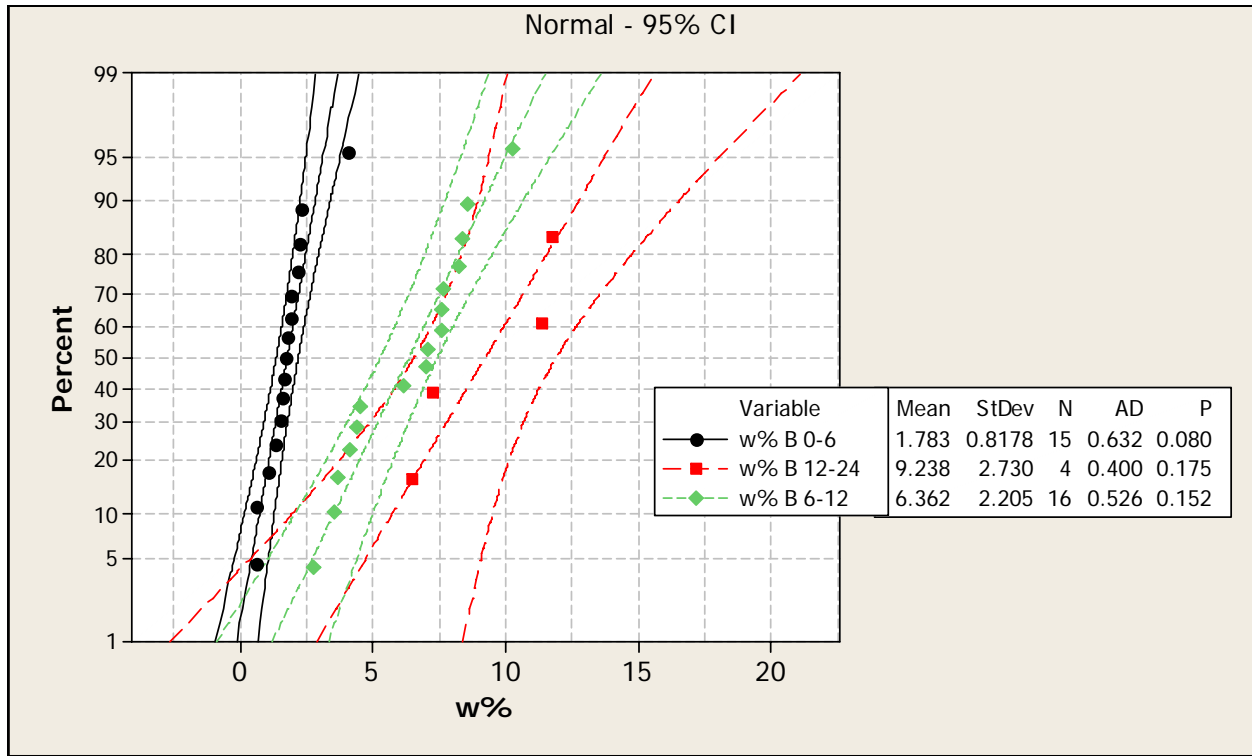


Figure 5-5: Probability plot of Soil B's field measured water contents (%) by depth range (in).

Soil B's surface was extremely dry with no exceptions. Laboratory samples combined the 0-6 and 6-12 inch samples to construct 8 inch tall specimens. The mixing increased the specimen moisture content to roughly 5%.

Table 5-3: Dry density (lbs/ft³) descriptive statistics by depth in Soil B.

Depth (in)	N	Mean	SE Mean	StDev	Minimum	Q1	Median	Q3	Maximum
0-6	15	81.3	2.6	10.05	66.7	70.8	83	89.5	98
6-12	16	92.08	1.41	5.63	84.1	87.35	91.65	95.45	104.4
12-24	4	94.18	1.48	2.97	91.2	91.43	94.15	96.95	97.2

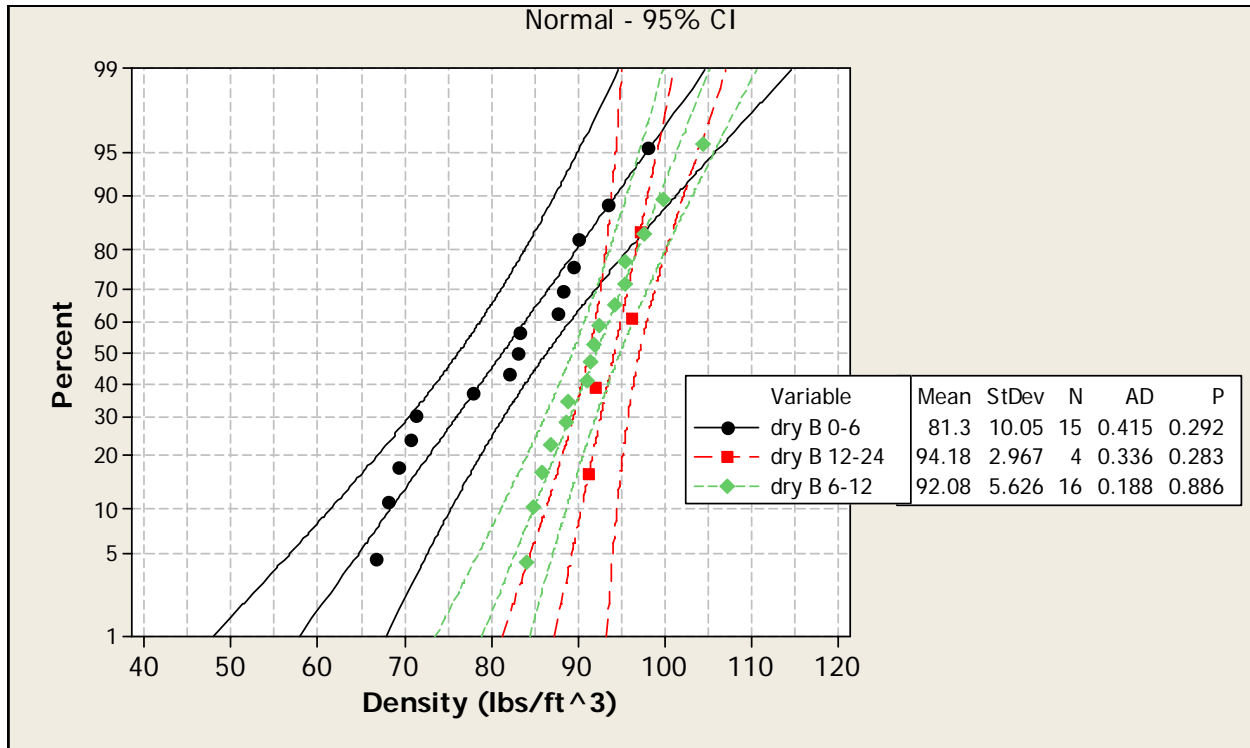


Figure 5-6: Probability plot of Soil B's dry densities (lbs/ft³) by depth range (in).

Taking the dry density as 81 lbs/ft³ (1.30 g/cm³) with a grain density of 2.78 g/cm³, the porosity n equals 53% using Equation 4-2. This porosity is 5% higher than Soil A, as expected for a looser soil. The measured porosity means 53% of the bulk volume of Soil B is comprised of void space, which leads to large deformations when combined with low shear strength.

5.5 Laboratory test data

Laboratory tests conducted on Soil B are presented in this section. The test log summarizes the tests using the triaxial apparatus.

Table 5-4: Test log for Cuddeback Soil B

Test ID	Sample ID	Type	Confining Pressure (psi)	Moisture content	Dry Density (lbs/ft ³)	Grain Density G _s (g/cm ³)	Porosity <i>n</i>
J3B08	CDS-17	Triax	2	4.31%	78.35	2.78	54.9%
D21D07	CDS-1	Triax	5	4.87%	77.24	2.78	55.5%
D19D07	CDS-11	Triax	10	3.15%	87.25	2.78	49.7%
J31B08	CDS-1,2	Triax	20	NA	NA	2.78	NA
J30B08	CDS-7,8	Triax	50	6.65%	76.55	2.78	55.9%
J22A08	CDS 9-12	Uniax	50	3.55%	78.22	2.78	54.9%
J22A08	CDS 9-12	Hydrostat	50	3.55%	78.22	2.78	54.9%

5.5.1 Moisture content

After testing specimens in the triaxial apparatus, pieces of the specimen were taken for moisture content testing. The samples were weighed, broken up to maximize surface area, and placed in a dish for overnight oven drying. The samples were weighed again to measure water loss. The water contents were computed as shown in 3.1.3. Fourteen tests were performed. Laboratory moisture contents on Soil B averaged 5%.

5.5.2 Grain density and grain size analysis

The grain density of Soil B was determined to be 2.78 g/cm³ by pycnometer. Figure 5-7 displays the dry sieve results for Soil B. As discussed in 3.1.2, there are two forms of sieve analysis. We believe the dry sieve analysis is misleading because the percent passing the #200 sieve is too low for the soil we were working with. We believe that many particles remained cemented together after being dried, and the dry sieve results are skewed toward the coarser side. A wet sieve analysis was run, and revealed much higher fines content.

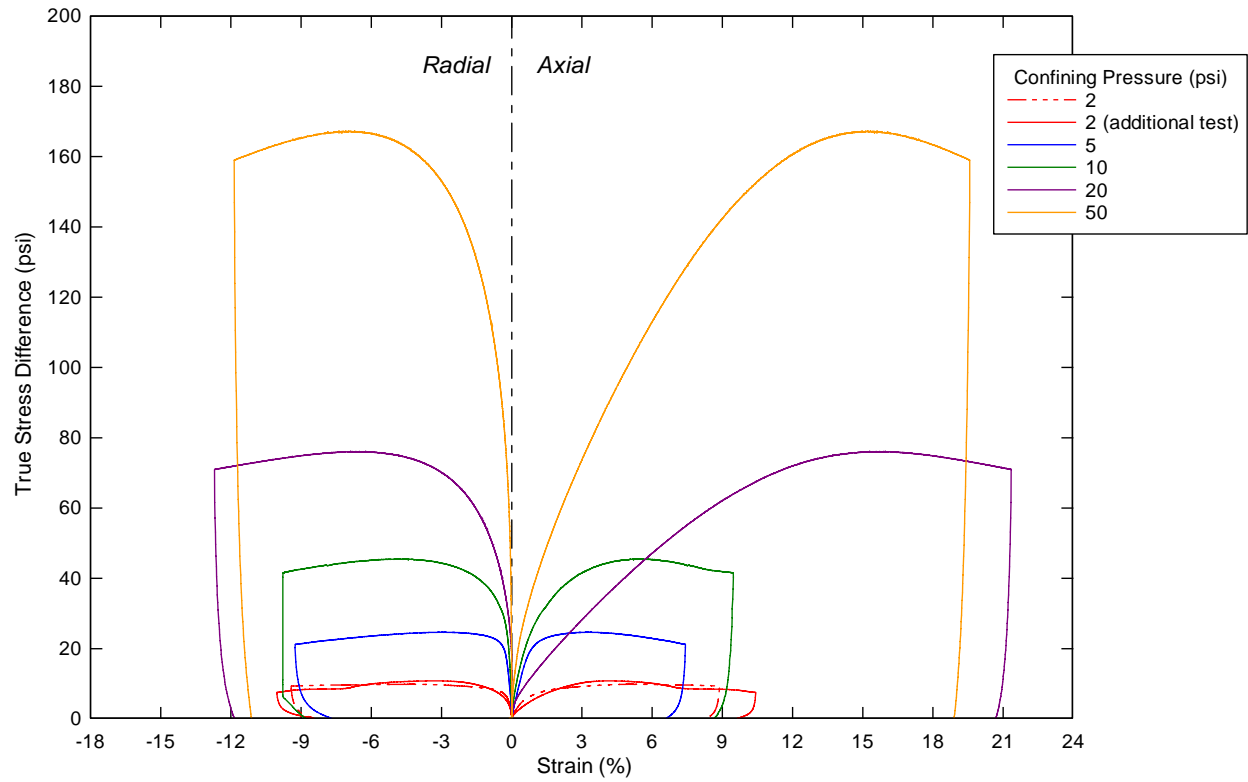


Figure 5-8: Soil B triaxial test results.

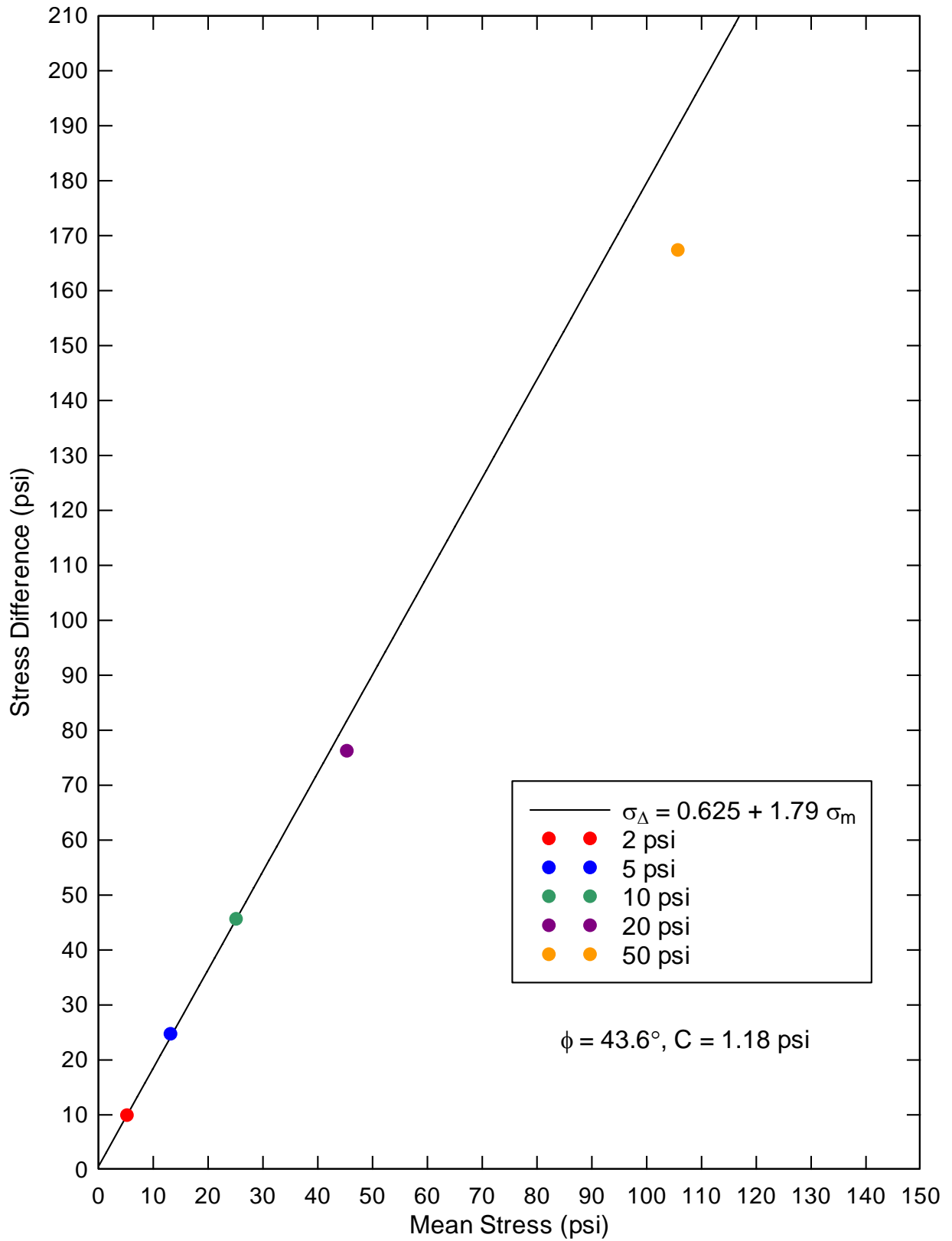


Figure 5-9: Soil B's strength envelope from triaxial data.

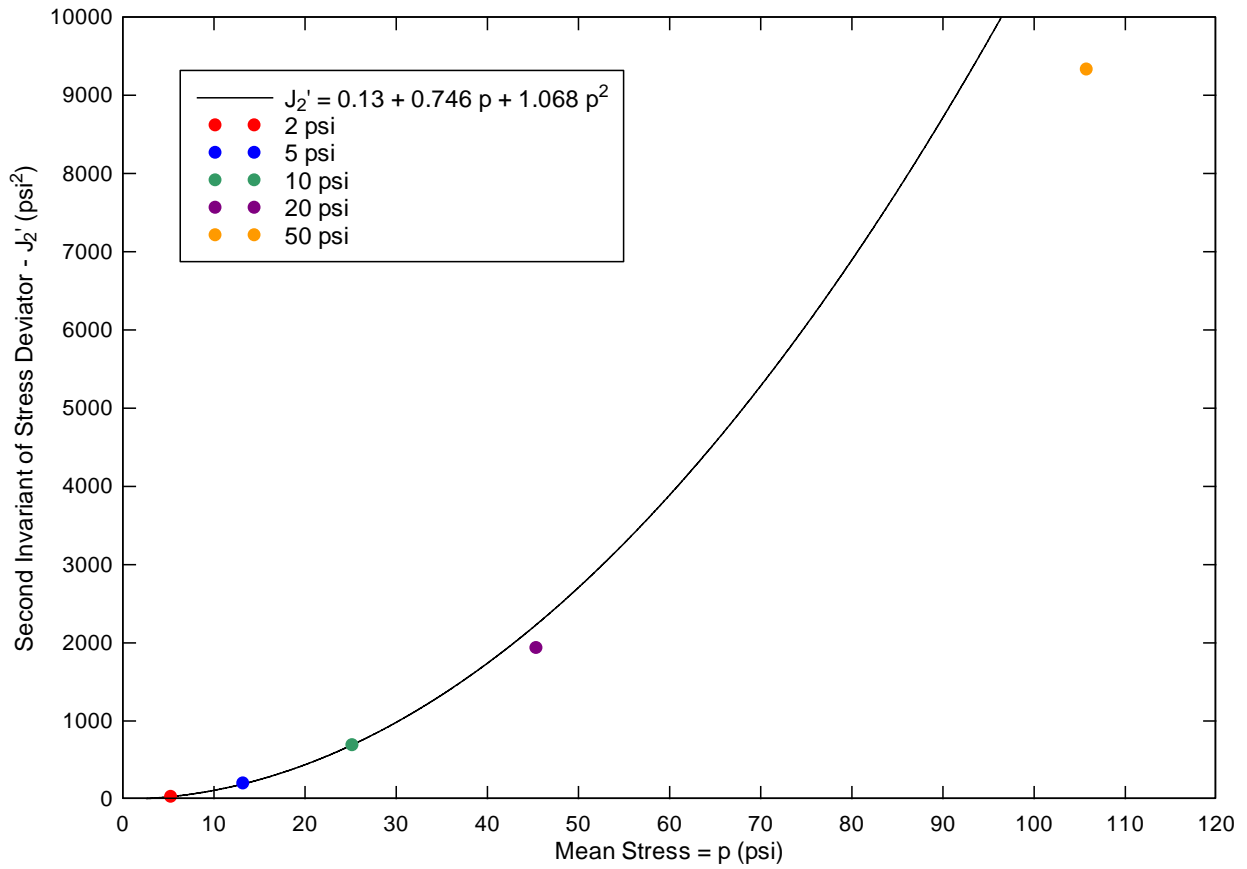


Figure 5-10: Soil B Material Model 5 yield surface fit from triaxial test data.

5.5.4 Hydrostatic compression

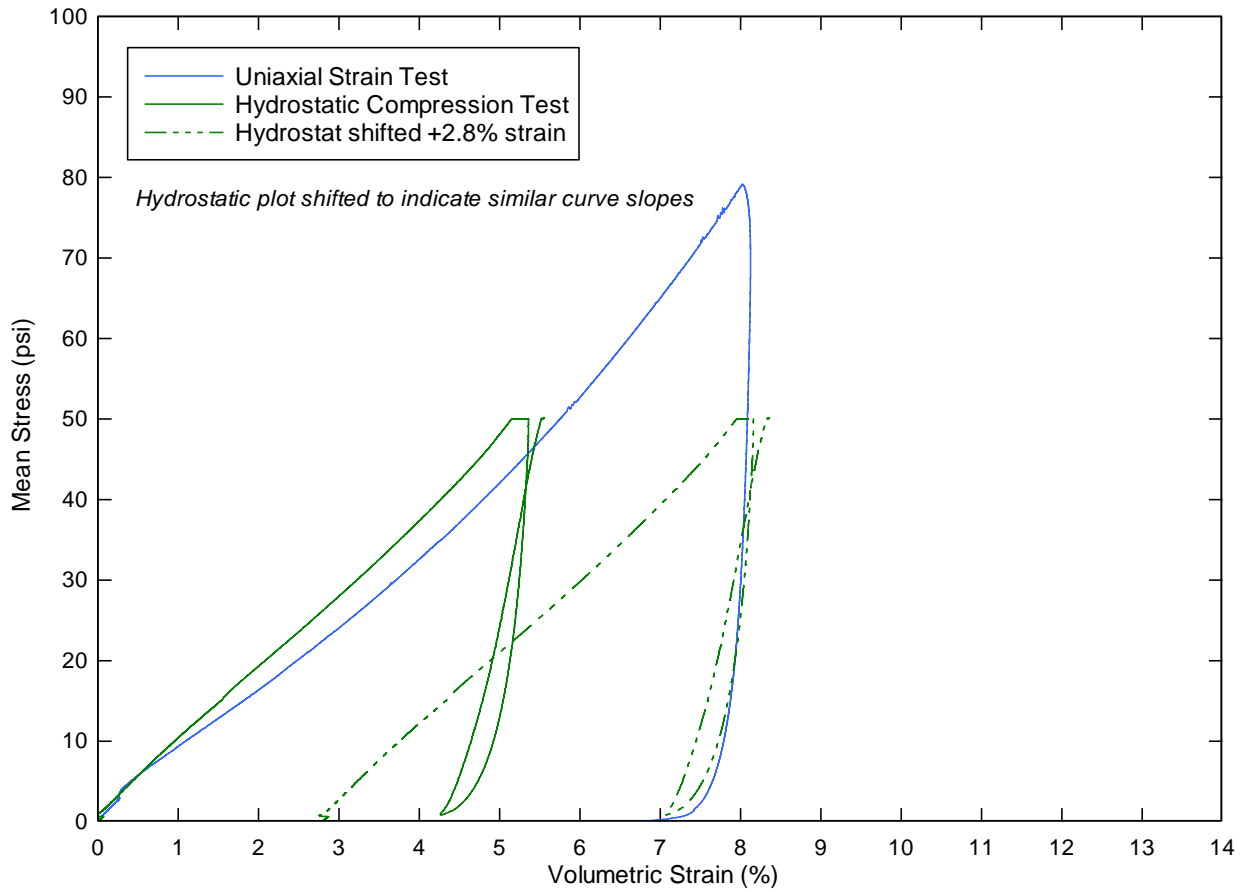


Figure 5-11: Soil B hydrostatic compression test. Soil B uniaxial strain data shown for comparison. Bulk unloading modulus is obtained from the unloading portion of the test.

5.5.5 Uniaxial strain

The uniaxial strain data for Soil B is shown on the next few pages.

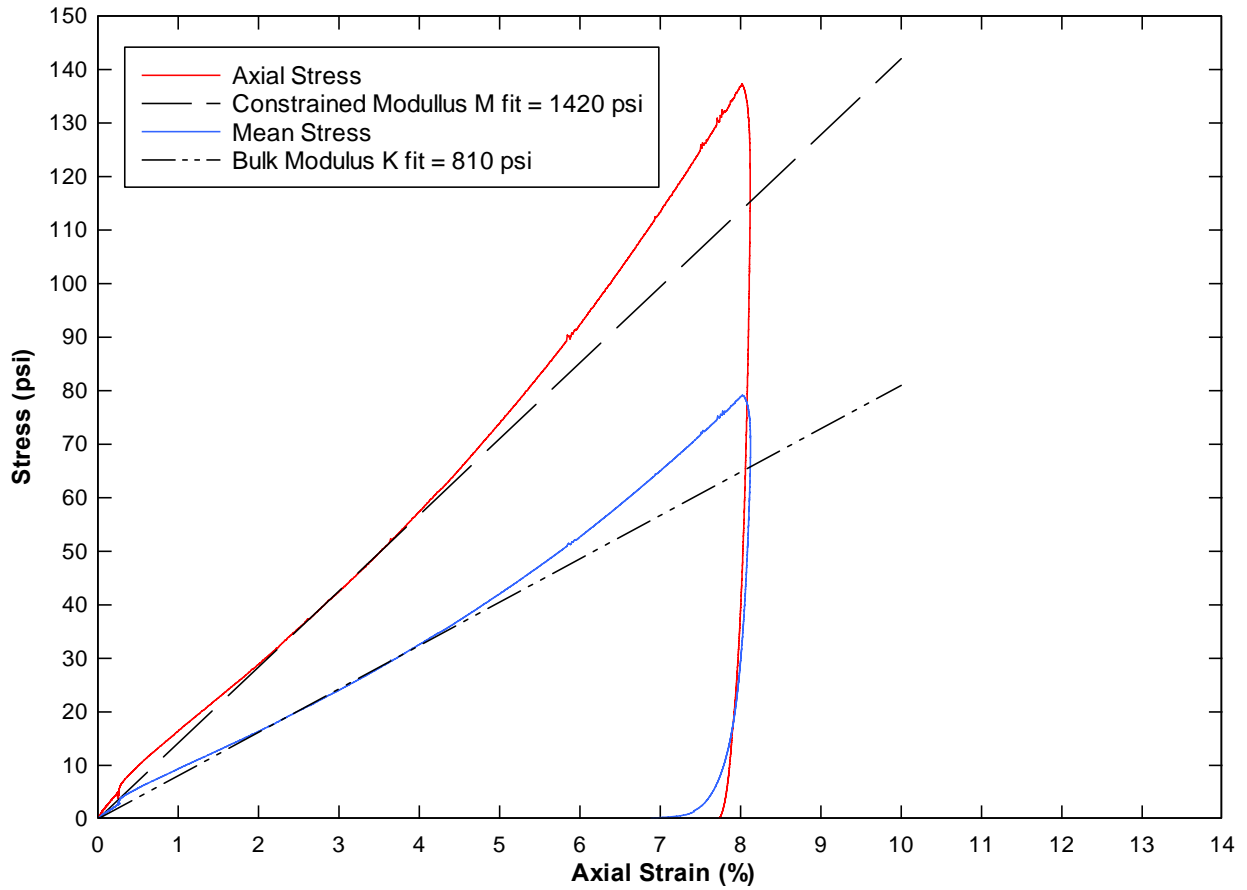


Figure 5-12: Soil B uniaxial strain test with constrained modulus M and bulk loading modulus K fitted.

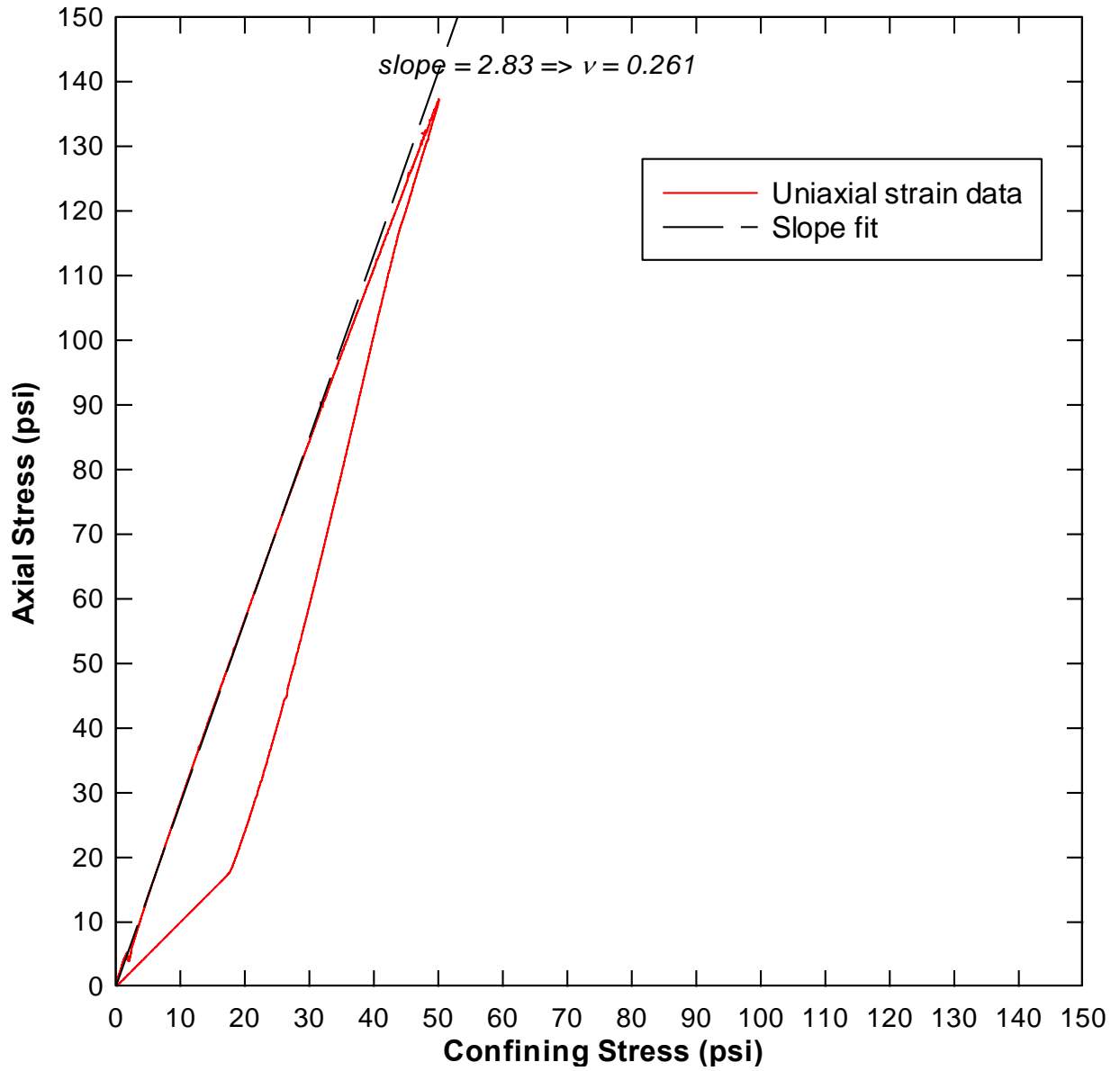


Figure 5-13: Soil B uniaxial strain test with Poisson's ratio calculated from confining pressure vs. axial stress slope.

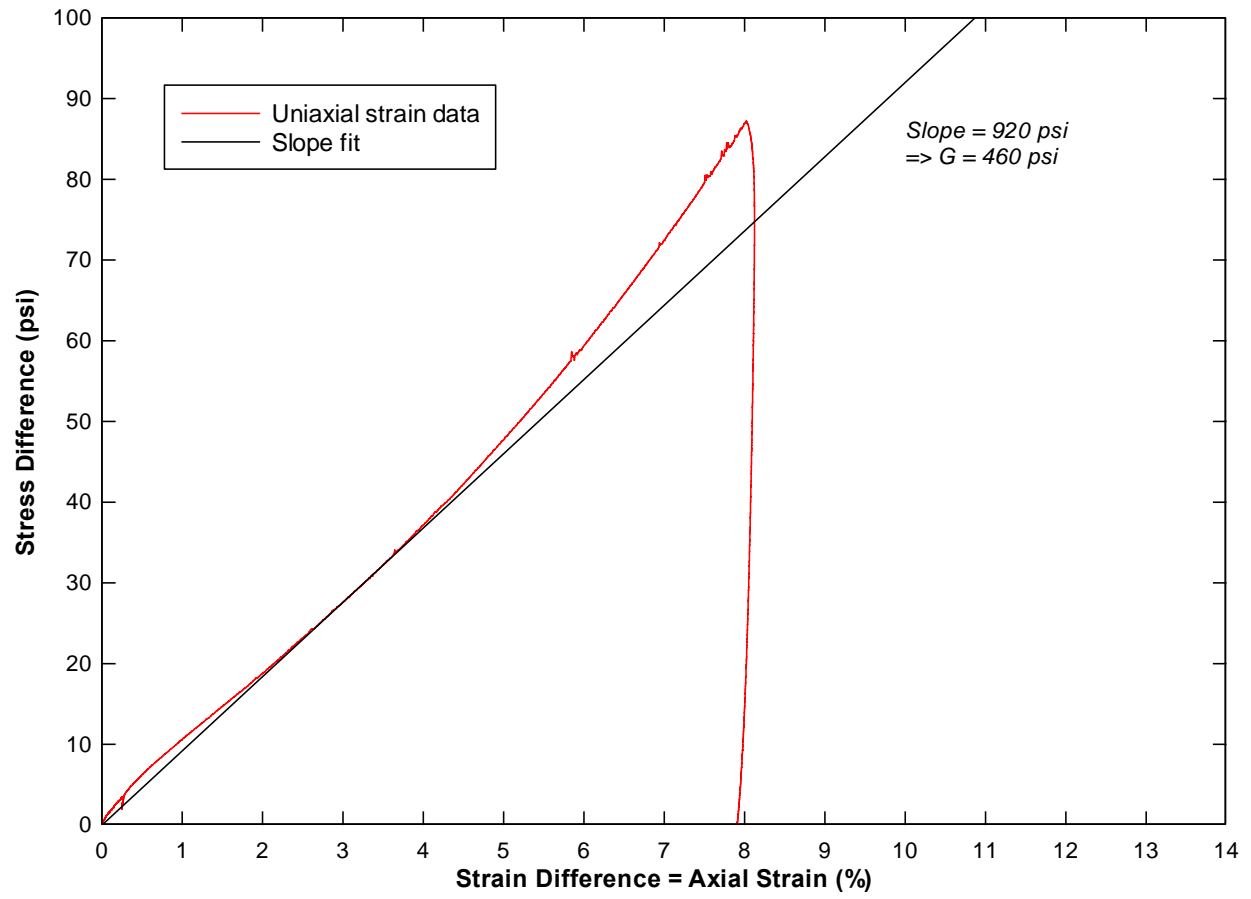


Figure 5-14: Soil B uniaxial strain test with shear modulus G calculated from shear strain slope.

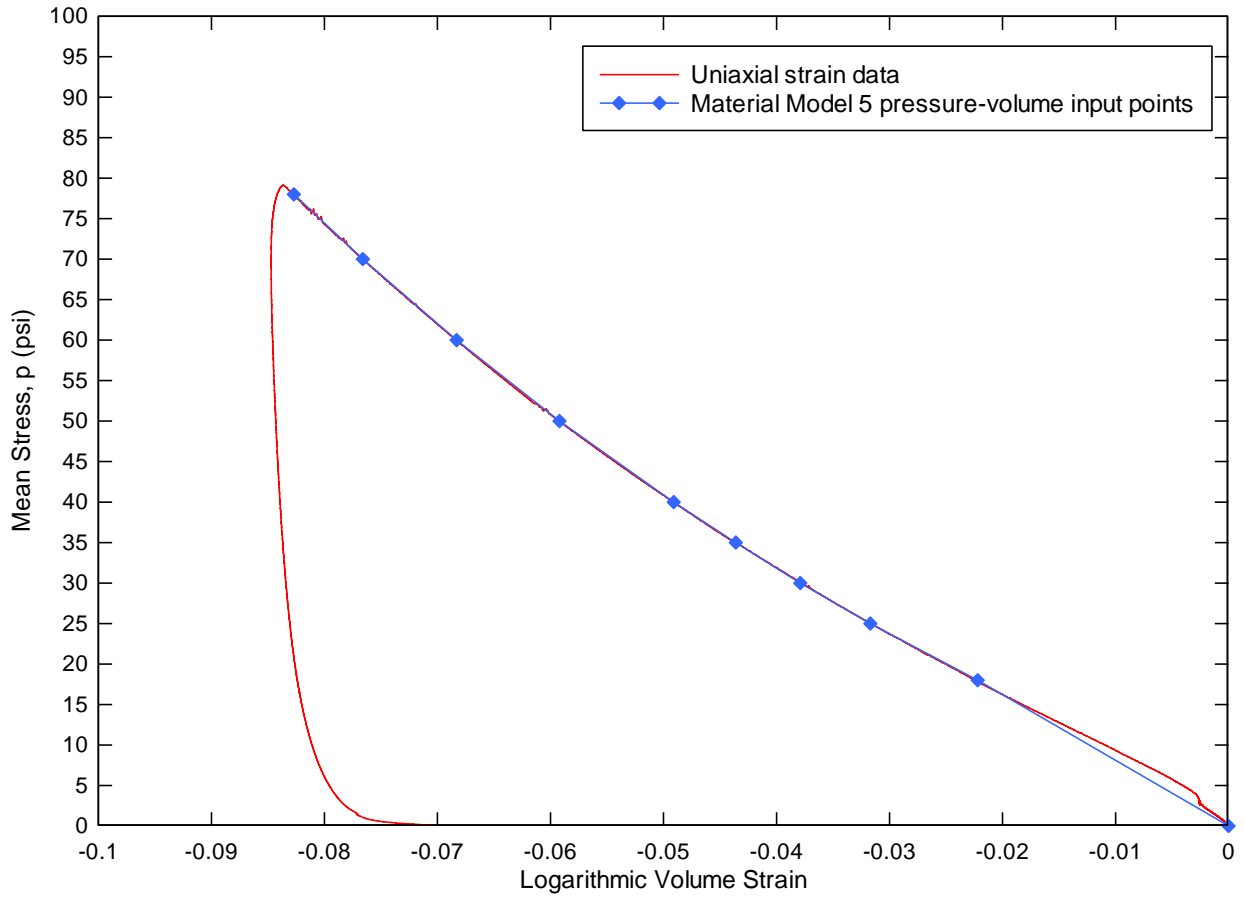


Figure 5-15: Soil B Material Model 5 pressure-logarithmic volume curve with 10 input points shown. Obtained from uniaxial strain test.

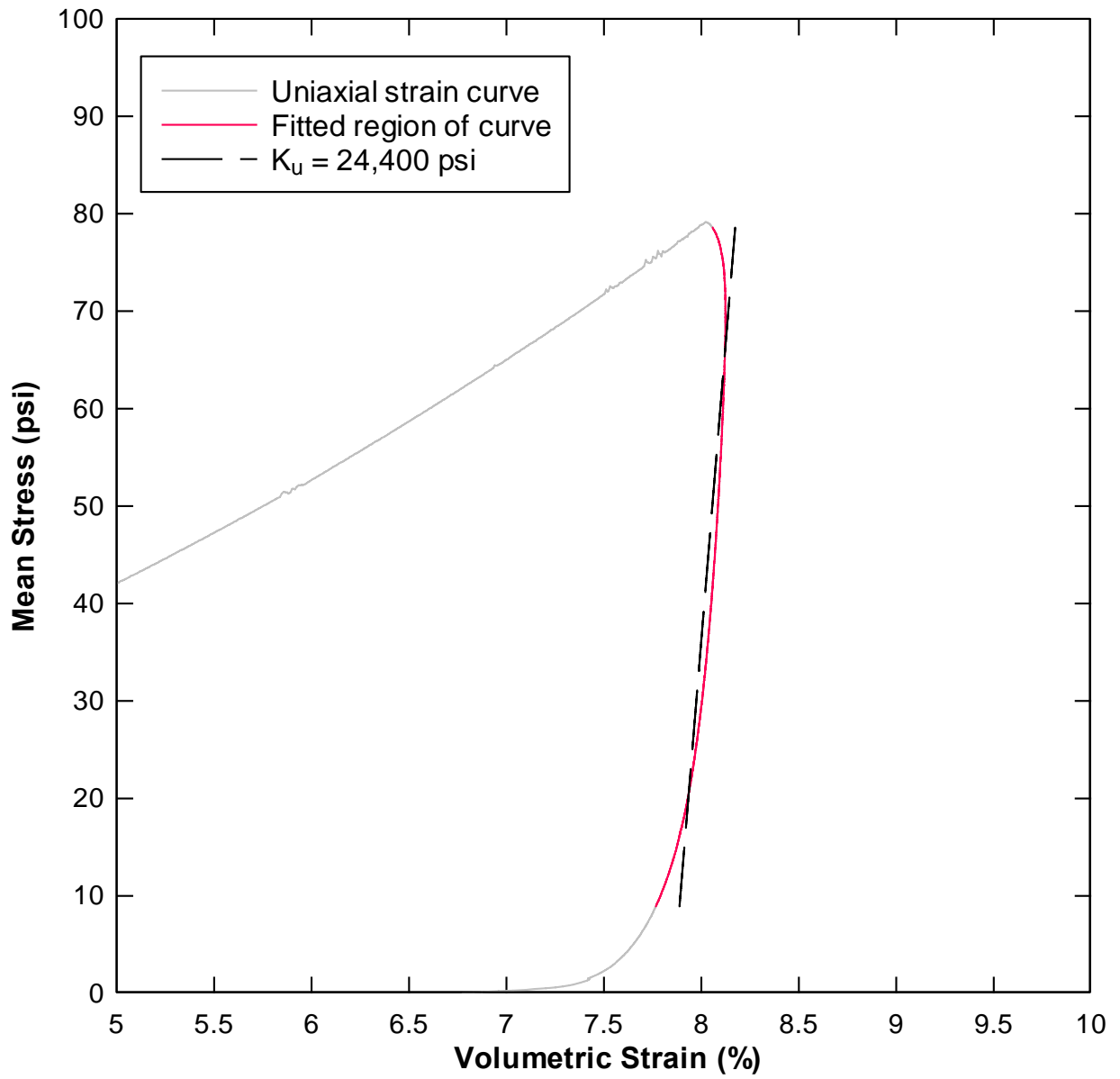


Figure 5-16: Soil B uniaxial strain test with bulk unloading modulus calculated from unloading portion of test

5.6 LS-DYNA Material Model 5 inputs

The recommended set of inputs for modeling Cuddeback Soil B in LS-DYNA Material Model 5: Soil and Foam is shown in the table below. It is assembled from field wet density, triaxial compression, hydrostatic compression, and uniaxial strain test data.

Table 5-5: Material Model 5 inputs for Soil B

	<u>Input</u>	<u>Value</u>	<u>Units</u>			
Density	RO	0.000121	lb s ² /in ⁴			
Shear modulus	G	460	psi			
Bulk unloading modulus	K	24400	psi			
Yield surface coefficient	A0	0.130	psi ²			
Yield surface coefficient	A1	0.746	psi			
Yield surface coefficient	A2	1.068	-			
Pressure cutoff	PC	0	psi			
	<u>Input</u>	<u>Value</u>	<u>Input</u>	<u>Value</u>	<u>Units</u>	
Pressure-volume point	EPS1	0.0000	P1	0	psi	
Pressure-volume point	EPS2	-0.0222	P2	18	psi	
Pressure-volume point	EPS3	-0.0317	P3	25	psi	
Pressure-volume point	EPS4	-0.0379	P4	30	psi	
Pressure-volume point	EPS5	-0.0436	P5	35	psi	
Pressure-volume point	EPS6	-0.0491	P6	40	psi	
Pressure-volume point	EPS7	-0.0592	P7	50	psi	
Pressure-volume point	EPS8	-0.0683	P8	60	psi	
Pressure-volume point	EPS9	-0.0766	P9	70	psi	
Pressure-volume point	EPS10	-0.0827	P10	78	psi	

Table 5-6: Summary of elastic constants

Constrained Modulus - M	1420	psi
Poisson's Ratio - v	0.261	
Young's Modulus - E	1160	psi
Bulk Modulus - K	810	psi
Shear Modulus - G	460	psi

5.7 Recommended range of model application

The Cuddeback Soil B model is only recommended for use in modeling dry conditions at Cuddeback Lake. The wet behavior of the soil is expected to be significantly different.

5.8 Recommended surrogate soil composition

The wet sieve analysis revealed a 73% fines content. Fines can be silt or clay. However, field observations revealed a powdery soil rather than cohesive. This leads to a high silt content conclusion. Atterberg limits testing confirmed the silt nature of the soil. The recommended starting point for a surrogate soil is 65% silt, 8% clay, and 27% sand. Surrogate soil determination is an iterative process, and can only reasonably be determined through additional testing on the surrogate soil to check if it matches field soil behavior. Surrogate testing and analysis is beyond the scope of this project.

6 Carson Sink Dry Soil

This chapter contains the field observations for Carson Sink in general, and describes the in situ “dry” soil model. The two models reported for Carson Sink represent a single soil at two moisture levels. The “dry” soil represents the field visit conditions, which are believed to be representative of most of the site for most of the year. The Carson Sink “wet” model represents the recently receded flood conditions, or the lower elevation pockets that retain water for longer periods of time.

6.1 Location

Carson Sink is located about 30 miles northeast of Fallon, NV. It is situated between the Humboldt, Hot Springs, and Stillwater Mountain Ranges. The southwest corner of the Fallon B20 bombing range is located ~2 km from the 10 km circular landing perimeter. The range is frequently used by the Naval Air Station. A complete weather station operated by the Western Regional Climate Center is located on the range. The weather station records wind speed, direction, temperature, and many other weather factors of interest to the landing engineer. The 24 hour, 365 days/year data is available online.

Fallon National Wildlife Refuge and Stillwater Wildlife Management Area border the landing zone to the south and west (Figure 6-2). These areas are managed by the United States Fish & Wildlife Service. To preserve wildlife habitat, vehicle access is confined to dirt roads in the wildlife management areas.

The landing zone is 10 km in diameter and centered at latitude 39.774° and longitude -118.49°. It is entirely contained on the flat playa. There are no shorelines as there are at Cuddeback Lake. Only sand dunes interrupt the flat playa on the southern edge of the zone. The sand dunes can easily be avoided by moving the landing zone 1 mile further north, where there seem to be no significant differences in soil. No roads exist on the playa. Any vehicle tracks are filled in by the next flood.

According to the BLM maps, the landing zone lies within shared private property area. The white checkered markings in Figure 6-2 indicate private land ownership. If Carson Sink is to be used for landing purposes, NASA should contact BLM to ascertain who the owner is and contact them.

Studying the topographic map in Figure 6-3, one will find that the landing zone gradually slopes downward to the northwest. During flood conditions, the northwest half of the zone will remain submerged for a longer period of time than the southeast half.

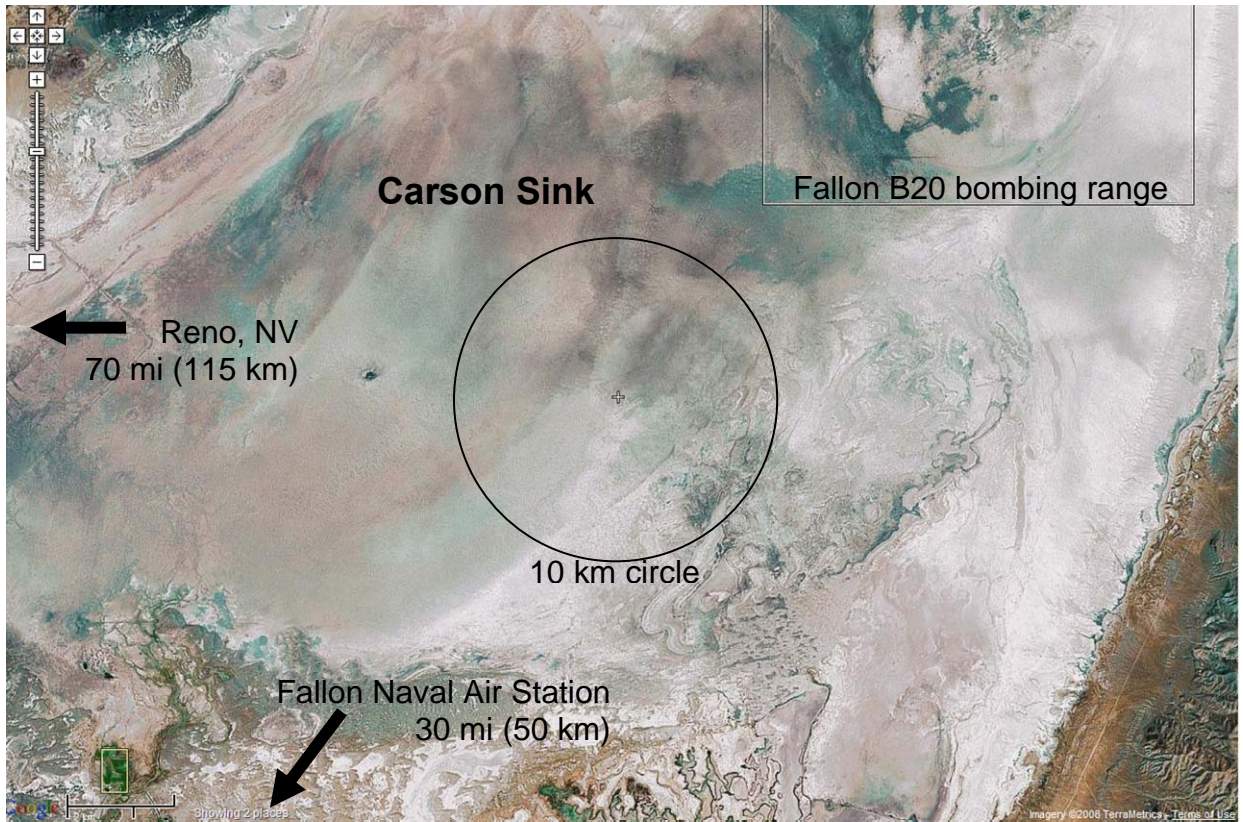


Figure 6-1: Aerial photo of Carson Sink with landing zone defined.

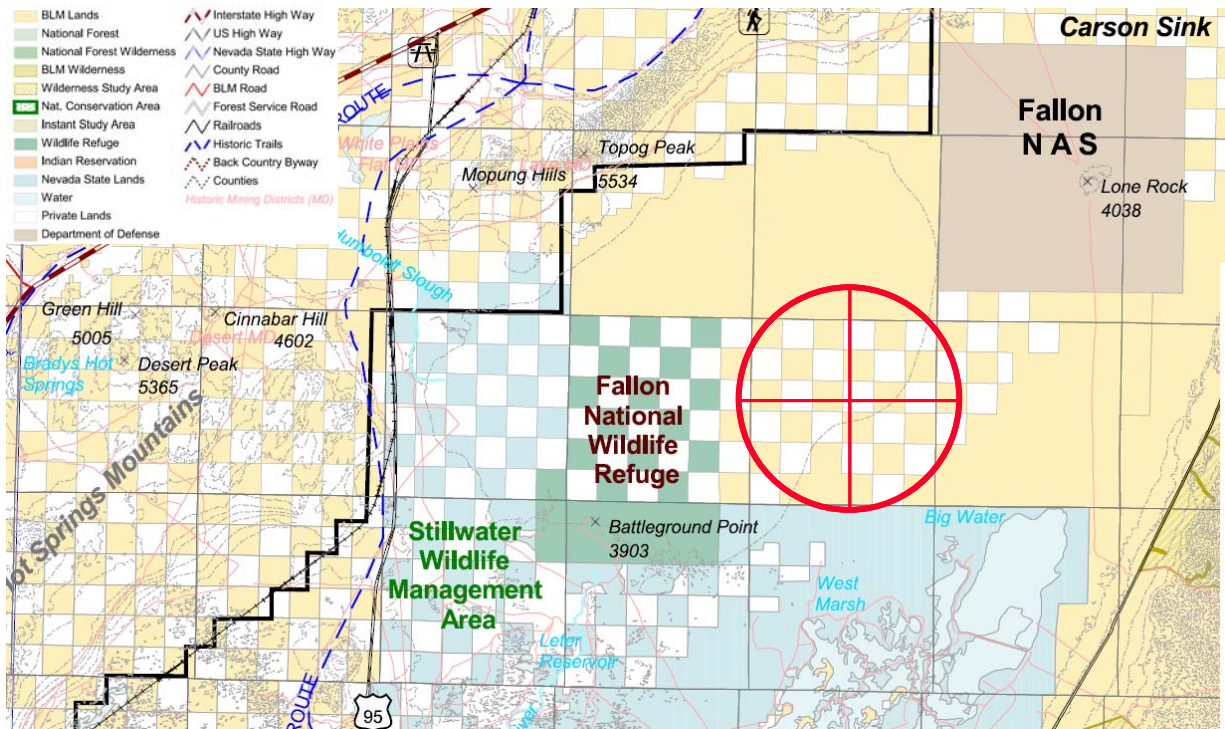


Figure 6-2: Bureau of Land Management (BLM) map of Carson Sink, indicating shared private land over the approximately placed landing zone. Wildlife areas border on the south and west. Elevations in ft.

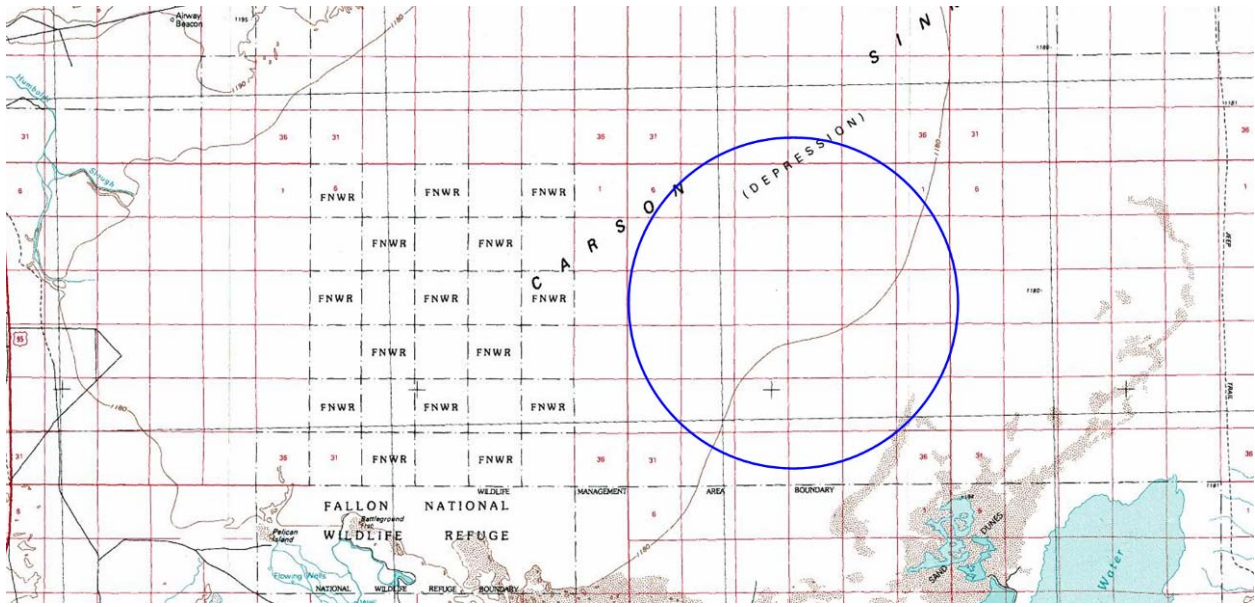


Figure 6-3: USGS topographic map of Carson Sink with 10 km diameter landing zone defined in blue. 1 square mile grid overlaid. Note the sand dune (shaded area) protrusion into the southeast perimeter. Elevations in meters.

6.2 General description

The Carson Sink dry soil model represents the in situ conditions encountered during the late October 2007 field visit. At the time, Carson Sink had no submerged areas. The soil surface was relatively dry, and moisture content increased with depth, much more so than Cuddeback Lake. Carson Sink's water table is approximately at four feet depth. Throughout the year, the underlying soil is always damp due to capillary water being drawn up from the water table.

It is important to note that only one type of soil was encountered at Carson Sink. Essentially, only the soil moisture content varied from one area to another. The higher moisture content areas corresponded to slightly lower elevations. While the elevation variation over the 10 km landing zone seemed to be no more than a few feet, the GPS devices used did not supply accurate enough elevation data. The NASA aerial elevation survey would provide fine enough elevation resolution for discerning low spots.

Carson Sink is a vast playa of approximately 300 square miles located in the Lahontan Valley in northwestern Nevada. Originally, the sink was a terminal lake fed by the Carson River. Currently, levees and channels control water flow in the area west of Carson Sink. The playa surface is cracked with sporadically placed wind-deposited sand dunes of a less than 6 inches in height. Outside the target landing area to the southeast there are significant dune deposits up to 8 feet in height, although generally, the target site is very flat. The soils that makeup the sink vary slightly in varying degrees of mainly clay soil mixed with silt or small amounts of sand. The clay/sand soil was mostly confined to the surface of the eastern edge of the site where the elevation is slightly higher, and closer to the sand dunes.

According to Fallon Naval Air Station (NAS) personnel, the northwestern portion of the sink can be intentionally flooded to relieve excess water from Humboldt Lake, situated north of Carson Sink. The lowest elevations are also in the northwest. Most of the year it appears that the playa is dry, particularly in the southeast. However, intentional flooding may submerge the northwest edge of the landing zone. One cannot say for sure whether flooding will occur because it depends on the amount of excess rainwater already present.

The soils at the Carson Sink site generally fall into two very similar soils, so treating all of Carson Sink as a single soil was an easy simplification. Clay was found over the entire site with a thickness of at least 4 inches. The deepest soil excavation was 27 inches at the northern location point where clay was observed from 3 to 27 inches (the bottom of the hole). The upper clay was generally moist and varied from soft to stiff as moisture decreased. The deeper clays, usually starting around 16 inches in depth, were always very wet and very soft. The softness is attributed to fat clay and moisture content. Fat clays are nearly pure clays. The other very similar soil type was confined to the eastern perimeter. It was mostly clay with silt or sand mixed on the surface. Because the surface soil was still very similar to the rest of the site, and the underlying soil was identical, it was considered the same soil for this analysis. The most defining attribute was Carson Sink's cohesion, or stickiness. If the weather remains dry for a significantly long time, Carson Sink could be as stiff as Cuddeback Soil A (Figure 6-4).



Figure 6-4: (left) Surface “flakes” from Carson Sink’s cementation. (center) Close up of Carson Sink soil, can be squeezed to form cohesive chunk. (right) After driving over, it is observed that drier portions of Carson Sink behave as stiff as Cuddeback Soil A.

6.2.1 Cementation

Drier pockets of Carson Sink soil exhibited a very thin ($< \frac{1}{4}$ inch) and weak layer of cemented soil on the surface. It is considered negligible in modeling and is not accounted for in this report. Carson Sink also displayed a cracked surface where the soil was drier. The wetter areas appeared very smooth (Figure 6-5).



Figure 6-5: (left) Drier Carson Sink areas were hard and appear cracked. (right) Wetter areas appeared almost completely smooth and significantly displaced under load.

6.2.2 Soil classification

Carson Sink is classified as inorganic clay of low to medium plasticity. The Unified Soil Classification System symbol is CL. The Atterberg limits test confirmed this. The surface of Carson Sink occasionally contains miniature sand dunes. The dunes are roughly 20 ft diameter pockets of wind-blown sand no more than 4 inches tall and probably move around with the wind. These dunes were not considered in the soil classification.

6.3 Field observations

Fallon NAS Search & Rescue provided helicopter support as a means of rapidly surveying the site. A bird's eye view is shown in Figure 6-6. Photographs and video of the helicopter survey are available on DVD. The pilot located the center of the target site, landed, and the evaluation team was able set foot on the ground make a quick evaluation of the soil. The pilot continued the tour stopping at the east, south, north, and west limits of the landing zone for further initial evaluation. Due to time restrictions, no soil was taken from the site that day. The relative softness of the Carson Sink soil was readily apparent during helicopter landings. The wetter areas, also visually darker colored from the helicopter survey, clearly had less shear strength, shown in Figure 6-7.



Figure 6-6: Helicopter survey revealed very uniform soil.



Figure 6-7: Huey H1 helicopter legs sinking into Carson Sink. The H1 weighs approximately 10,000 lbs.

The team returned to the site the next day and began soil sampling and nuclear density tests. Five location points were selected for the initial evaluation of the site, similar to the locations that were selected for the helicopter landing locations the day before. One location each was selected at the center, eastern, northern, western, and southern most points of the 10 km landing zone. Soil descriptions and density, moisture, shear vane, and DCP measurements were made at each location.

Midway through the first day, light rain fell and the soil started sticking to the wheels of the survey vehicles. It became readily apparent how quickly Carson Sink soil loses shear strength when moisture is added. The soil cohesion skyrocketed. Clearly the optimum moisture content was already surpassed, and any additional moisture reduced the strength of the soil. Although not enough rain fell to cause ponding, the entire sink was colored darker by the addition of water. We retreated before getting stuck on Carson Sink. This highlights one of the practical considerations NASA must face if Carson Sink is to be used for landing. The recovery of craft from Carson Sink could be extremely difficult if conducted during wet conditions.

By the next day, Carson Sink had mostly recovered from the rains. It was capable of supporting the vehicles the next day which is some indication of the rain recovery rate. The amount of fallen rain on the site was likely less than a tenth of an inch. The following days remained rain free and the Sink continued to dry.

There were no man made obstructions observed on the landing zone. There was no vegetation on the playa itself within the landing zone. Only the sand dunes harbored any kind of plants.

6.3.1 Sampling and sample locations

Four locations were chosen for sampling. The center location happened to be the wettest, and thus samples were taken. The eastern location was clay with silt/fine sand. The northern site was somewhat wet clay. The southern site was dry clay. The soil sample was taken from the eastern location point as indicated on the map in figure 4.

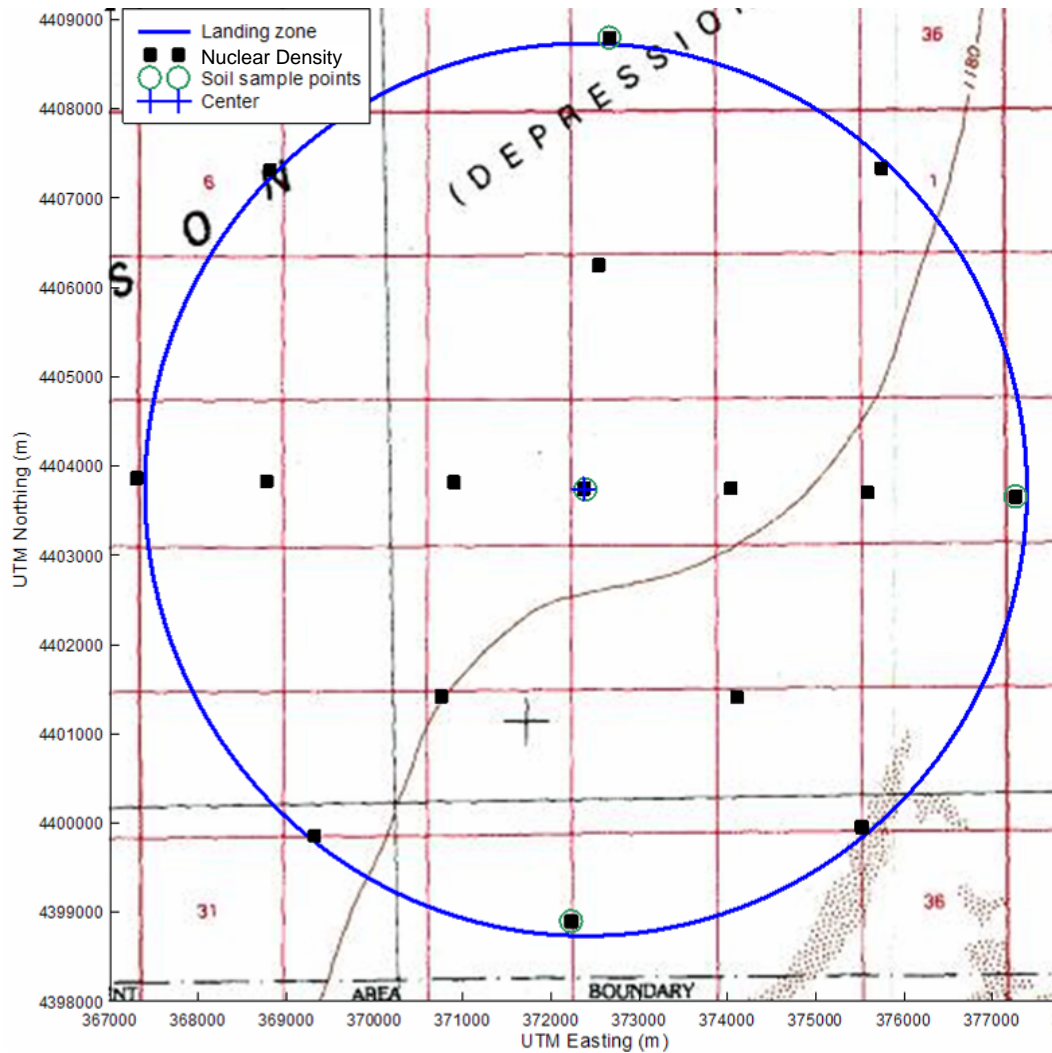


Figure 6-8: Soil sampling and nuclear density test locations superimposed on Carson Sink topographic map. Four sample points were chosen, circled in green. Sixteen nuclear density locations used. Coordinates and elevations in meters.

6.3.2 Nuclear density and moisture data

Converse Consultants of Reno, NV was subcontracted to perform nuclear density and nuclear moisture field tests for Carson Sink. The nuclear density gage was a Humboldt Scientific Model 5001 EZ. The device was calibrated against a standard block of known density every morning before use.

The nuclear density test procedure involves driving a 3/4 inch spike into the ground before inserting the nuclear source probe. The spike makes a hole for the probe. Because of the higher moisture content, the cohesion of Carson Sink soil was high enough that the hole never caved in.

A total of 62 nuclear density tests were performed in Carson Sink. The descriptive statistics of the nuclear density and moisture data are presented on the following pages.

Table 6-1: Carson Sink Dry (in situ moisture) model, wet densities (lbs/ft³) by depth range (in).

Depth (in)	N	Mean	SE Mean	StDev	Minimum	Q1	Median	Q3	Maximum
0-2	18	76.71	3.68	15.59	32	70.45	79	84.98	101.4
2-3	3	77.23	1.3	2.25	75.3	75.3	76.7	79.7	79.7
0-6	18	86.29	1.58	6.7	76.9	81.43	84.85	90.55	101.3
6-12	18	92.91	1.26	5.34	84	88.13	93.65	96.25	102.2
12-18	5	88.62	2.21	4.95	82.8	83.85	89.5	92.95	95.4

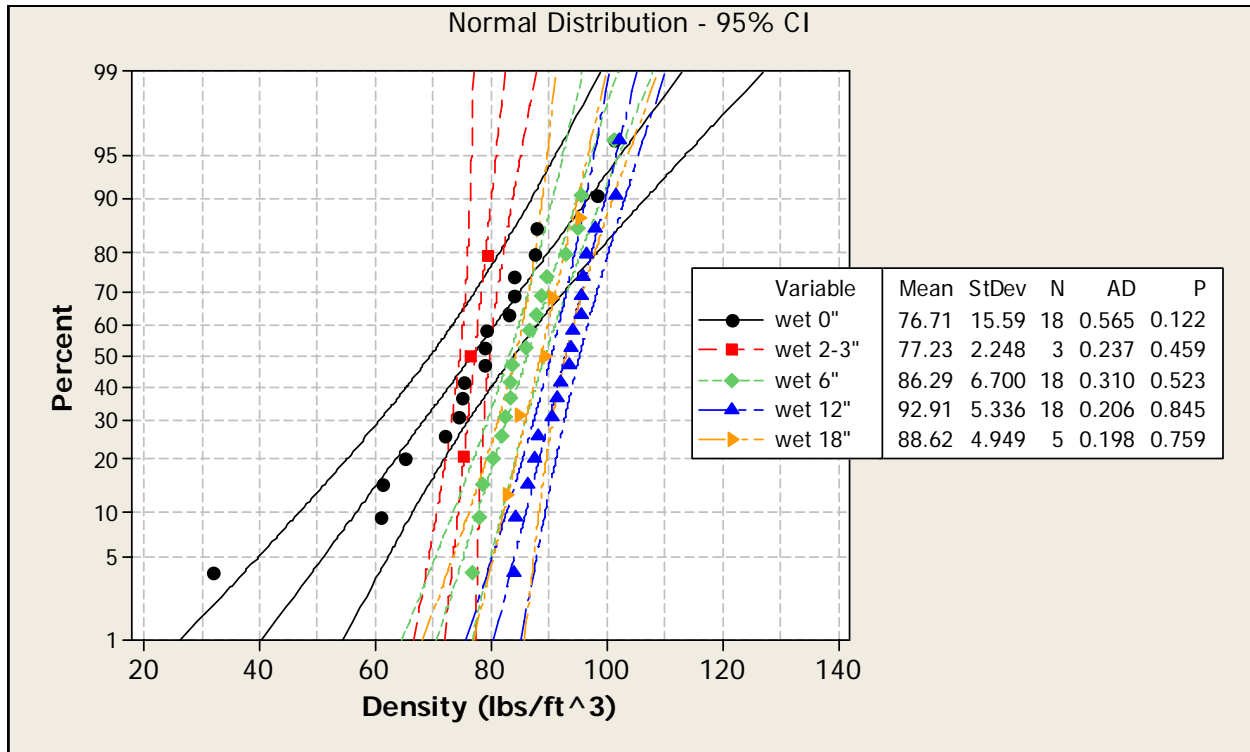


Figure 6-9: Probability plot of Carson Sink Dry (in situ moisture) model's wet densities by depth (in).

Surface densities at Carson Sink were much lower than at Cuddeback Soil A. The 0-2 inch depth range's density varied widely. The wet density for laboratory specimen testing was 86 lbs/ft³. This wet density represented the 0-6 inch depth range average.

Table 6-2: Carson Sink Dry model's water contents (%) by depth range (in).

Depth (in)	N	Mean	SE Mean	StDev	Minimum	Q1	Median	Q3	Maximum
0-2	18	4.639	0.512	2.171	1.5	2.95	4.05	6.125	9.2
2-3	3	3.133	0.384	0.666	2.7	2.7	2.8	3.9	3.9
0-6	18	3.967	0.494	2.097	1.2	2.475	3.35	5.225	9.6
6-12	18	3.828	0.469	1.991	1	2.575	3.4	4.675	9.4
12-18	5	15.94	1.63	3.65	12.5	12.6	14.9	19.8	20

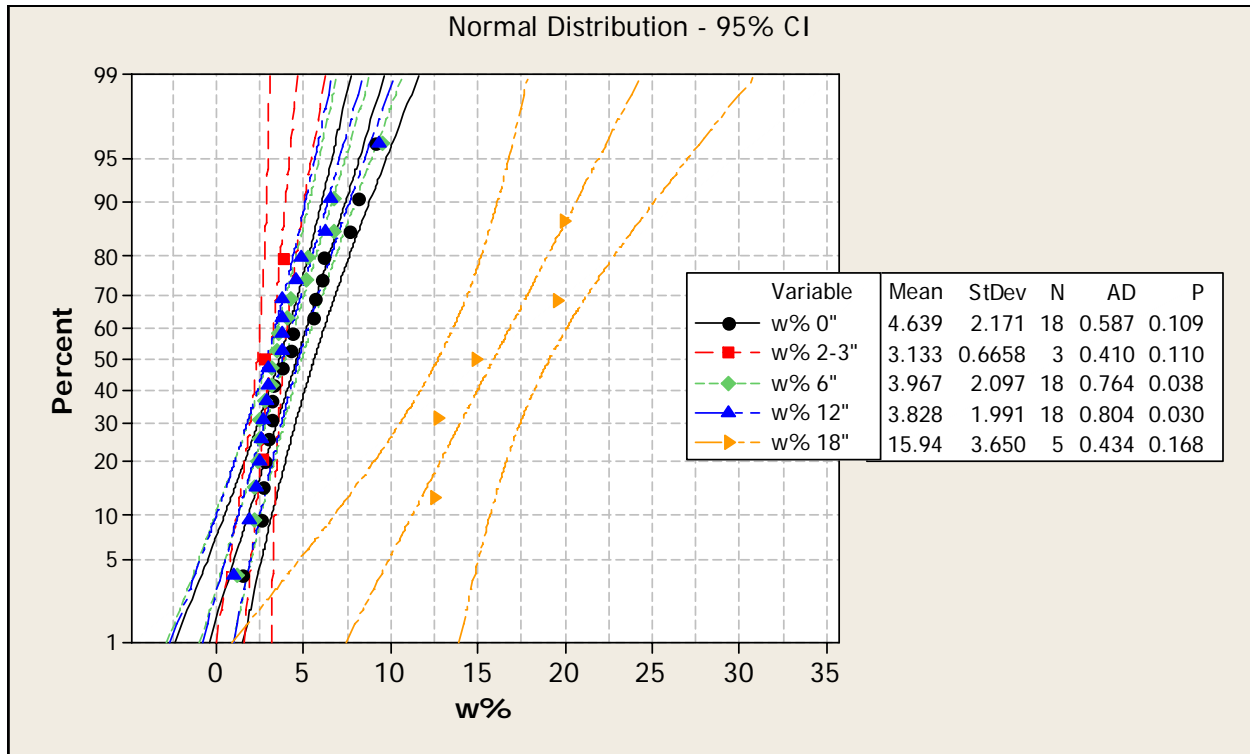


Figure 6-10: Probability plot of Carson Sink Dry model's water contents (%) by depth range (in).

Nearly all of the surface soil down to 12 inches depth ranged from 3 to 10% moisture content. The wetter pockets of soil at Carson Sink had 6 to 10% water contents. The 12-18 inch depth shows a clear departure from this range because the fat clays lie within these depths. Fat clays are mostly pure clays and can retain quite a lot of water, especially if near the water table.

Table 6-3: Carson Sink Dry (in situ moisture) model's dry densities (lbs/ft³) by depth range (in).

Depth	N	Mean	SE Mean	StDev	Minimum	Q1	Median	Q3	Maximum
dry 0"	18	73.48	3.51	14.89	29.7	69.03	75	80.88	97
dry 2-3"	3	74.9	1.04	1.81	73.2	73.2	74.7	76.8	76.8
dry 6"	18	82.98	1.55	6.56	75.1	76.98	82.35	86.75	100.1
dry 12"	18	89.52	1.31	5.56	79.2	84.88	89.85	92.5	100.5
dry 18"	5	76.56	2.65	5.94	69	71.45	75.7	82.1	84.8

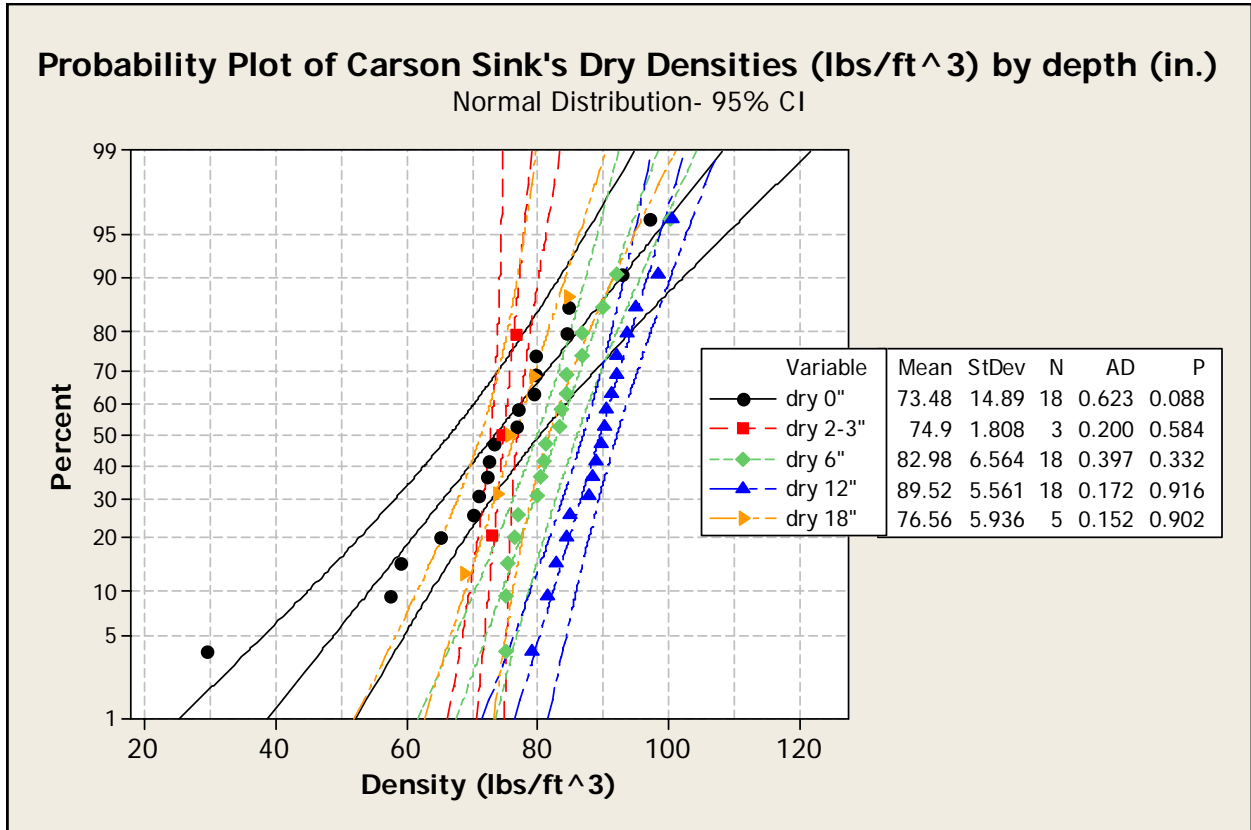


Figure 6-11: Probability plot of Carson Sink Dry (in situ moisture) model's dry densities (lbs/ft³) by depth range (in).

For developing the Carson Sink Wet model, the dry density of 83 lbs/ft³ was maintained while adding water. The wet Carson Sink sample was reconstituted to the same dry density as the Carson Sink Dry soil. This density was used because temporary flooding does not change the dry density of the soil. The water replaces the air in the voids, but does not displace soil grains.

6.4 Laboratory test data

This section contains the results of laboratory testing on Carson Sink Dry soil. The test log summarizes the tests using the triaxial apparatus.

Table 6-4: Test log for Carson Sink Dry soil.

Test ID	Sample ID	Type	Confining Pressure (psi)	Moisture content	Dry Density (lbs/ft ³)	Grain Density G _s	Porosity <i>n</i>
D12B07	CAR 65	Triax	2	8.89%	79.26	2.78	54.3%
D11C07	CAR 64	Triax	5	7.87%	80.01	2.78	53.9%
D7B07	CAR 55	Triax	10	8.68%	79.41	2.78	54.2%
D10B07	CAR 53	Triax	20	6.48%	81.05	2.78	53.3%
J30G08	CAR 61	Triax	50	8.89%	79.57	2.78	54.2%
J23A08	CAR 59	Uniax	50	8.28%	80.03	2.78	53.9%
J23A08	CAR 59	Hydrostat	50	8.28%	80.03	2.78	53.9%

6.4.1 Moisture content

The laboratory oven dried moisture content for Carson Sink specimens averaged 8%. This moisture content corresponds to an in situ saturation of about 20%. Nine moisture tests were conducted.

6.4.2 Atterberg limits

Carson Sink is classified as a clay with medium to high plasticity. The majority of the soil consists of clay. Silts cannot achieve this level of plasticity.

Table 6-5: Atterberg results for Carson Sink soil.

Soil ID	Liquid Limit	Liquid Limit	Plasticity Index	Soil Classification
CAR-53	26	16	10	CL
CAR-32	47	18	29	CL

6.4.3 Grain density and grain size analysis

The grain density of Carson Sink soil was determined to be 2.78 g/cm^3 by pycnometer. Two grain size distributions, one based on wet sieving and one dry, are shown in Figure 6-12. The dramatic difference between wet and dry sieving is due to particle cementation during the oven drying process for dry sieving. Individual particles bind together creating larger particles, skewing the distribution toward more coarse soil. Wet sieving is considered much more accurate.

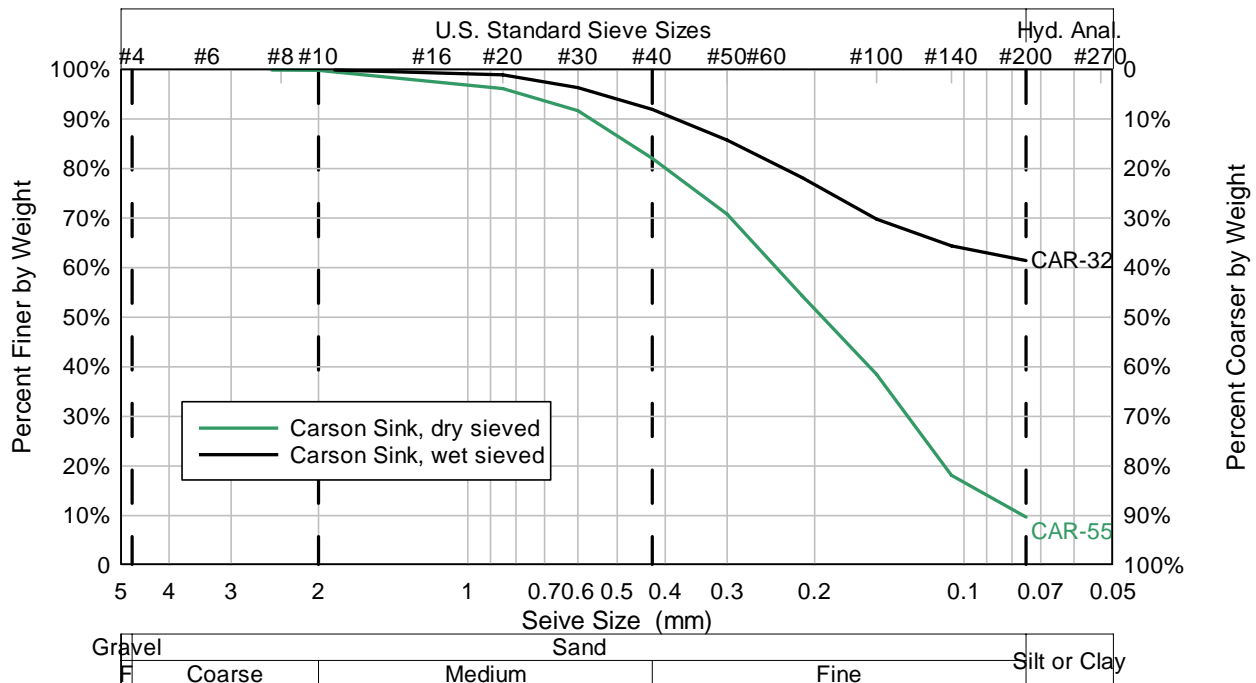
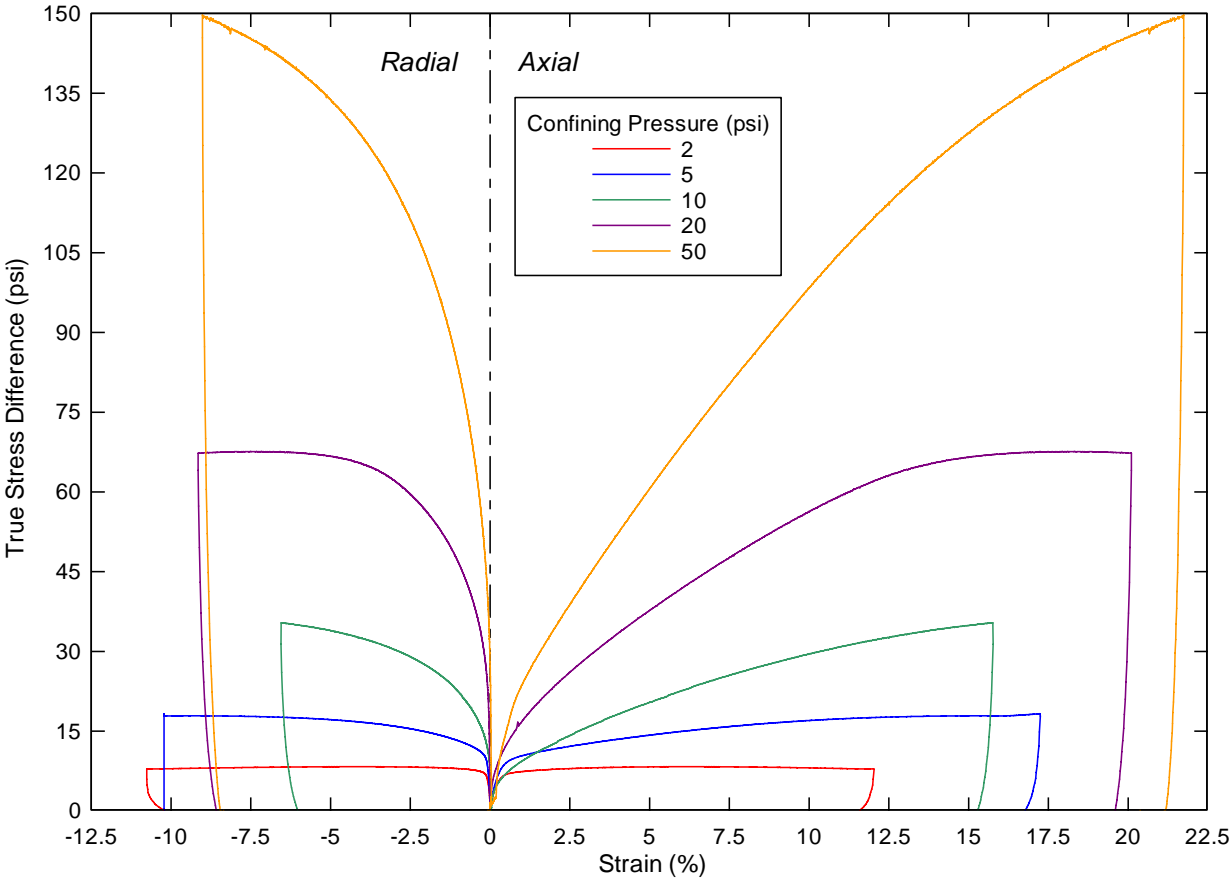


Figure 6-12: Wet and dry sieve grain size distribution for Carson Sink.

6.4.4 Triaxial compression

Using the same regimen as was used for the Cuddeback Lake soils, a series of 5 triaxial tests were carried out on Carson Sink dry soil at 2, 5, 10, 20, and 50 psi confining pressures.

Triaxial Compression Tests Carson Sink



CarD Triax.grf

Figure 6-13: Carson Sink Dry model's triaxial compression test results.

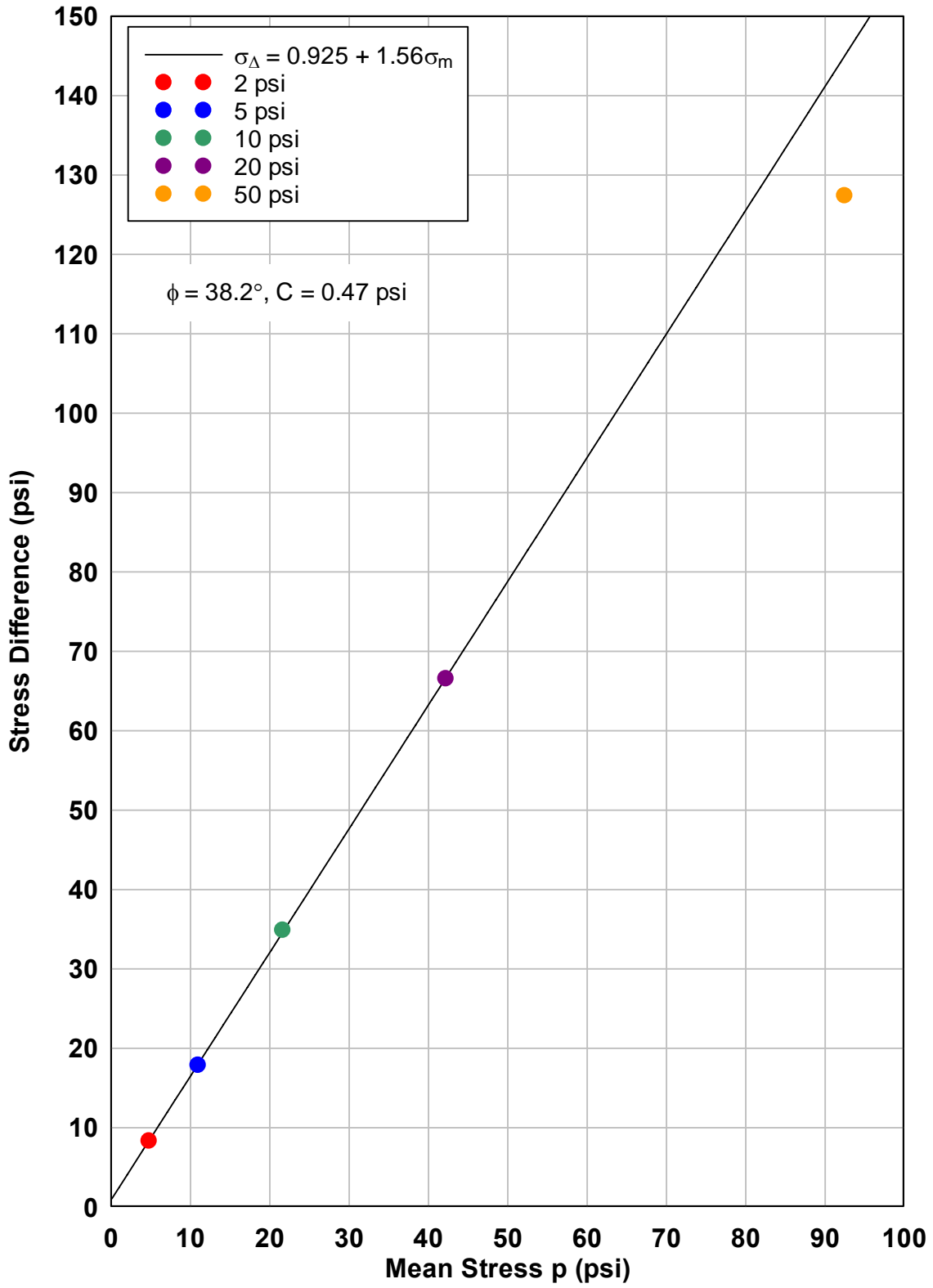


Figure 6-14: Carson Sink Dry model's strength envelope.

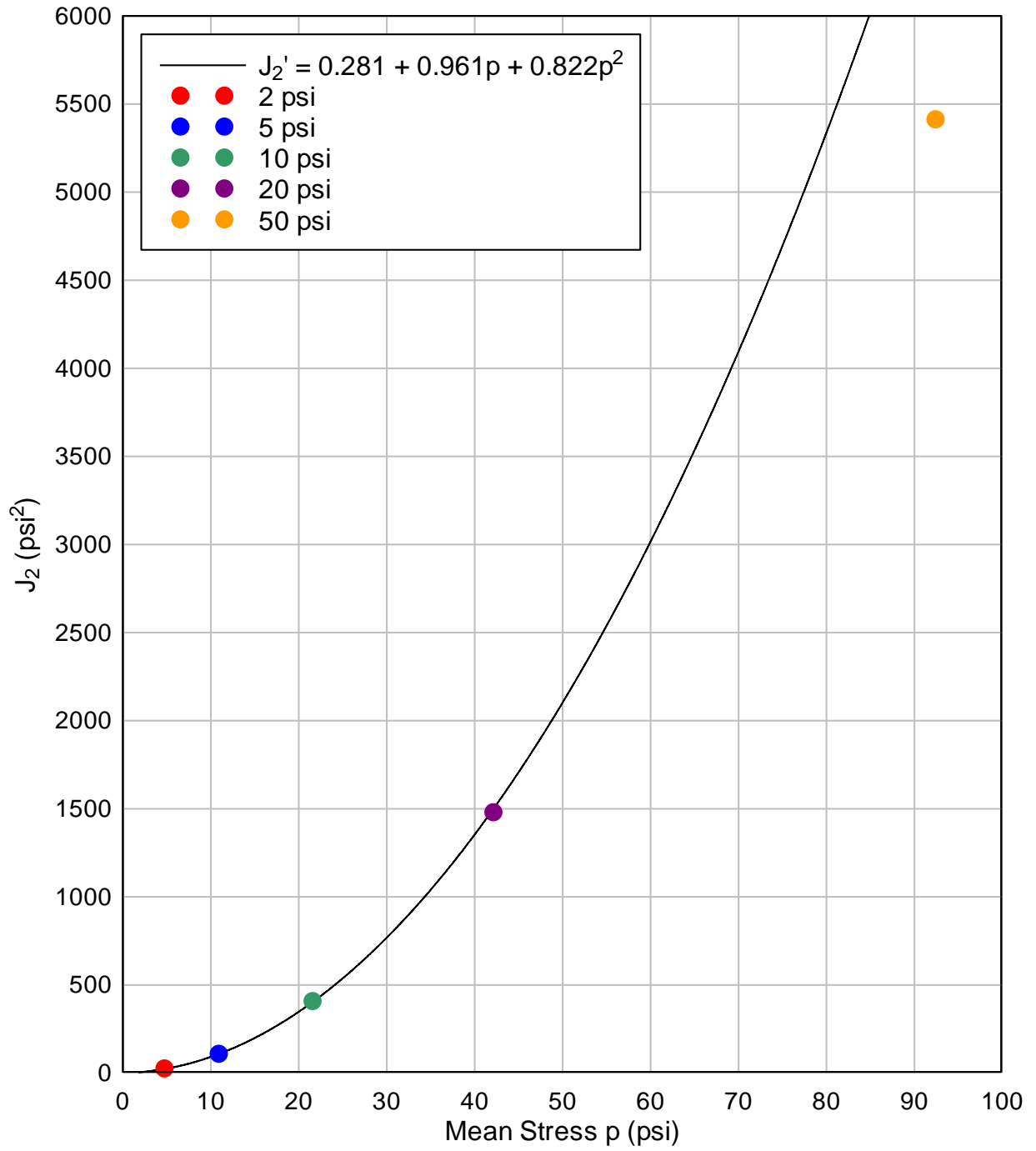


Figure 6-15: Carson Sink Dry Material Model 5 yield surface fit from triaxial data.

6.4.5 Hydrostatic compression

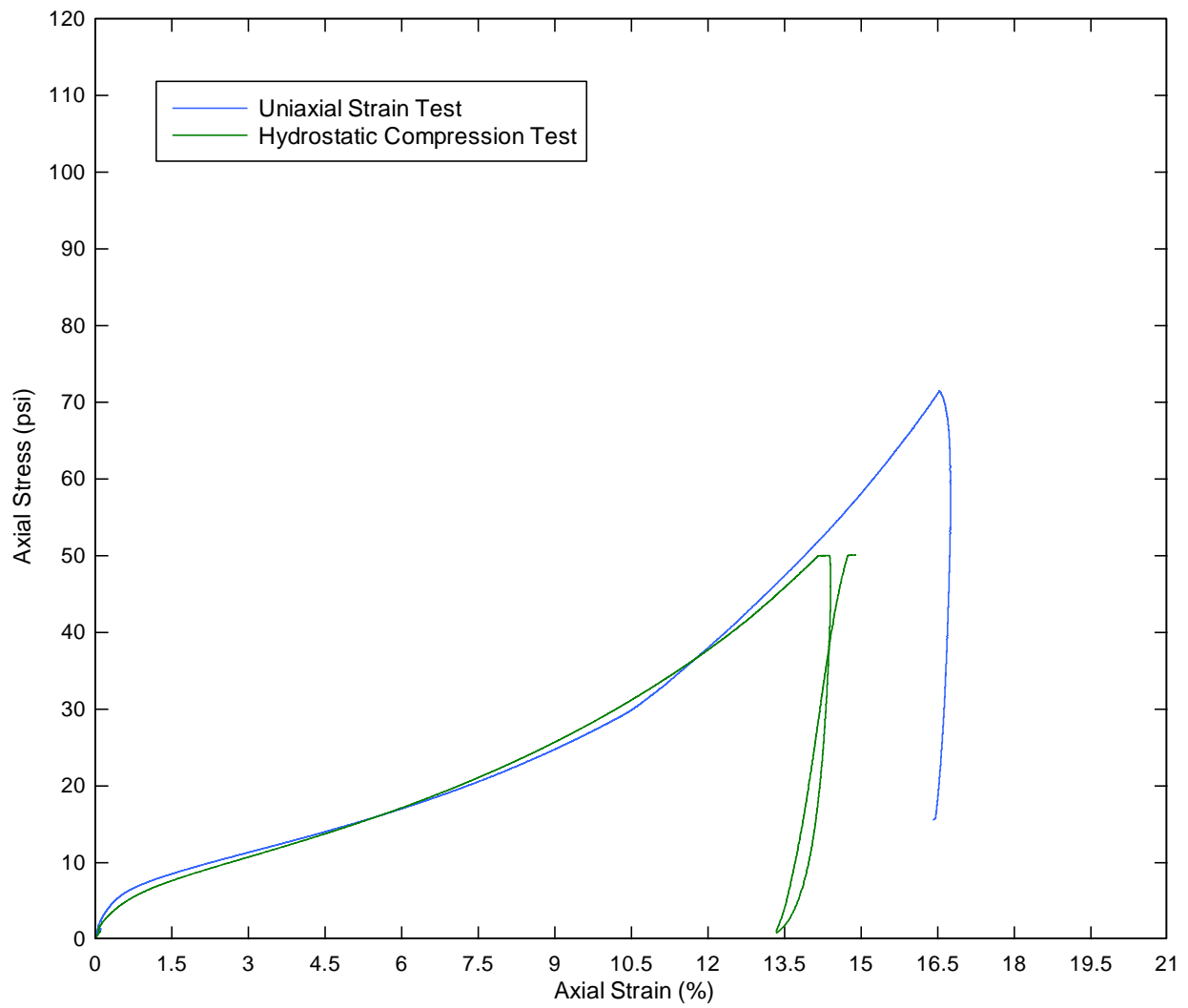


Figure 6-16: Hydrostatic compression test results compared to uniaxial strain.

6.4.6 Uniaxial strain

Carson Sink Dry model's uniaxial strain test results follow on the next few pages.

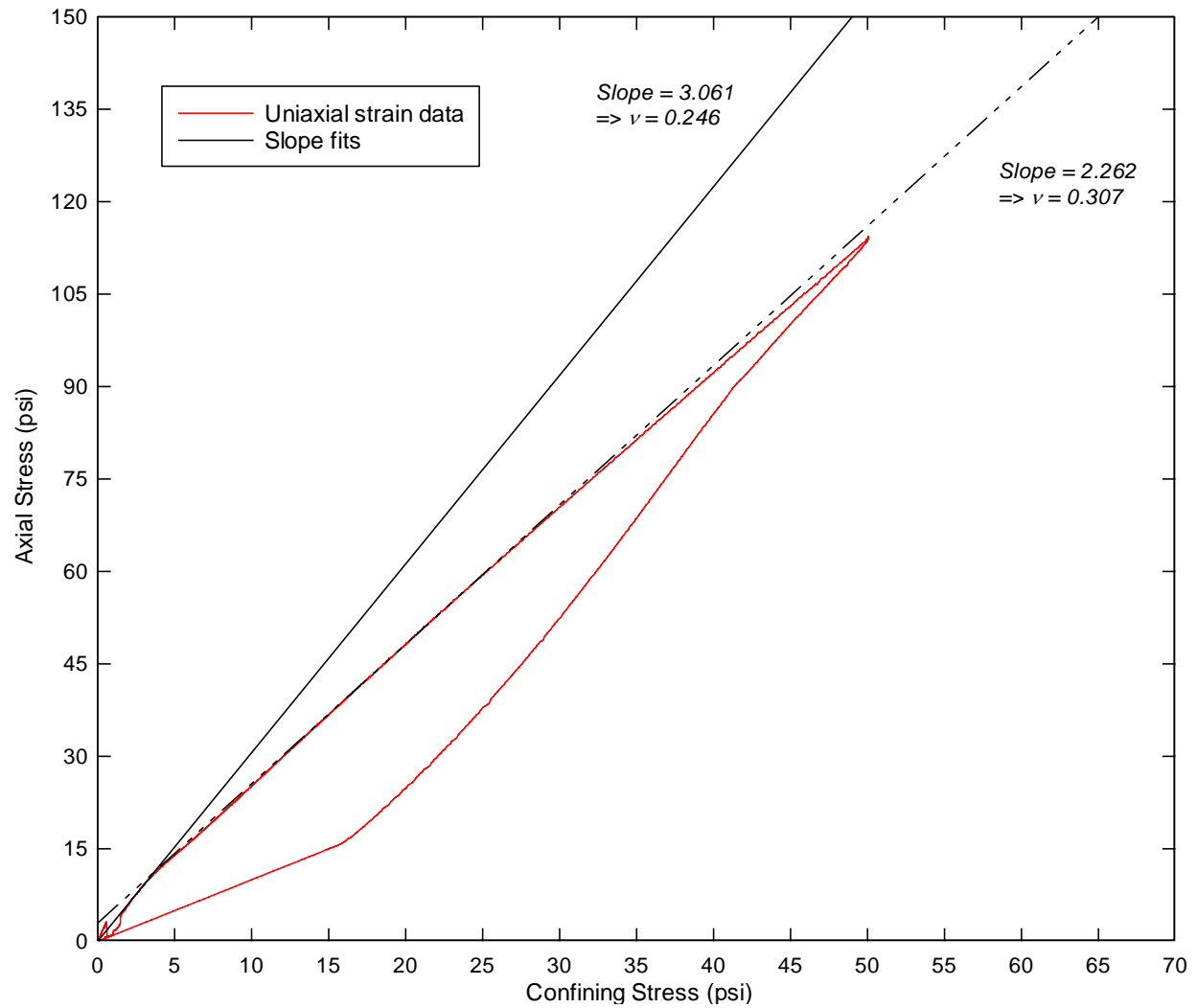


Figure 6-17: Carson Sink Dry model's uniaxial strain test. Axial stress vs. confining stress plotted to calculate Poissons ratio from slopes.

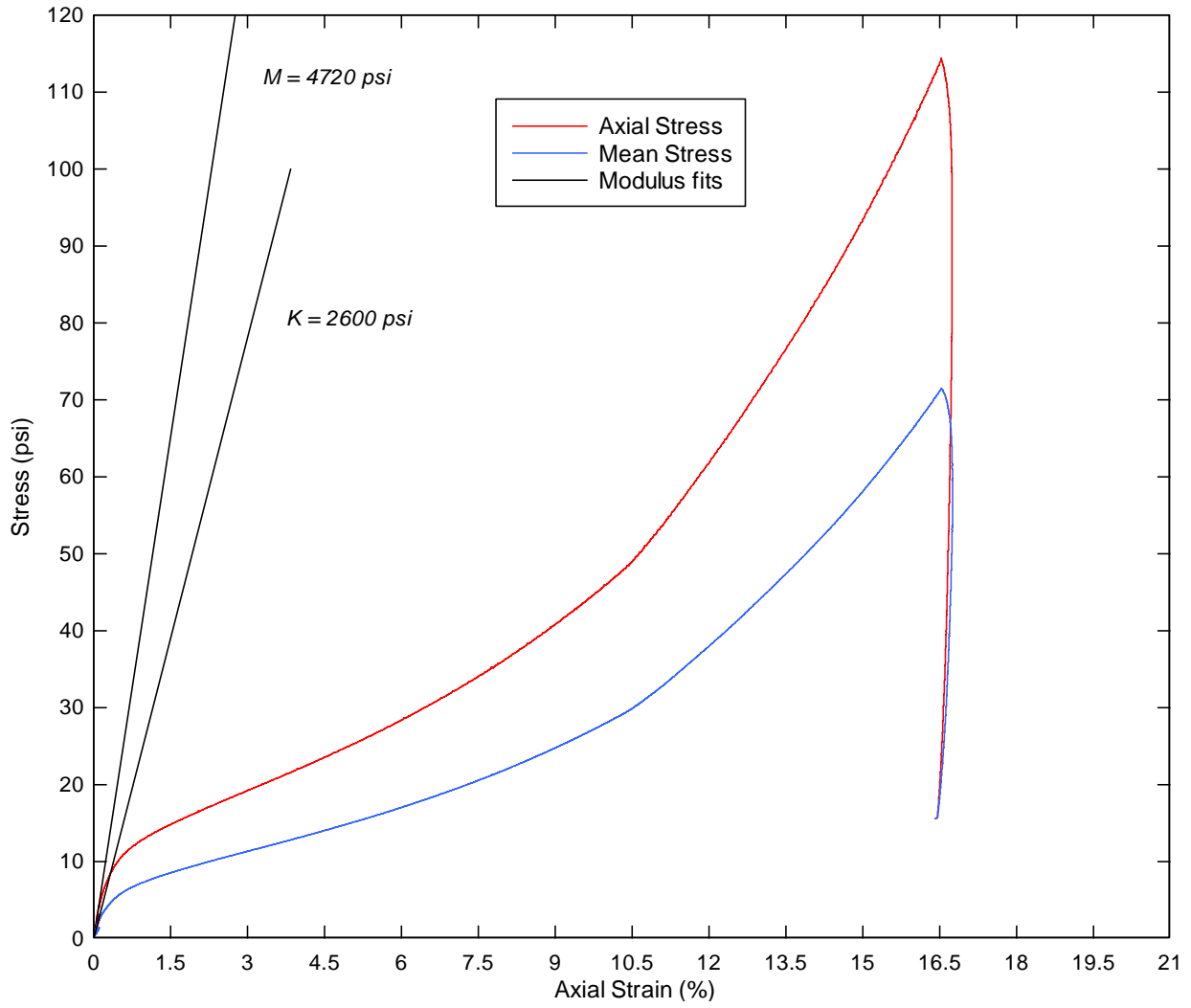


Figure 6-18: Carson Sink Dry model's uniaxial strain test. Stress vs. axial strain plotted to obtain constrained modulus from axial stress and bulk modulus from mean stress.

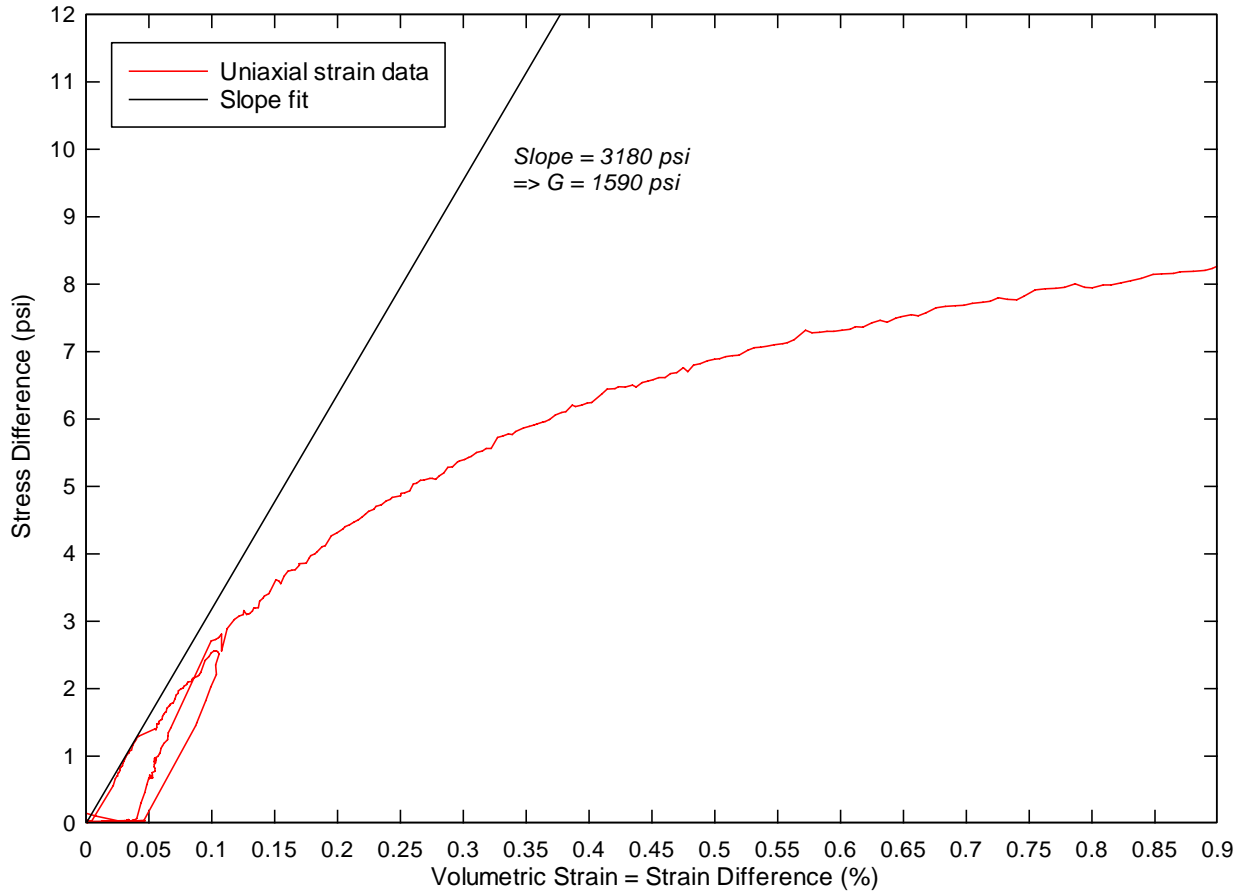


Figure 6-19: Carson Sink Dry model's uniaxial strain test. Stress difference vs. strain difference plotted to obtain shear modulus G.

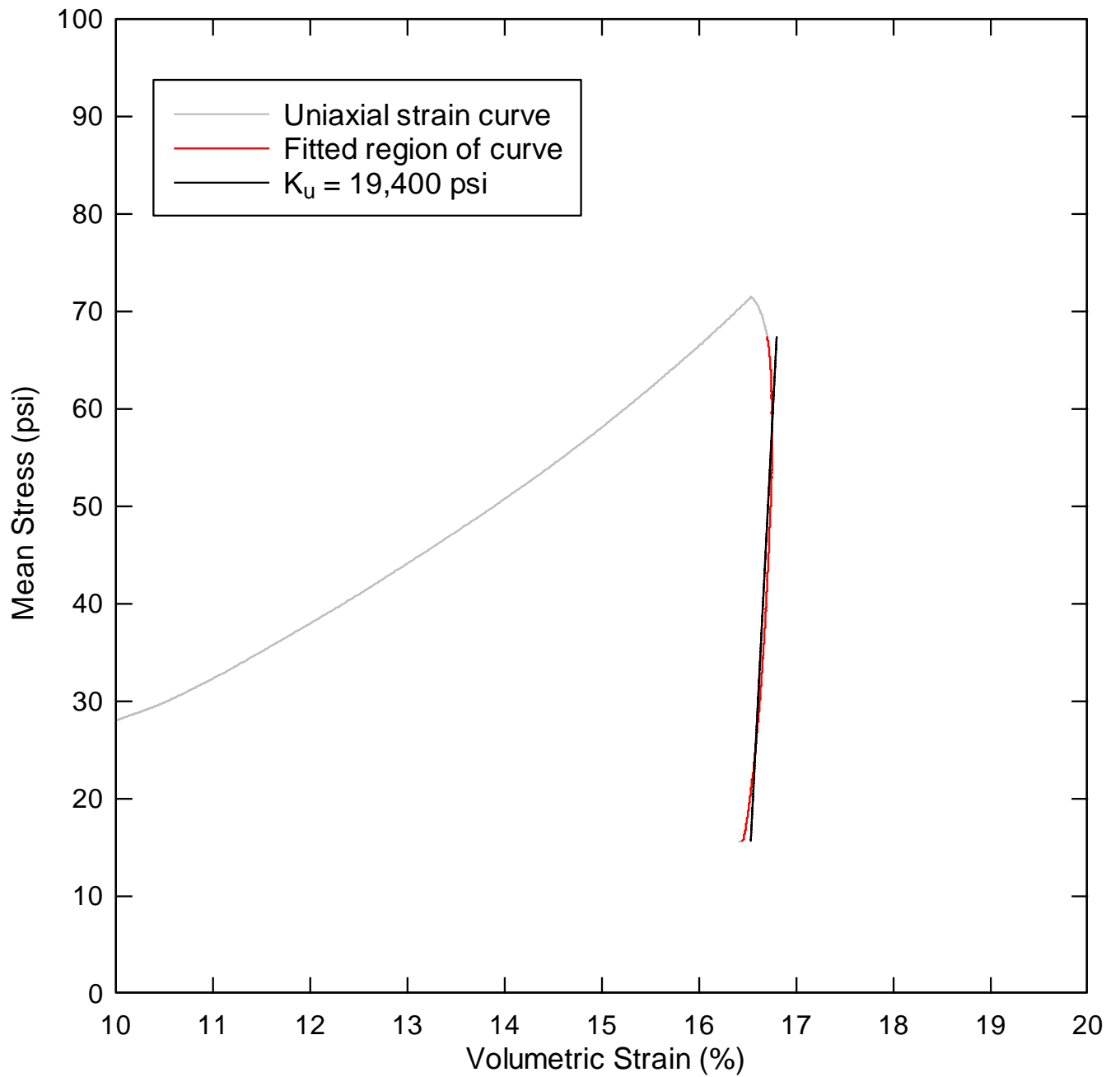


Figure 6-20: Carson Sink Dry model's uniaxial strain test, unloading portion. Mean stress vs. volumetric strain plotted to obtain bulk unloading modulus K_u (BULK). Black line represents slope of K_u . Red line represented fitted portion of test curve.

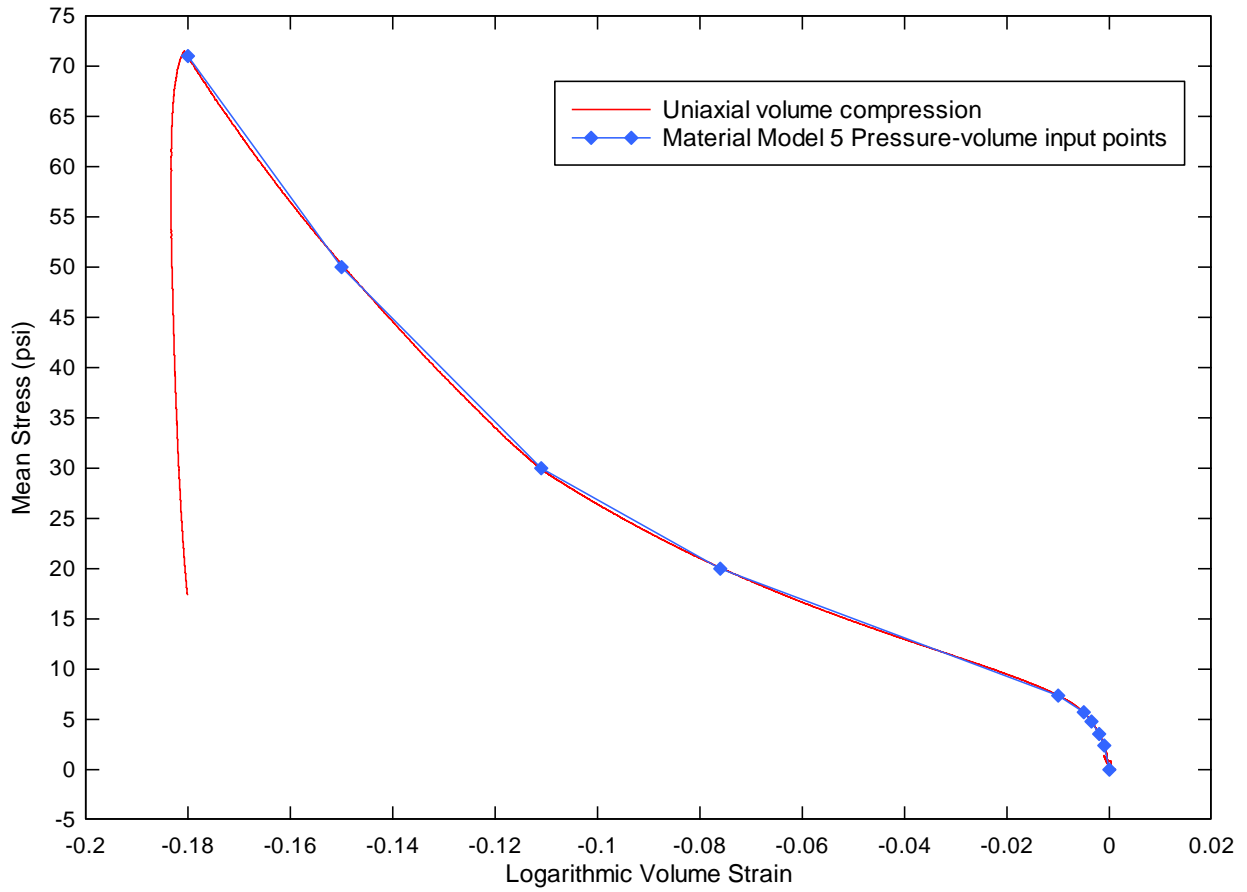


Figure 6-21: Carson Sink Dry model's uniaxial strain test. Mean stress vs. logarithmic volume strain plotted to obtain 10 pressure-volume points for Material Model 5 compressibility curve.

6.5 LS-DYNA Material Model 5 inputs

The recommended set of inputs for modeling Carson Sink Dry in LS-DYNA Material Model 5: Soil and Foam is shown in the table below. It is assembled from field wet density, triaxial compression, hydrostatic compression, and uniaxial strain test data.

Table 6-6: Material Model 5 inputs for Carson Sink Dry soil.

	<u>Input</u>	<u>Value</u>	<u>Units</u>			
Mass density	RO	0.000129	lb s ² /in ⁴			
Shear modulus	G	1590	psi			
Bulk unloading modulus	K	19400	psi			
Yield surface coefficient	A0	0.281	psi ²			
Yield surface coefficient	A1	0.961	psi			
Yield surface coefficient	A2	0.822	-			
Pressure cutoff	PC	0	psi			
	<u>Input</u>	<u>Value</u>		<u>Input</u>	<u>Value</u>	<u>Units</u>
Pressure-volume point	EPS1	0.000		P1	0	psi
Pressure-volume point	EPS2	-0.001		P2	2.4	psi
Pressure-volume point	EPS3	-0.002		P3	3.56	psi
Pressure-volume point	EPS4	-0.004		P4	4.8	psi
Pressure-volume point	EPS5	-0.005		P5	5.72	psi
Pressure-volume point	EPS6	-0.010		P6	7.37	psi
Pressure-volume point	EPS7	-0.076		P7	20	psi
Pressure-volume point	EPS8	-0.111		P8	30	psi
Pressure-volume point	EPS9	-0.150		P9	50	psi
Pressure-volume point	EPS10	-0.180		P10	71	psi

Table 6-7: Summary of elastic constants for Carson Sink Dry soil.

Constrained Modulus - M	4720	psi
Poisson's Ratio - v	0.246	
Young's Modulus - E	3960	psi
Bulk Modulus - K	2600	psi
Shear Modulus - G	1590	psi

6.6 Recommended range of model application

The Carson Sink Dry model is intended for modeling Carson Sink during the dry season. It is middle strength soil in between Cuddeback Soil A and Soil B. The wet version of Carson Sink soil is in the next chapter.

6.7 Recommended surrogate soil composition

Carson Sink's base soil material is about 50% clay based on wet sieve analysis and Atterberg limits tests. The percent passing the #200 sieve can only be clay or silt particles. The Atterberg limits test results suggest that these particles are clay. The assumption is that not all #200 passing particles are clay, and 1/6th of the passing are assumed to be silt. With 60% passing the #200 sieve, this makes 50% clay and 10% silt. About 10% is made of medium coarse sand, and an additional 30% is fine sand or silt. In summary, the "ingredients" are 50% clay, 30% fine sand/silt, 10% silt, 10% medium coarse sand.

The recommended water content for reconstituting this soil is 8%. The grain density should be as near as possible to 2.78 g/cm³. The wet density should be reconstituted to 86 lbs/ft³.

These recommendations are only a first guess at a surrogate soil. Laboratory testing of the surrogate soil is needed to confirm matching strength and deformation behavior.

7 Carson Sink Wet Soil

The Carson Sink Wet model is the weakest soil in this report. Water was added in the laboratory to Carson Sink Dry soil to create a wet version of the same soil. Therefore, all field observations and general descriptions are the same as provided in the Carson Sink Dry model chapter.

7.1 General description

The physical description for Carson Sink Wet soil is similar to the low elevation wet soils discussed in the Carson Sink Dry model chapter. The Carson Sink Wet soil was reconstituted to 86.3 lbs/ft³ wet density for laboratory testing.



Figure 7-1: Center coordinate at Carson Sink. This area would most closely represent the Carson Sink Wet model in the field. Moisture contents here measured 10% on the nuclear gage. Soil was extremely cohesive.

7.2 Laboratory test data

This section covers the laboratory tests conducted on Carson Sink Wet soil. The test log summarizes the tests using the triaxial apparatus.

Table 7-1: Test log for Carson Sink Wet soil tests.

Test ID	Sample ID	Type	Confining Pressure (psi)	Moisture content	Dry Density (lbs/ft ³)	Grain Density G _s (g/cm ³)	Porosity <i>n</i>
J24A08	CAR 57,58	Triax	2	12.34%	80.03	2.78	53.9%
J24C08	CAR 57,58	Triax	5	12.29%	80.07	2.78	53.9%
J25B08	CAR 62	Triax	10	12.60%	79.88	2.78	54.0%
J25D08	CAR 62	Triax	20	12.44%	79.99	2.78	53.9%
J30E08	CAR 62,59	Triax	50	12.33%	80.04	2.78	53.9%
J22B08	CAR 54,56	Uniax	50	11.86%	80.34	2.78	53.7%
J22B08	CAR 54,56	Hydrostat	50	11.86%	80.34	2.78	53.7%

7.2.1 Moisture content

The average moisture content was 12%, corresponding to a saturation of about 30%. Seven moisture content tests were conducted.

7.2.2 Triaxial compression

Triaxial compression data for Carson Sink Wet soil is shown on the next few pages.

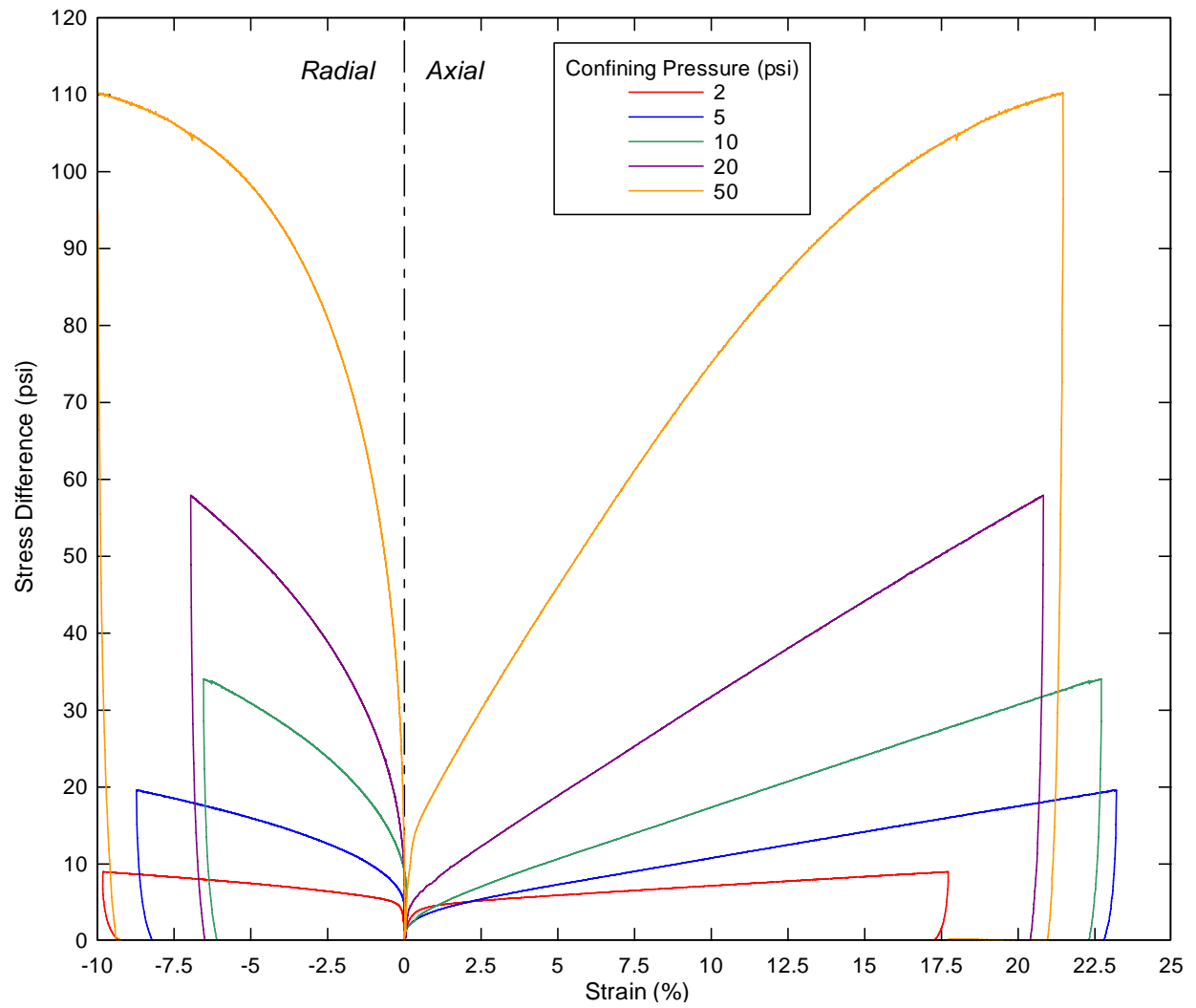


Figure 7-2: Carson Sink Wet model's triaxial test results.

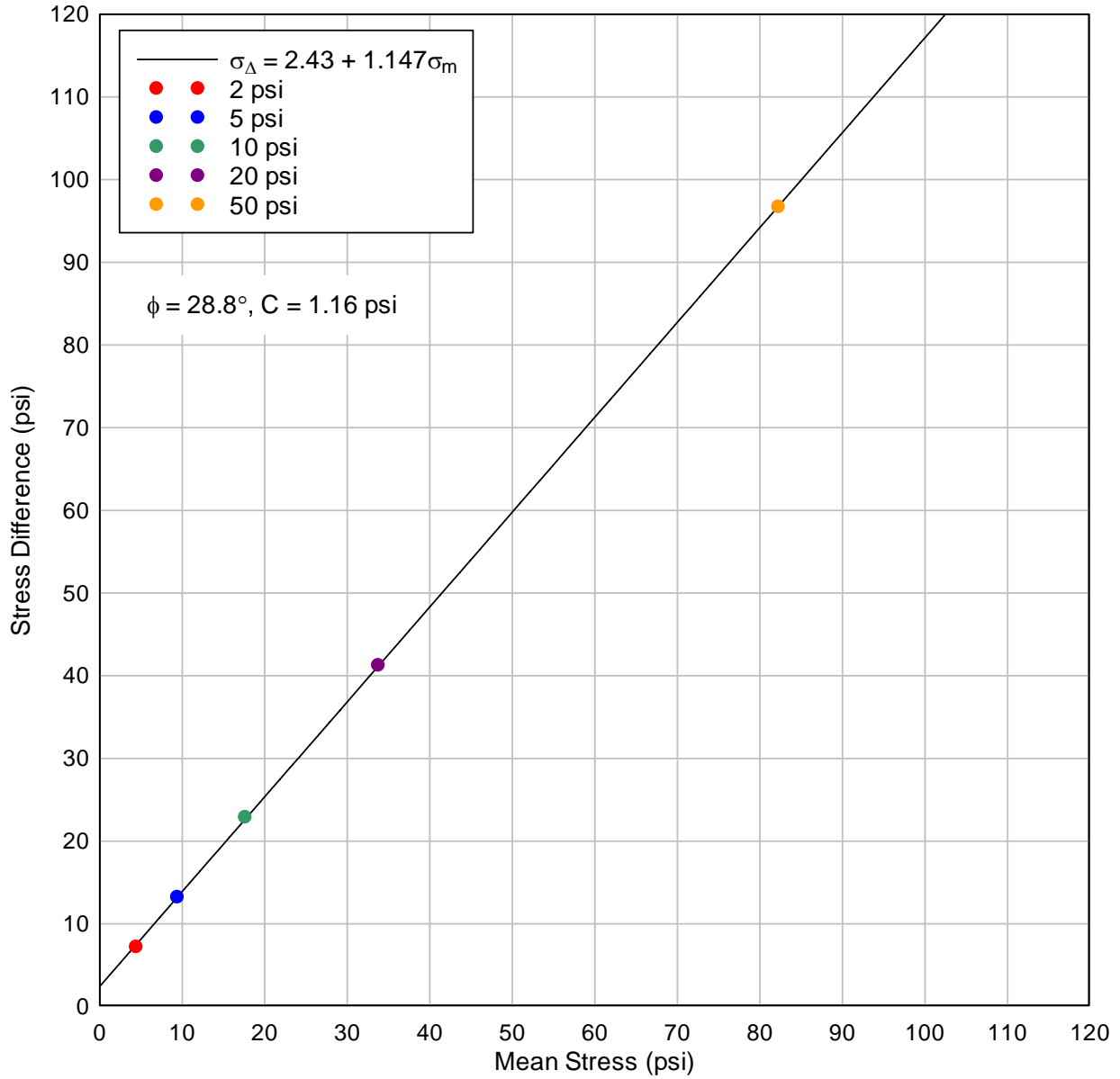


Figure 7-3: Carson Sink Wet model's strength envelope from triaxial tests. Failure based on 15% strain.

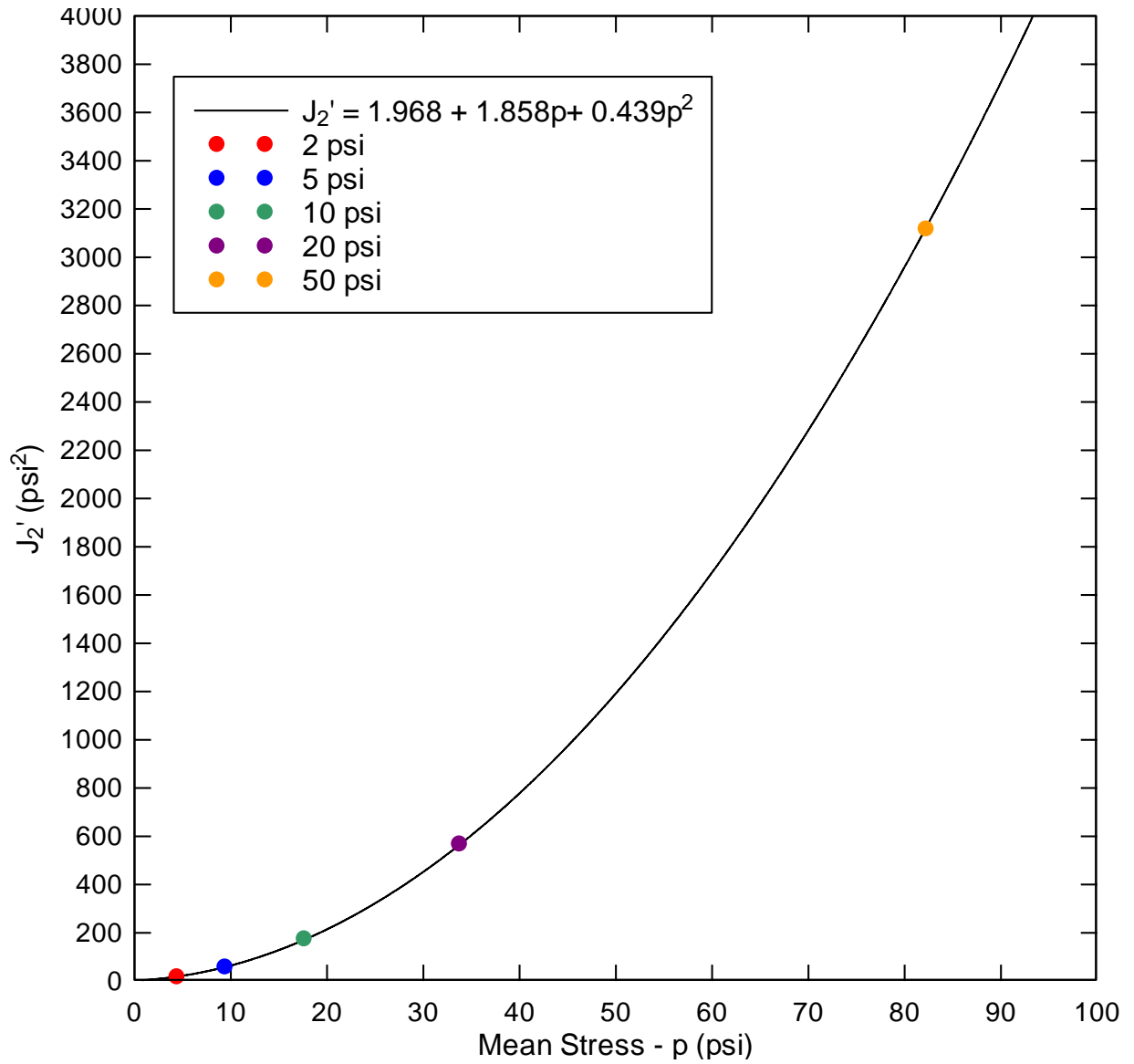


Figure 7-4: Carson Sink Wet Material Model 5 yield surface fit from strength envelope data. Failure based on 15% strain.

7.2.3 Hydrostatic compression

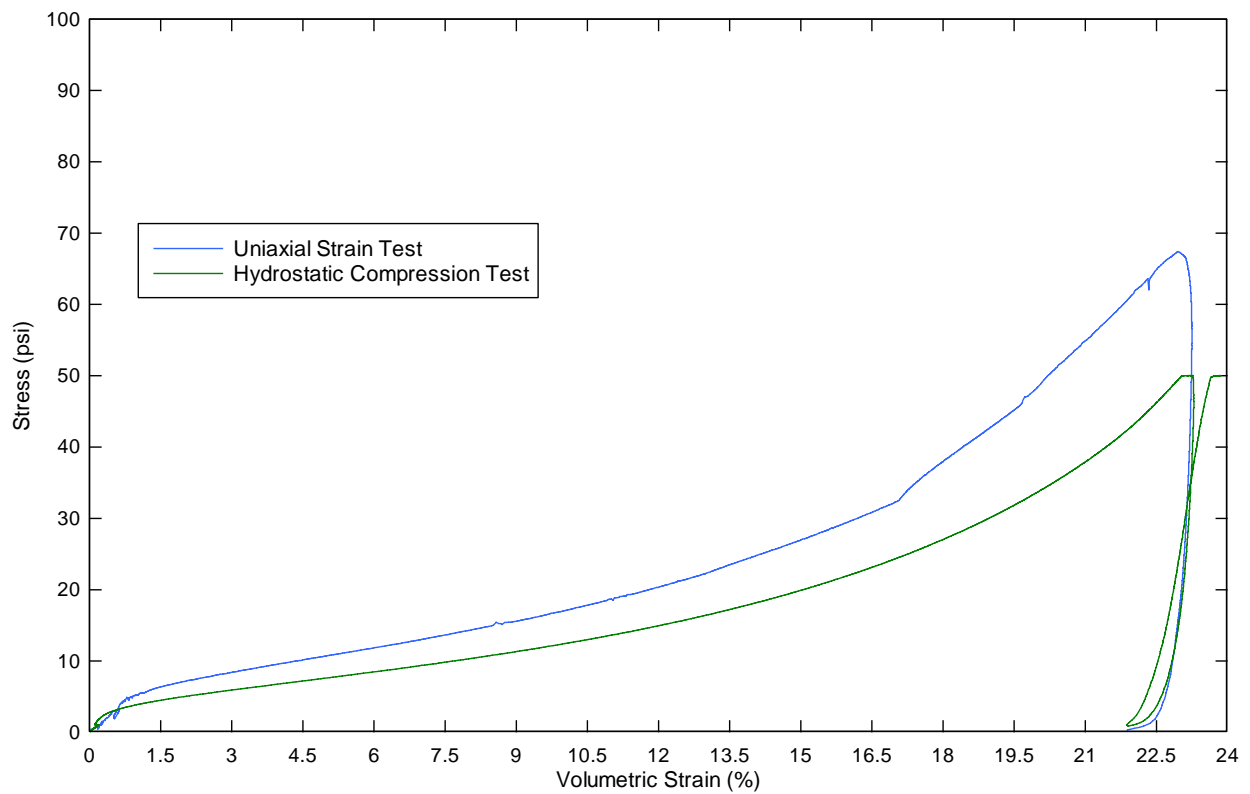


Figure 7-5: Carson Sink Wet soil hydrostatic compression test results. Uniaxial strain data shown for comparison. Note similar slopes.

7.2.4 Uniaxial strain

Uniaxial strain tests for Carson Sink Wet model are shown in the following five figures.

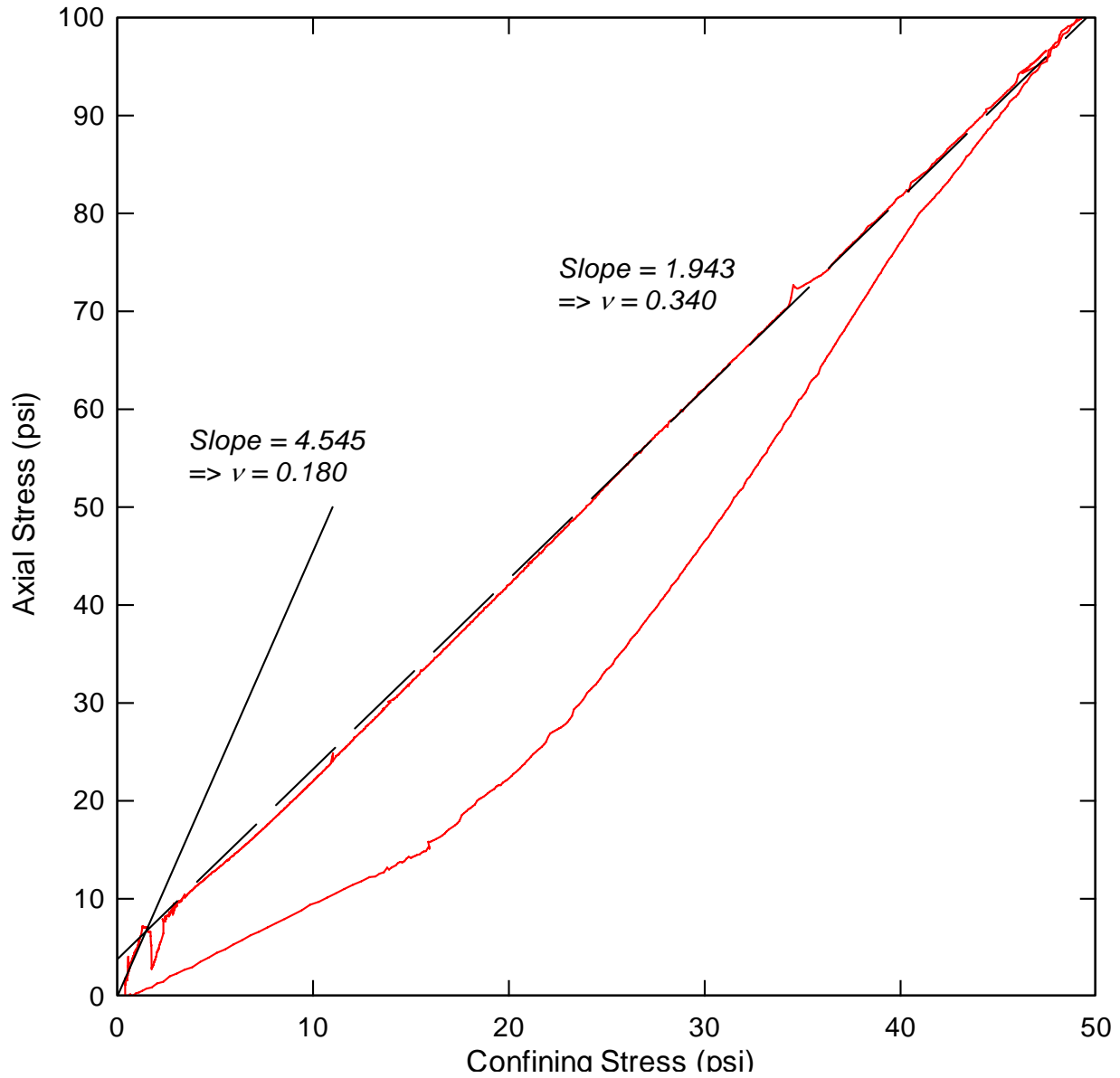


Figure 7-6: Carson Sink Wet model's uniaxial strain test. Axial stress vs. confining stress plotted to obtain Poisson's ratio from slopes.

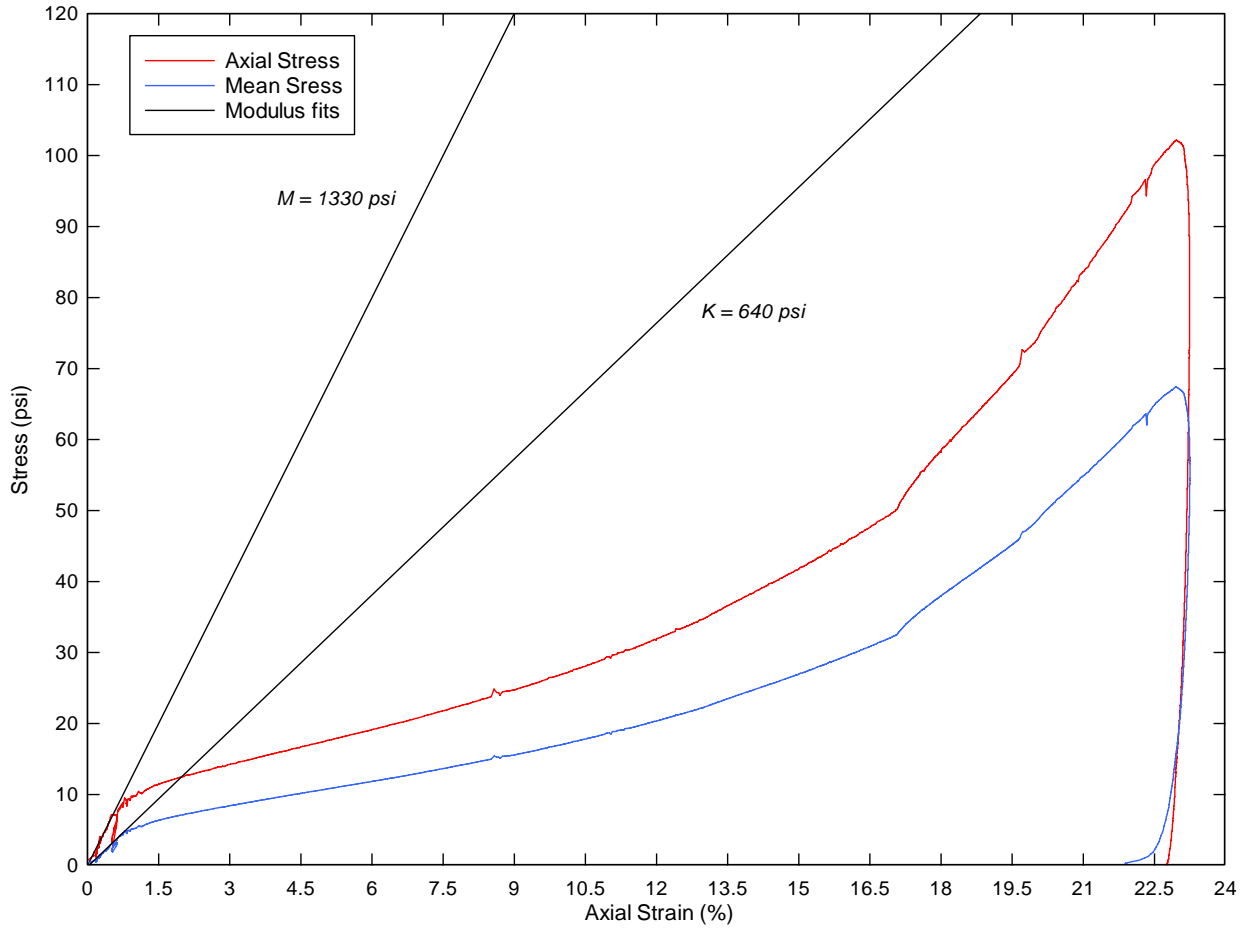


Figure 7-7: Carson Sink Wet model's uniaxial strain test. Stress vs. strain plotted to obtain constrained modulus M and bulk modulus K.

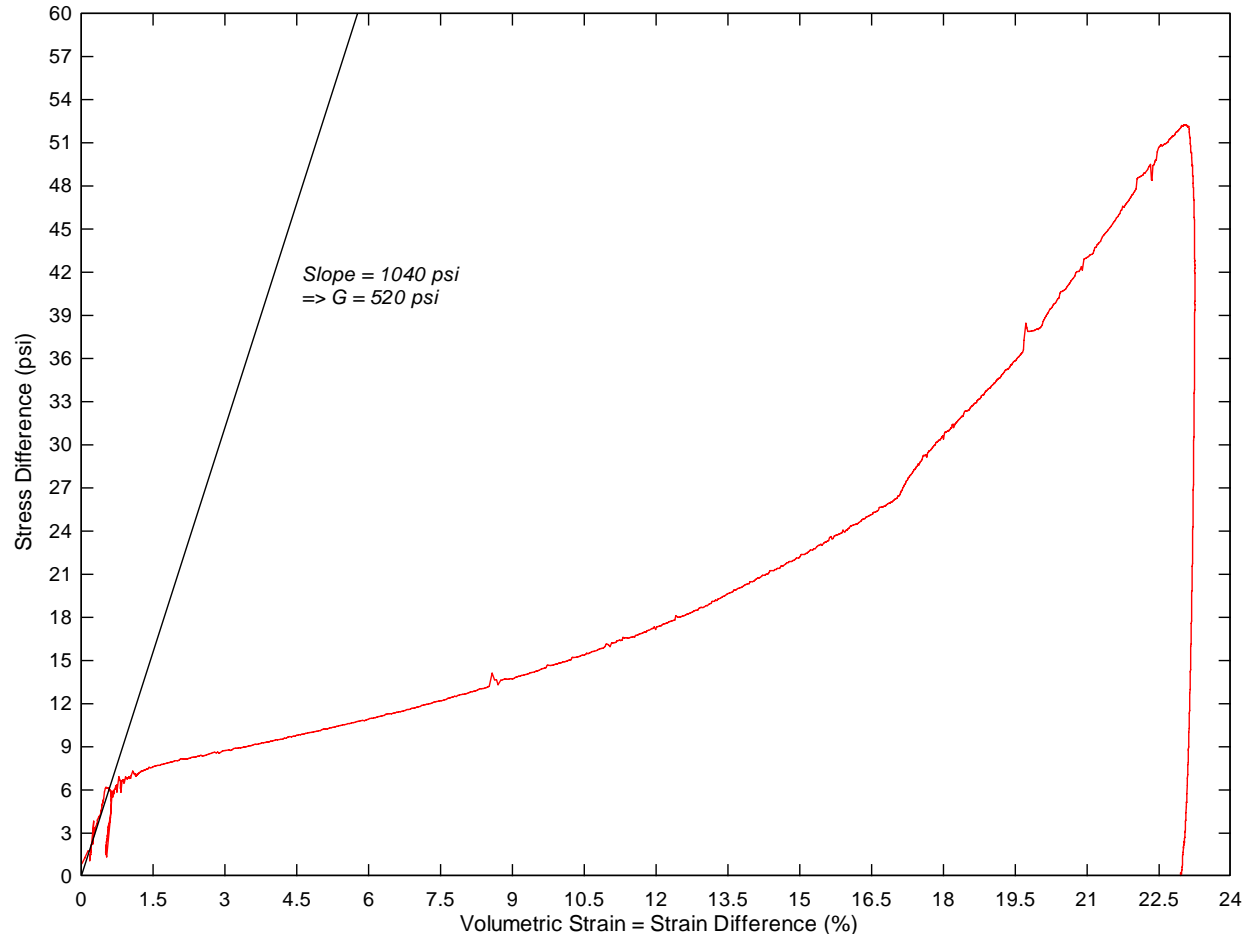


Figure 7-8: Carson Sink Wet model's uniaxial strain test. Stress difference vs. strain difference plotted to obtain shear modulus G from initial slope.

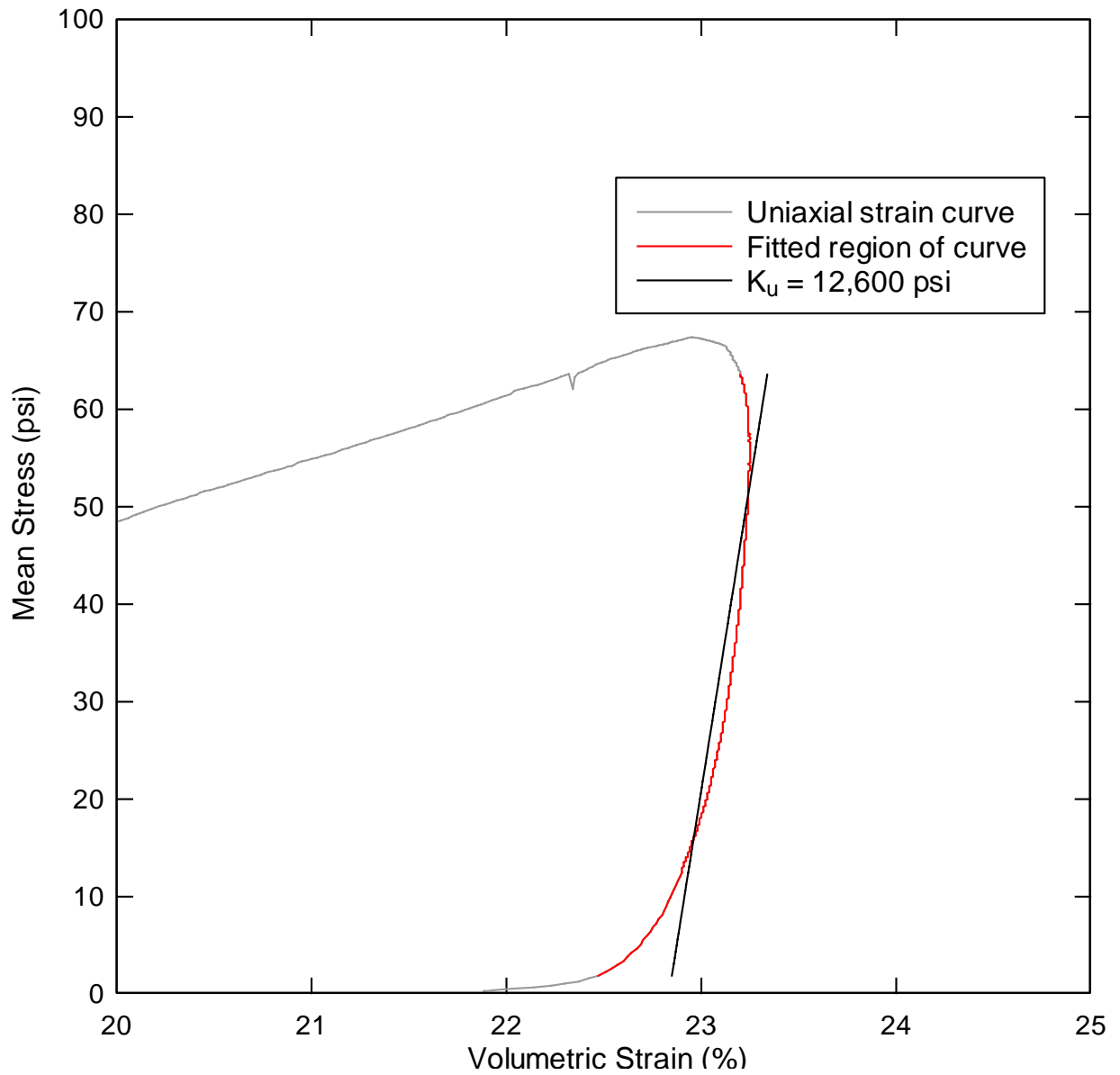


Figure 7-9: Carson Sink Wet model's uniaxial strain test. Mean stress vs. volumetric strain plotted to obtain bulk unload modulus K_u (BULK). Black line is linear fit to the red portion of the test data curve.

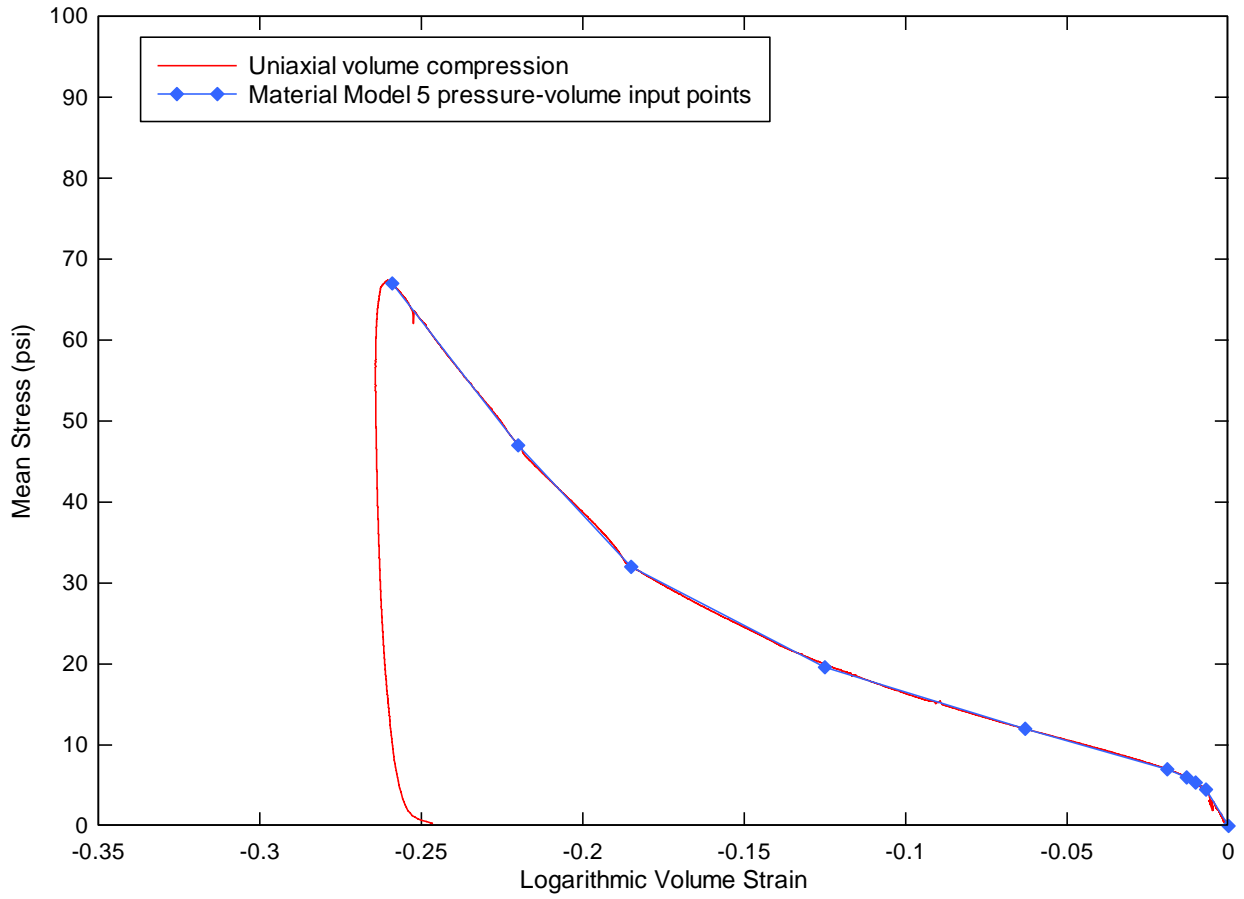


Figure 7-10: Carson Sink Wet model uniaxial strain test. Mean stress vs. logarithmic volume strain plotted to obtain 10 points on Material Model 5's pressure-volume curve.

7.3 LS-DYNA Material Model 5 inputs

The recommended set of inputs for modeling Carson Sink Wet in LS-DYNA Material Model 5: Soil and Foam is shown in the table below. It is assembled from field wet density, triaxial compression, hydrostatic compression, and uniaxial strain test data.

Table 7-2: Material Model 5 inputs for Carson Sink Wet soil.

	<u>Input</u>	<u>Value</u>	<u>Units</u>			
Mass density	RO	0.000135	lb s ² /in ⁴			
Shear modulus	G	500	psi			
Bulk unloading modulus	K	12600	psi			
Yield surface coefficient	A0	1.968	psi ²			
Yield surface coefficient	A1	1.858	psi			
Yield surface coefficient	A2	0.439	-			
Pressure cutoff	PC	-1.0	psi			
	<u>Input</u>	<u>Value</u>	<u>Input</u>	<u>Value</u>	<u>Units</u>	
Pressure-volume point	EPS1	0	P1	0	psi	
Pressure-volume point	EPS2	-0.007	P2	4.5	psi	
Pressure-volume point	EPS3	-0.0102	P3	5.36	psi	
Pressure-volume point	EPS4	-0.013	P4	6	psi	
Pressure-volume point	EPS5	-0.019	P5	7	psi	
Pressure-volume point	EPS6	-0.063	P6	12	psi	
Pressure-volume point	EPS7	-0.125	P7	19.6	psi	
Pressure-volume point	EPS8	-0.185	P8	32	psi	
Pressure-volume point	EPS9	-0.22	P9	47	psi	
Pressure-volume point	EPS10	-0.259	P10	67	psi	

Table 7-3: Summary of elastic constants for Carson Sink Wet soil.

Constrained Modulus - M	1330	psi
Poisson's Ratio - n	0.18	
Young's Modulus - E	1220	psi
Bulk Modulus - K	640	psi
Shear Modulus - G	520	psi

7.4 Recommended range of model application

The Carson Sink Wet model is recommended for use during the wet season at Carson Sink. It can also be used as an estimate for the wet season environment at Cuddeback Lake.

8 Soil to soil comparisons

Plots of model to model comparisons are shown here to demonstrate the relative strengths and softness of each soil model. Ranked from strongest to weakest in terms of strength envelopes, the order is: Cuddeback Soil A, Cuddeback Soil B, Carson Sink Dry, and Carson Sink Wet. The ranking order in terms of deformation (softness), is the same. The next two figures illustrate this comparison.

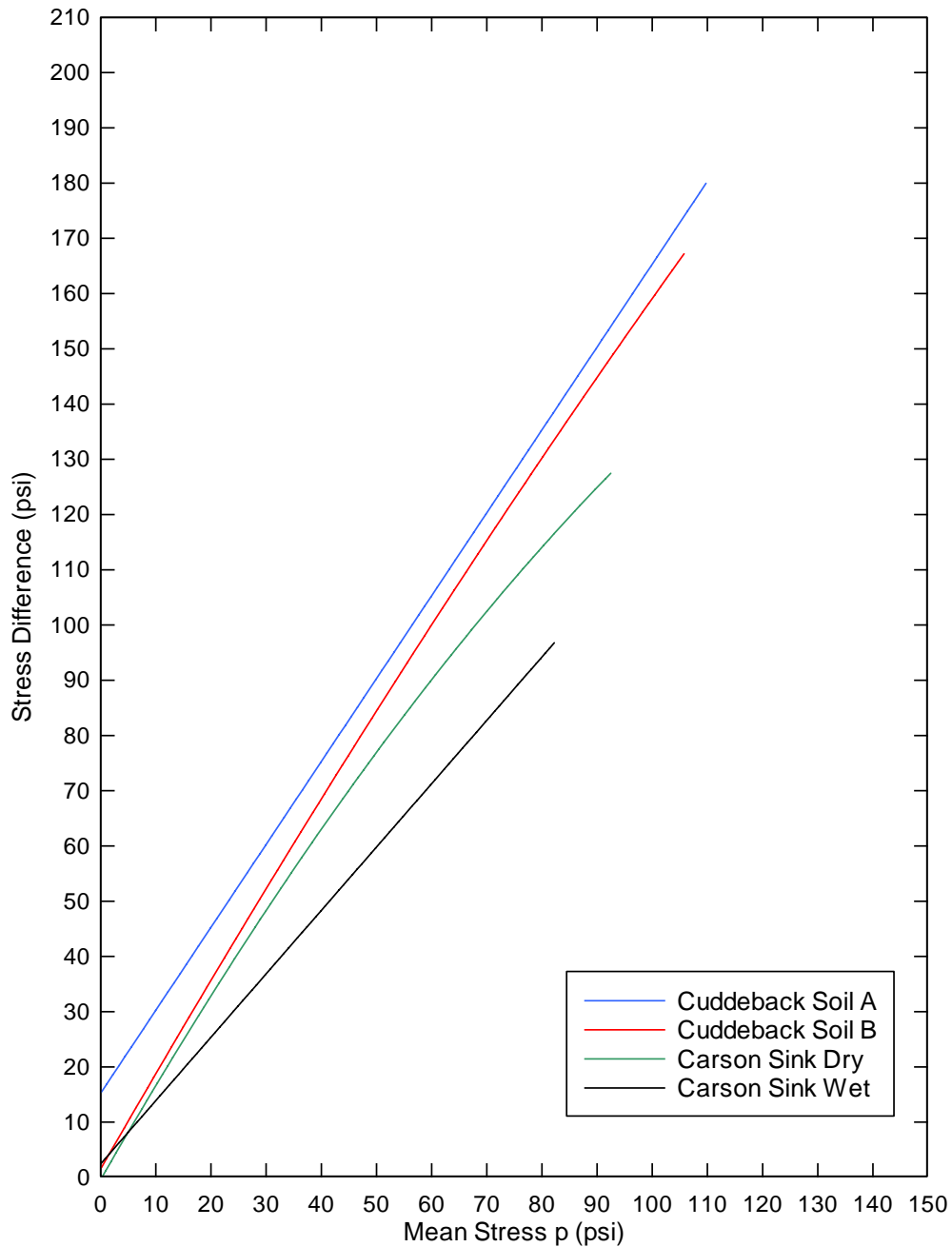


Figure 8-1: Comparison of soil strengths between models.

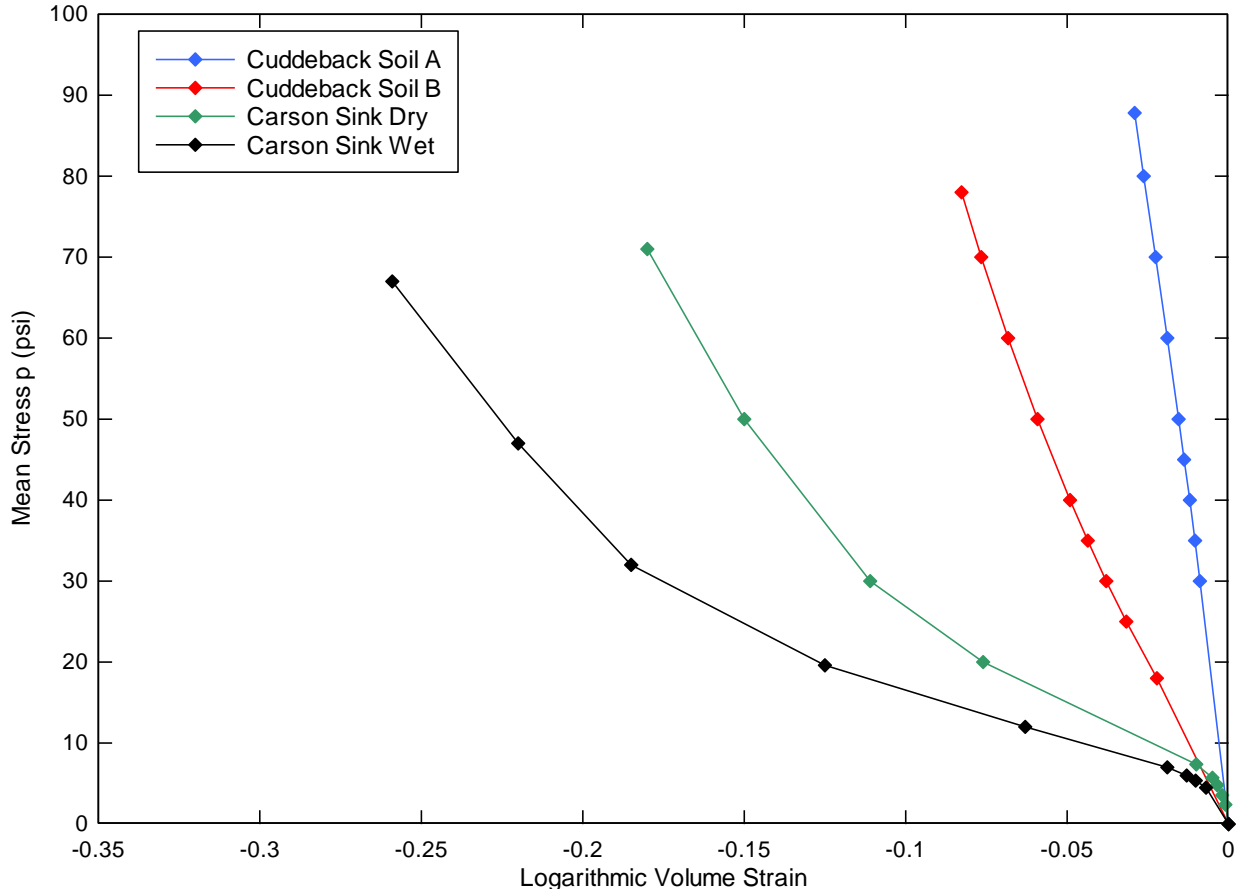


Figure 8-2: Comparison of soil softness between models.

9 Closing Remarks

The soil models presented here are based on static strength and compressibility tests. No attempt was made at impact loading the soil, nor accounting for strain rate effects. All test specimens were reconstituted from field dug samples.

LS-DYNA *Material Model 5: Soil and Foam* is a basic model well suited for preliminary design purposes. However, this is not the only soil model available. There have been many pressure-dependent material strength models developed for LS-DYNA, one of which is Material Model 25, the *Geological Cap* model. It is more complex than Material Model 5 because it uses kinematic hardening parameters. It uses two surfaces, an initial yield surface and a failure surface. The kinematic hardening parameters alter the behavior of the soil when moving from the initial yield to failure. This feature makes Material Model 25 a higher fidelity soil model because it accounts for more dynamic effects. The laboratory tests required to construct Material Model 25 are the same as Material Model 5. Using the test data for presented here with additional calibration effort, it is possible to construct a *Geological Cap* model.

Appendix A: LS-DYNA Theory Manual for Material Model 5

Appendix A is taken from the “LS-DYNA Theory Manual,” 2006, Livermore Software Technology Corporation, Livermore, California. The excerpts shown below are from the Material Model 5 description starting on Page 19.21 of the LS-DYNA Theory Manual.

LS-DYNA is a registered trademark of the Livermore Software Technology Corporation.

The following boxed figures are copied from the LS-DYNA Theory Manual. The copied pages refer to the equations used in deriving constitutive parameters in Chapter 3.

Material Model 5: Soil and Crushable Foam

This model, due to Krieg [1972], provides a simple model for foam and soils whose material properties are not well characterized. We believe the other foam models in LS-DYNA are superior in their performance and are recommended over this model which simulates the crushing through the volumetric deformations. If the yield stress is too low, this foam model gives nearly fluid like behavior.

A pressure-dependent flow rule governs the deviatoric behavior:

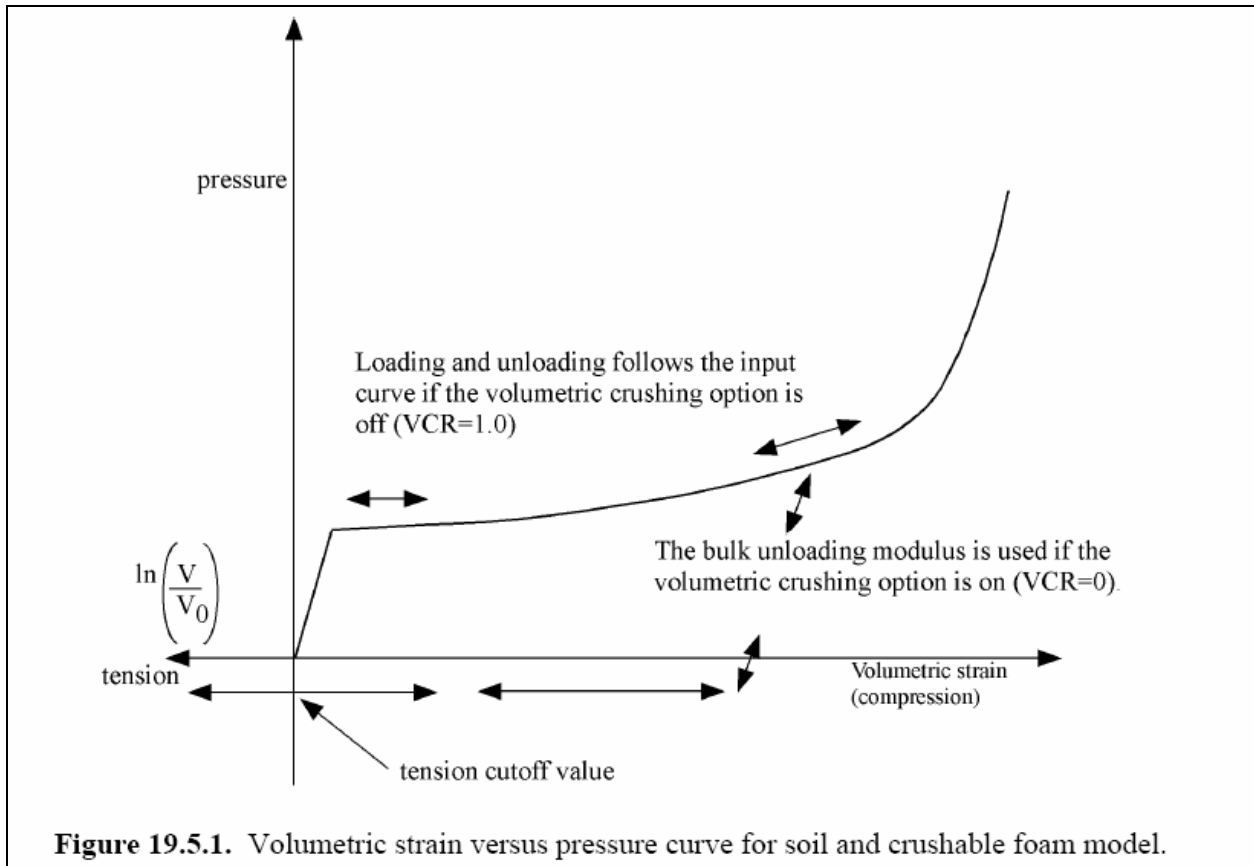
$$\phi_s = \frac{1}{2} s_{ij} s_{ij} - (a_0 + a_1 p + a_2 p^2) \quad (19.5.1)$$

where a_0 , a_1 , and a_2 are user-defined constants. Volumetric yielding is determined by a tabulated curve of pressure versus volumetric strain. Elastic unloading from this curve is assumed to a tensile cutoff as illustrated in Figure 19.5.1.

Implementation of this model is straightforward. One history variable, the maximum volumetric strain in compression, is stored. If the new compressive volumetric strain exceeds the stored value, loading is indicated. When the yield condition is violated, the updated trial stresses, s_{ij}^* , are scaled back using a simple radial return algorithm:

$$s_{ij}^{n+1} = \left(\frac{a_0 + a_1 p + a_2 p^2}{\frac{1}{2} s_{ij}^* s_{ij}^*} \right)^{1/2} s_{ij}^* \quad (19.5.2)$$

If the hydrostatic tension exceeds the cutoff value, the pressure is set to the cutoff value and the deviatoric stress tensor is zeroed.



Krieg, R. D., "A Simple Constitutive Description for Cellular Concrete," Sandia National Laboratories, Albuquerque, NM, Rept. SC-DR-72-0883 (1972).

Appendix B: Field Data

The field summary, documenting physical observations at each site, is attached in Appendix B. Raw DCP data for Carson Sink and Cuddeback Lake are also attached.

Soil Evaluation Samples				Unified	WGS84 N (m)	WGS84 E (m)	Elevation (m)	GeoVane 19mm	GeoVane 34mm		Test Depth	WGS84 N (m)	WGS84 E (m)	Wet Density (lbs/ft ³)	Water content (%) w%=Mwater / Msoil	Dry Density (lbs/ft ³)	Tech's Notes				
Location	Sample	Depth	Description														Comment	Test #			
Cuddeback Lake	CD	1	0-6"	Brown fine to coarse sand with silt, occasional gravel and trace clay, moist, med dense to dense	SM	3905170.862	453029.8415	2665		60,129.60,53,125 (0-2")	Non-cohesive soil	0'-6"	3905171	453030	105.30	0.96	104.30		1	1	
													3905171	453030	104.20		104.20		2	1	
													3905171	453030	104.40	0.66	103.70		3	1	
													3905171	453030	101.80	1.01	100.80		4	1	
													3905171	453030	102.40	1.40	101.00		5	1	
Cuddeback Lake	CD	2	0-6"	Brown fine to coarse sand with silt, occasional gravel, cobble and trace clay, moist, loose to dense (w/depth)	SM	3905942.342	454673.2532	2602		44,47,50,52,70,62 (0-2") 32 (10-12")	Non-cohesive soil	0'-2"	3905907	454666	99.70	0.33	99.40		7	2	
													Surface	3905907	454666	101.10	0.36	100.80		8	2
													0'-10"	3905907	454666	97.90	1.11	96.90		9	2
													0'-12"	3905907	454666	103.40		103.40		10	2
													0'-12"	3905907	454666	102.80	1.27	101.70		11	2
													0'-12"	3905907	454666	101.90	1.36	100.60		12	2
													0'-12"	3905907	454666	101.50	1.24	100.30		13	2
													0'-12"	3905907	454666	99.30	1.52	97.80	2 ft to the north	14	2
Cuddeback Lake	CD	3	0-6"	Brown sandy silt with clay moist and soft (moisture increased with depth)	ML	3906345.987	455981.8244	2550	56 (7-10")	78,54,114,16,22,37 (0-2") 40,17,130 (7-10")	Cohesive soil	0'-6"	3906339	455983	71.80	0.64	71.40		15	3	
													3906339	455983	70.20	1.37	69.30		16	3	
													3906339	455983	72.40	2.23	70.80		17	3	
													3906339	455983	69.50	1.96	68.20		18	3	
													3906339	455983	84.80	2.17	83.00	2 ft to the north	19	3	
													6'-12"	3906339	455983	101.30	6.14	95.47		20	4
													6'-12"	3906339	455983	99.10	7.05	92.50		21	4
													6'-12"	3906339	455983	95.50	7.59	88.70		22	4
													6'-12"	3906339	455983	98.00	7.06	91.50		23	4
													Cuddeback Lake	CD	4	0-6"	Brown clay with silt moist and stiff	CH/CH	3906562.954	456522.9434	2537
3906560	456527	94.10	3.78	90.70	2 ft to the north	25	4														
3906560	456527	91.70	4.28	87.90		26	4														
3906560	456527	88.90	4.18	85.30		27	4														
0'-6"	3906560	456527	91.20	4.09	87.70		28	4													
0'-6"	3906560	456527	92.10	3.92	88.70		29	4													
0'-6"	3906560	456527	92.90	3.80	89.40		30	4													
0'-6"	3906560	456527	88.30	3.83	85.10		31	4													

Soil Evaluation Samples				Unified	WGS84 N (m)	WGS84 E (m)	Elevation (m)	GeoVane 19mm	GeoVane 34mm		Test Depth	WGS84 N (m)	WGS84 E (m)	Wet Density (lbs/ft ³)	Water content (%) w%=Mwater / Msoil	Dry Density (lbs/ft ³)	Tech's Notes			
Location	Sample	Depth	Description														Comment	Test #		
Cuddeback Lake	CD	5	4-12"	Brown silt with sand and clay moist and stiff	ML/MH	3907853.495	459710.87	2557'	10,12,14,32,28 (0-2") 110, 140+ (6-8")		Cohesive soil	0'-6"	3907854	459253	95.00	1.69	83.40		32	5
												0'-6"	3907854	459253	91.80	2.35	89.50		33	5
												0'-6"	3907854	459253	89.90	1.78	88.30		34	5
												0'-6"	3907854	459253	89.10	1.54	87.70		35	5
												6'-12"	3907854	459253	98.60	6.24	91.10		36	5
												6'-12"	3907854	459253	103.50	8.41	95.40		37	5
												6'-12"	3907854	459253	107.50	7.67	99.90		38	5
												6'-12"	3907854	459253	102.40	8.57	94.30		39	5
												Cuddeback Lake	CD	6	0-6"	Brown silty fine to coarse sand with occasional gravel, moist and med dense	SM	3906795.278	486564.9325	2895'
Cuddeback Lake	CD	7	0-6"	Brown silt with occasional sand, moist to dry and soft (Dune)	ML	3907667	458466	774	none measured	none measured	Sand Dune	0'-6"	3907667	458466	81.20	1.75	79.80		69	
												6'-9"	3907667	458466	83.20	3.40	80.50	20 ft to the east	70	
												9'-12"	3907667	458466	81.90	4.28	77.00		71	
												12"-23"	3906414	457289	105.90	11.16	95.20		72	
												12"-18"	3906414	457289	104.70	11.87	93.60		73	
												0'-8"	3906414	457289	88.50	3.50	85.50		74	
												0'-6"	3906414	457289	88.40	3.55	85.40	20 ft to the east	75	
												0'-4"	3906414	457289	90.00	3.52	86.90	20 ft to the east	76	
												0'-2"	3906414	457289	88.30	3.84	85.10	20 ft to the east	77	
												6'-16"	3906414	457289	98.90	6.82	92.50		78	
												6'-14"	3906414	457289	96.40	6.46	90.50		79	
6'-12"	3906414	457289	91.70	6.54	86.10		80													
6'-10"	3906414	457289	85.10	7.19	79.40		81													
Cuddeback Lake	CD	8	0-6"	Light Brown/white silty fine to coarse sand with occasional gravel, trace organics (sagebrush, lichen/moss type of plant life) moist medium dense	SM/ML	3902682.921	454610.4838	781	none measured	none measured	Shoreline Area	6'-8"	3906414	457289	78.30	7.89	72.50	10 ft to the east	82	
												0'-6"	3902690	454629	103.70	9.30	103.40		83	
												6'-12"	3902690	454629	104.00	2.66	101.30		84	
												0'-6"	3902690	454629	102.40	0.45	101.90	5 ft to the east	85	
												6'-12"	3902690	454629	106.90	2.57	104.20		86	

Sample 1 (Lakebed Soil "Type A")				WGS84 N	WGS84 E	Elevation	GeoVane	GeoVane	Test Depth	WGS84	WGS84 E	Wet Density	Water content (%)	Dry Density	Comment	Tech's Notes	
Location	Sample	Depth	Description	Unified	(m)	(m)	(m)	19mm	34mm	(m)	(m)	(lbs/ft^3)	w%=Mwater / Msoil	(lbs/ft^3)		Test #	
Cuddeback Lake	CDL	1	no sample		3904616	457515	79.92.98 (0-6")					3.52	95.2	92.5			
Cuddeback Lake	CDL	2	no sample		3904249	456326	90.110.160 (0-6")					none					
Cuddeback Lake	CDL	3	no sample		3902691	455826	140+70,114.52 (0-2")					none					
Cuddeback Lake	CDL	4	0-6" Clay with occasional sand moist very stiff		3906414.102	457268.6827	64.86.86 (0-6")					3.23	93.5	90.6			
Cuddeback Lake	CDL	5	?														
Cuddeback Lake	CDL	6	0-6" Clay with occasional sand moist very stiff		3906416.277	458190.1251	None Measured	None Measured									
Cuddeback Lake	CDL	7	6-12" Clay with occasional sand moist very stiff		3906416.277	458190.1251	None Measured	None Measured									
Cuddeback Lake	CDL	8	0-6" Clay with occasional sand moist very stiff		3906416.277	458190.1251	None Measured	None Measured									
Cuddeback Lake	CDL	9	12-15" Clay with occasional sand moist very stiff		3906416.277	458190.1251	None Measured	None Measured									
Cuddeback Lake	CDL	10	15-18" Clay with occasional sand moist very stiff		3906416.277	458190.1251	None Measured	None Measured									
Cuddeback Lake	CDL	11	15-18" Clay with occasional sand moist very stiff		3906416.277	458190.1251											
Cuddeback Lake	CDL	12	0-5" Mud cracks, Clay with silt, occasional sand and gravel, almost dry and very stiff	CL/CH	3902191	455664	783	None Measured	None Measured	0'-6"	3902192	455661	92.60	4.81	88.30		
Cuddeback Lake	CDL	13	0.5-3" Lt Brown Clay with silt, occasional sand and gravel, almost dry and very stiff	CL/CH	3902191	455664	783	None Measured	None Measured	6"-12"	3902192	455661	90.00	6.54	84.40		87
Cuddeback Lake	CDL	14	3-6" Lt Brown Clay with silt, occasional sand, almost dry and very stiff	CL/CH	3902191	455664	783	None Measured	None Measured	12"-23"	3902192	455661	101.90	9.09	93.40		88
Cuddeback Lake	CDL	15	6-9" Lt Brown Clay with silt, occasional sand, almost dry and very stiff	CL/CH	3902191	455664	783	None Measured	None Measured	12"-18"	3902192	455661	96.40	9.49	88.10		89
Cuddeback Lake	CDL	16	9-12" Lt Brown Clay with silt, occasional sand, moist and very stiff	CL/CH	3902191	455664	783	None Measured	None Measured	0'-9"	3902192	455661	96.40	3.98	92.70		90
Cuddeback Lake	CDL	17	12-18" grey to Brown Clay with silt, occasional sand and gravel, almost dry and very stiff	CL/CH	3902191	455664	783	None Measured	None Measured	0'-6"	3902192	455661	92.50	4.48	88.50		91
Cuddeback Lake	CDL	18	0-6" Lt Brown Clay with silt, occasional sand and gravel, almost dry and very stiff	CL/CH	3902191	455664	783	None Measured	None Measured	0'-3"	3902192	455661	90.10	4.42	86.30	10 ft to the east	92
Cuddeback Lake	CDL	19	0-6" Lt Brown Clay with silt, occasional sand and gravel, almost dry and very stiff	CL/CH	3902191	455664	783	None Measured	None Measured	6'-16"	3902192	455661	94.60	6.70	87.90	10 ft to the east	93
Cuddeback Lake	CDL	20	0-3" Lt Brown Clay with silt, occasional sand, almost dry and very stiff	CL/CH	3903870	456122	783	None Measured	None Measured	6'-12"	3902192	455661	96.10	7.87	89.10		94
Cuddeback Lake	CDL	21	3-6" Lt Brown Clay with silt, occasional sand, almost dry and very stiff	CL/CH	3903870	456122	783	None Measured	None Measured	6'-9"	3902192	455661	93.90	8.65	86.40		95
Cuddeback Lake	CDL	22	6-9" Lt Brown Clay trace silt, occasional sand, moist and very stiff	CL/CH	3903870	456122	783	None Measured	None Measured	0'-6"	3903867	456122	92.30	3.74	88.90	20 ft to the east	96
Cuddeback Lake	CDL	23	9-12" Lt Brown Clay trace silt, occasional sand, moist and very stiff	CL/CH	3903870	456122	783	None Measured	None Measured	6'-12"	3903867	456122	95.60	7.94	88.60		101
Cuddeback Lake	CDL	24	12-15" Lt Brown Clay trace silt, occasional sand, moist and very stiff	CL/CH	3903870	456122	783	None Measured	None Measured								102
Cuddeback Lake	CDL	25	15-18" Lt Brown Clay trace silt, occasional sand, moist and very stiff	CL/CH	3903870	456122	783	None Measured	None Measured								
Cuddeback Lake	CDL	26	0-6" Lt Brown Clay with silt, occasional sand and gravel, almost dry and very stiff	CL/CH	3903870	456122	783	None Measured	None Measured								
Cuddeback Lake	CDL	27	0-6" Lt Brown Clay with silt, occasional sand and gravel, almost dry and very stiff	CL/CH	3903870	456122	783	None Measured	None Measured								

Sample 2 (Shoreline Soil "Type B")																	
Location	Sample	Depth	Description	Unified	WGS84 N (m)	WGS84 E (m)	Elevation (m)	GeoVane 19mm	GeoVane 34mm	Test Depth	WGS84 (m)	WGS84 E (m)	Wet Density (lbs/ft^3)	Water content (% w%=Mwater / Msoil)	Dry Density (lbs/ft^3)	Tech's Notes	
Cuddeback Lake	CDS	1	0-3'	Lt Brown Sandy Silt with occasional gravel moist to dry and loose	SMML	3906195	455969	785	10,13,4,8,9,10,22,8,6,7,10(0-3")	0'-6"	3906195	455969	68.00	1.91	66.70		
Cuddeback Lake	CDS	2	3-6'	Lt Brown Sandy silt medium dense moist med dense	SMML	3906195	455969	785	36,38,18,42,20,36,26,35 (3-6")	6'-12"	3906195	455969	93.50	7.59	86.90	107	
Cuddeback Lake	CDS	3	6-9'	lt brown with orange mottling, Sandy silt, moist and hard	SMML	3906195	455969	785	too hard	9'-15"	3906195	455969	94.70	10.26	85.90	108	
Cuddeback Lake	CDS	4	9-12'	lt Brown Sandy silt, moist and hard	SMML	3906195	455969	785	too hard	12'-23"	3906195	455969	101.60	11.36	91.20	109	
Cuddeback Lake	CDS	5	12-15'	lt Brown Sandy silt, moist and hard	SMML	3906195	455969	785	too hard	12'-18"	3906195	455969	102.90	11.80	92.10	110	
Cuddeback Lake	CDS	6	15-18'	lt Brown Sandy silt, moist and hard	SMML	3906195	455969	785	too hard							111	
Cuddeback Lake	CDS	7	0-6'	Lt Brown Sandy Silt with moist to dry and soft	ML	3906195	455962	785	22,30,34,20 (0-6")								
Cuddeback Lake	CDS	8	0-6'	Lt Brown Sandy Silt with moist to dry and soft	ML	3906192	455962	785	None Measured	None Measured							
Cuddeback Lake	CDS	9	0-6'	Lt Brown Silty fine to coarse Sand with occasional gravel moist to wet and loose	SM	3907979	458424	785	34,33,28,42,14,36,22	0'-6"	3907979	458422	82.50	0.61	82.00		
Cuddeback Lake	CDS	10	0-6'	Lt Brown Silty fine to coarse Sand with occasional gravel moist to wet and loose	SM	3907976	458427	785		6'-17"	3907976	458422	109.00	4.38	104.40	20 ft to the east	
Cuddeback Lake	CDS	11	0-3'	Lt Brown Silty fine to coarse Sand, loose and moist to wet	SM	3907980	458425	784	None Measured	None Measured	6'-12"	3907979	458422	101.20	3.70	97.60	113
Cuddeback Lake	CDS	12	3-6'	Lt Brown Silty fine to coarse Sand, loose and moist to wet	SM	3907980	458425	784	None Measured	None Measured	12'-18"	3907979	458422	103.50	6.50	97.20	114
Cuddeback Lake	CDS	13	6-9'	lt Brown Sandy silt, moist and hard	SMML	3907980	458425	784	None Measured	None Measured	18'-24"	3907979	458422	103.90	7.29	96.20	115
Cuddeback Lake	CDS	14	9-12'	lt Brown Sandy silt, moist and hard	SMML	3907980	458425	784	None Measured	None Measured						116	
Cuddeback Lake	CDS	15	12-15'	lt Brown Sandy silt, moist and hard	SMML	3907980	458425	784	None Measured	None Measured							
Cuddeback Lake	CDS	16	15-18'	lt Brown Sandy silt, moist and hard	SMML	3907980	458425	784	None Measured	None Measured							
Cuddeback Lake	CDS	17	0-3'	Red-Brown Silty fine to coarse Sand with occasional gravel, moist and Medium dense	SM	3907210	458872		8,6,14,16	0'-6"	3907210	458872	84.60	1.59	83.30		
Cuddeback Lake	CDS	18	3-6'	Red-Brown silty fine to coarse Sand, moist and loose	SM	3907210	458872		None Measured	None Measured	6'-12"	3907210	458872	87.10	3.59	84.10	10 ft to the east
Cuddeback Lake	CDS	19	6-9'	Red-Brown silt with sand, moist and medium stiff	SMML	3907210	458872		None Measured	None Measured	9'-20"	3907210	458872	93.70	4.07	90.00	
Cuddeback Lake	CDS	20	9-12'	Red-Brown silt with sand, moist and stiff	SMML	3907210	458872		74,90,94,70,72,91	0'-6"	3907210	458872	78.80	1.11	77.90	5 ft to the north	
Cuddeback Lake	CDS	21	12-15'	Red-Brown silt with sand, moist and stiff	SMML	3907210	458872		None Measured	None Measured	6'-12"	3907210	458872	84.50	4.56	88.50	5 ft to the north
Cuddeback Lake	CDS	22	15-18'	Red-Brown silt with sand, moist and stiff	SMML	3907210	458872		None Measured	None Measured	6'-17"	3907210	458872	88.40	4.16	84.90	5 ft to the north
Cuddeback Lake	CDS	23	0-6'	Red-Brown Silty fine to coarse Sand with occasional gravel, moist and Med dense to loose	SM	3907210	458872		16,13,20,22,26							121	
Cuddeback Lake	CDS	24	0-6'	Red-Brown Silty fine to coarse Sand with occasional gravel, moist and Med dense to loose	SM	3907210	458872		None Measured	None Measured						122	

General Density Sampling	Test D	WGS84 N	WGS84 E	Wet Density (lbs/ft ³)	Water content (%) w%=Mwater / Msoil	Dry Density (lbs/ft ³)	Comment	Tech's Notes
		(m)	(m)					Test #
	0'-6"	3902952	455829	94.60	3.73	91.20		97
	6'-12"	3902952	455829	97.80	6.87	91.50		98
	0'-6"	3903526	455997	93.30	3.87	89.80		99
	6'-12"	3903526	455997	92.20	8.28	85.20		100
	0'-6"	3904986	455981	101.10	1.71	99.40		103
	6'-12"	3904986	455981	94.10	6.32	88.50		104
	0'-6"	3904638	457326	99.70	1.73	98.00		105
	6'-9"	3904638	457326	94.40	2.81	91.80	10 ft to the east	106
	0'-2"	3906862	462003	93.80	0.28	93.50		40
	0'-2"	3906862	462003	93.30	0.02	93.30		41
	0'-2"	3906862	462003	92.20	0.52	91.70		42
	0'-2"	3906862	462003	92.40	0.45	92.00		43
	6'-8"	3906862	462003	96.30	1.39	95.00		44
	6'-8"	3906862	462003	92.70	1.39	91.47	20 ft to the east	45
	6'-8"	3906862	462003	93.70	1.44	92.30		46
	6'-8"	3906862	462003	95.90	1.93	94.10		47
	0'-6"	3906624	456733	88.10	4.20	84.60		48
	0'-6"	3906686	456905	89.70	4.12	86.20		50
	6'-12"	3906686	456905	95.90	7.34	89.40		51
	0'-6"	3906691	457397	89.10	4.26	85.50		52
	6'-12"	3906691	457397	93.80	6.14	88.30		53
	0'-6"	3906786	456498	92.40	3.30	89.50		54
	6'-12"	3906786	456498	94.50	6.75	88.50		55
	0'-6"	3905616	457514	95.20	3.52	91.90		56
	6'-12"	3905616	457514	96.20	7.63	91.30	20 ft to the east	57
	0'-6"	3904249	456325	89.60	3.43	86.60		58
	6'-12"	3904249	456325	101.90	5.75	96.40		59
	0'-6"	3904249	456325	91.10	3.61	88.00		60
	0'-6"	3902692	455828	100.30	3.22	97.10		61
	6'-12"	3902692	455828	93.70	9.81	85.30	5 ft to the east	62
	0'-6"	3902692	455828	95.00	3.51	91.70		63
	6'-12"	3902692	455828	96.60	6.27	90.90		64
	0'-6"	3901889	456445	100.20	0.80	99.40		65
	6'-12"	3901889	456445	100.70	4.50	96.40	10 ft to the east	66
	0'-6"	3906414	457269	93.50	3.23	90.60		67
	6'-12"	3906414	457269	93.80	6.16	88.40		68

Carson Sink Soil Descriptions															WGS84 N	WGS84 E	Elevation	Location	Depth	34mm GeoVane Data	Depth	34mm GeoVane Data	UTM Northing	UTM Easting	Date	Test #	Latitude (degrees only)	Longitude (degrees only)	Depth tested	Wet Density (lbs/ft ³)	Water content (% w/w-Mwater / Msol)	Dry Density (lbs/ft ³)	UTM Northing	UTM Easting	Depth Code
(E) East	Carson Sink	CAR	1	1-4"	Brown silty fine sand trace clay moist to dry and loose	SM	4403658	377268	1182	CAR Nuc	1	0-4"	52,58,84,70,50	4-8"	140+	4403660	377001	10/30/2007	1	39.774	118.43308	0 to 2"	65.2	2.7	65.2	4403656.068	377268.0456	0							
	Carson Sink	CAR	2	4-13"	Brown clayey fine sand trace silt moist to dry and med dense	SM	4403658	377268	1182									10/30/2007	2	39.774	118.43308	3-4"	75.3	2.8	73.2	4403656.068	377268.0456	3							
	Carson Sink	CAR	3	13-17"	Brown to grey clay moist to wet moderately stiff	CL/CH	4403658	377268	1182									10/30/2007	3	39.774	118.43308	6"	83.6	2.2	81.2	4403656.068	377268.0456	6							
	Carson Sink	CAR	4	17-21"	Brown clayey fine sand trace silt moist to dry and med dense	SM	4403658	377268	1182									10/30/2007	4	39.774	118.43308	12"	96.7	1.9	94.9	4403656.068	377268.0456	12							
																		10/30/2007	5	39.774	118.43308	18"	90.5	19.6	75.7	4403656.068	377268.0456	18							
(C) Center	Carson Sink	CAR	5	0-6"	Grey clay with occasional sand and trace silt moist and soft	ML/MH	4403750	372369	1177	CAR Nuc	4	0-4"	90,118,126	4-8"	140+	4403736	372393	10/30/2007	14	39.774	118.49017	0 to 2"	101.4	9.2	92.9	4403749.204	372378.7621	0							
	Carson Sink	CAR	6	6-12"	Grey clay with occasional sand and trace silt moist and moderately stiff	ML/MH	4403750	372369	1177									10/30/2007	15	39.774	118.49017	6"	95.0	9.6	86.7	4403749.204	372378.7621	6							
																		10/30/2007	16	39.774	118.49017	12"	96.1	9.4	87.8	4403749.204	372378.7621	12							
(C) Center	Carson Sink	CAR	7	0-5"	surface on lakebed wind deposited short dunes of less than a few inches are common, this sample was	SM	4403750	372369	1177									10/30/2007	17	39.774	118.49027	20' x 30'	87.6	3.3	84.8	4403744.907	372370.1236	0							
(N) North	Carson Sink	CAR	8	0-3"	Brown silty/clayey fine sand moist loose to med dense	SM	4408794	372670	1177									10/31/2007	44	39.8196	118.48782	0"	83.2	4.4	79.7	4408797.155	372664.0052	0							
	Carson Sink	CAR	9	3-6"	Brown clay with fine sand moist and very stiff	CL/CH	4408794	372670	1177									10/31/2007	45	39.8196	118.48782	6"	83.5	4.3	80.0	4408797.155	372664.0052	6							
	Carson Sink	CAR	10	6-22"	Brown-grey clay occasional sand moist and stiff	CL/CH	4408794	372670	1177									10/31/2007	46	39.8196	118.48782	12"	93.5	3.8	90.1	4408797.155	372664.0052	12							
	Carson Sink	CAR	11	22-27"	grey clay occasional sand moist med stiff to soft	CL/CH	4408794	372670	1177									10/31/2007	47	39.8196	118.48782	18"	95.4	12.5	84.8	4408797.155	372664.0052	18							
(S) South	Carson Sink	CAR	13	0-4"	Brown silty fine sand med moist and loose to medium dense	SM	4398894	372232		CAR Nuc	11	0-4"	28,42,40,48	4-8"	140+	4398853	372226	10/31/2007	33	39.7304	118.49095	2"	79.7	3.9	76.8	4398896.619	372231.1734	2							
	Carson Sink	CAR	14	4-7"	Brown clay with sand moist and moderately stiff	CL/CH	4398894	372232										10/31/2007	34	39.7304	118.49095	0"-2"	61.0	3.2	59.2	4398896.619	372231.1734	0							
	Carson Sink	CAR	15	7-16"	Brown clay occasional sand moist and stiff	CL/CH	4398894	372232										10/31/2007	35	39.7304	118.49095	6"	76.9	2.5	75.1	4398896.619	372231.1734	6							
	Carson Sink	CAR	16	16-24"	Grey clay moist and soft	CL/CH	4398894	372232										10/31/2007	36	39.7304	118.49095	12"	86.5	2.3	84.5	4398896.619	372231.1734	12							
																		10/31/2007	37	39.7304	118.49095	18"	89.5	12.7	79.4	4398896.619	372231.1734	18							
(W) West	Carson Sink	West		0-4"	Brown silty fine sand, moist, medium dense	SM	4404070	367302										10/31/2007	51	39.7744	118.54951	0"	79.3	8.2	73.3	4403866.55	367297.0764	0							
	Carson Sink	West		4-20"	Brown/Grey clay occasional sand, moist and med stiff to stiff	CL/CH	4404070	367302										10/31/2007	52	39.7744	118.54951	6"	81.8	6.8	76.6	4403866.55	367297.0764	6							
																		10/31/2007	53	39.7744	118.54951	12"	88.3	6.6	82.9	4403866.55	367297.0764	12							

Carson Sink Soil Descriptions																												
						WGS84 N	WGS84 E	Elevation	Location	Depth	34mm GeoVane Data	Depth	34mm GeoVane Data	UTM Northing	UTM Easting	Date	Test #	Latitude (degrees only)	Longitude (degrees only)	Depth tested	Wet Density (lbs/ft ³)	Water content (%) w%=Mwater / Msoil	Dry Density (lbs/ft ³)	UTM Northing	UTM Easting	Depth Code		
(E) East	Carson Sink	CAR	1	1-4"	Brown silty fine sand trace clay moist to dry and loose	SM	4403658	377268	1182	CAR Nuc	1	0-4"	52,58,84,70,50	4-8"	140+	4403660	377001	10/30/2007	1	39.774	118.43308	face to 2"	65.2	2.7	65.2	4403656.068	377268.0456	0
	Carson Sink	CAR	2	4-13"	Brown clayey fine sand trace silt moist to dry and med dense	SM	4403658	377268	1182									10/30/2007	2	39.774	118.43308	3-4"	75.3	2.8	73.2	4403656.068	377268.0456	3
	Carson Sink	CAR	3	13-17"	Brown to grey clay moist to wet moderately stiff	CL/CH	4403658	377268	1182									10/30/2007	3	39.774	118.43308	6"	83.6	2.2	81.2	4403656.068	377268.0456	6
	Carson Sink	CAR	4	17-21"	Brown clayey fine sand trace silt moist to dry and med dense	SM	4403658	377268	1182									10/30/2007	4	39.774	118.43308	12"	96.7	1.9	94.9	4403656.068	377268.0456	12
																		10/30/2007	5	39.774	118.43308	18"	90.5	19.6	75.7	4403656.068	377268.0456	18
(C) Center	Carson Sink	CAR	5	0-6"	Grey clay with occasional sand and trace silt moist and soft	ML/MH	4403750	372369	1177	CAR Nuc	4	0-4"	90,118,126	4-8"	140+	4403736	372393	10/30/2007	14	39.7741	118.49017	face to 2"	101.4	9.2	92.9	4403749.204	372378.7621	0
	Carson Sink	CAR	6	6-12"	Grey clay with occasional sand and trace silt moist and moderately stiff	ML/MH	4403750	372369	1177									10/30/2007	15	39.7741	118.49017	6"	95.0	9.6	86.7	4403749.204	372378.7621	6
																		10/30/2007	16	39.7741	118.49017	12"	96.1	9.4	87.8	4403749.204	372378.7621	12
(C) Center	Carson Sink	CAR	7	0-5"	surface on lakebed wind deposited short dunes of less than a few inches are common, this sample was	SM	4403750	372369	1177									10/30/2007	17	39.7741	118.49027	20' x 30'	87.6	3.3	84.8	4403744.907	372370.1236	0
(N) North	Carson Sink	CAR	8	0-3"	Brown silty/clayey fine sand moist loose to med dense	SM	4408794	372670	1177									10/31/2007	44	39.8196	118.48782	0"	83.2	4.4	79.7	4408797.155	372664.0052	0
	Carson Sink	CAR	9	3-6"	Brown clay with fine sand moist and very stiff	CL/CH	4408794	372670	1177									10/31/2007	45	39.8196	118.48782	6"	83.5	4.3	80.0	4408797.155	372664.0052	6
	Carson Sink	CAR	10	6-22"	Brown-grey clay occasional sand moist and stiff	CL/CH	4408794	372670	1177									10/31/2007	46	39.8196	118.48782	12"	93.5	3.8	90.1	4408797.155	372664.0052	12
	Carson Sink	CAR	11	22-27"	grey clay occasional sand moist med stiff to soft	CL/CH	4408794	372670	1177									10/31/2007	47	39.8196	118.48782	18"	95.4	12.5	84.8	4408797.155	372664.0052	18
(S) South	Carson Sink	CAR	13	0-4"	Brown silty fine sand med moist and loose to medium dense	SM	4398894	372232		CAR Nuc	11	0-4"	28,42,40,48	4-8"	140+	4398853	372226	10/31/2007	33	39.7304	118.49095	2"	79.7	3.9	76.8	4398896.619	372231.1734	2
	Carson Sink	CAR	14	4-7"	Brown clay with sand moist and moderately stiff	CL/CH	4398894	372232										10/31/2007	34	39.7304	118.49095	0"-2"	61.0	3.2	59.2	4398896.619	372231.1734	0
	Carson Sink	CAR	15	7-16"	Brown clay occasional sand moist and stiff	CL/CH	4398894	372232										10/31/2007	35	39.7304	118.49095	6"	76.9	2.5	75.1	4398896.619	372231.1734	6
	Carson Sink	CAR	16	16-24"	Grey clay moist and soft	CL/CH	4398894	372232										10/31/2007	36	39.7304	118.49095	12"	86.5	2.3	84.5	4398896.619	372231.1734	12
																	10/31/2007	37	39.7304	118.49095	18"	89.5	12.7	79.4	4398896.619	372231.1734	18	
(W) West	Carson Sink		West	0-4"	Brown silty fine sand, moist, medium dense	SM	4404070	367302										10/31/2007	51	39.7744	118.54951	0"	79.3	8.2	73.3	4403866.55	367297.0764	0
	Carson Sink		West	4-20"	Brown/Grey clay occasional sand, moist and med stiff to stiff	CL/CH	4404070	367302										10/31/2007	52	39.7744	118.54951	6"	81.8	6.8	76.6	4403866.55	367297.0764	6
																		10/31/2007	53	39.7744	118.54951	12"	88.3	6.6	82.9	4403866.55	367297.0764	12

Test Samples	Location	Sample	Depth	Description	Unified	WGS84 N	WGS84 E	Elevation	Location	Depth	34mm GeoVane Data	Depth	34mm GeoVane Data	UTM Northing	UTM Easting	Test #	Latitude (degrees only)	Longitude (degrees only)	Depth tested	Wet Density (lbs/ft³)	Water content (% w=Mwater / Msoil)	Dry Density (lbs/ft³)	UTM Northing	UTM Easting	Depth Code				
(C) Center (Sample)	Carson Sink	CAR	17	3-12"	Brown clay occasional sand moist and stiff	CL/CH	4403750	372369	1177	CAR Nuc	0-4"	90,118,126	4-8"	140+	4403736	372393	14	39.77412	118.49017	Surface to 2'	101.4	9.2	92.9	4403749.204	372378.7621	0			
	Carson Sink	CAR	18	3-12"	Brown clay occasional sand moist and stiff	CL/CH	4403750	372369	1177								15	39.77412	118.49017	6"	95.0	9.6	86.7	4403749.204	372378.7621	6			
	Carson Sink	CAR	19	3-12"	Brown clay occasional sand moist and stiff	CL/CH	4403750	372369	1177								16	39.77412	118.49017	12"	96.1	9.4	87.8	4403749.204	372378.7621	12			
	Carson Sink	CAR	20	3-12"	Brown clay occasional sand moist and stiff	CL/CH	4403750	372369	1177																				
	Carson Sink	CAR	21	3-12"	Brown clay occasional sand moist and stiff	CL/CH	4403750	372369	1177																				
	Carson Sink	CAR	22	3-12"	Brown clay occasional sand moist and stiff	CL/CH	4403750	372369	1177																				
	Carson Sink	CAR	23	3-12"	Brown clay occasional sand moist and stiff	CL/CH	4403750	372369	1177																				
	Carson Sink	CAR	24	3-12"	Brown clay occasional sand moist and stiff	CL/CH	4403750	372369	1177																				
	Carson Sink	CAR	25	3-12"	Brown clay occasional sand moist and stiff	CL/CH	4403750	372369	1177																				
	Carson Sink	CAR	26	3-12"	Brown clay occasional sand moist and stiff	CL/CH	4403750	372369	1177																				
	Carson Sink	CAR	27	3-12"	Brown clay occasional sand moist and stiff	CL/CH	4403750	372369	1177																				
	Carson Sink	CAR	28	3-12"	Brown clay occasional sand moist and stiff	CL/CH	4403750	372369	1177																				
	Carson Sink	CAR	29	3-12"	Brown clay occasional sand moist and stiff	CL/CH	4403750	372369	1177																				
	Carson Sink	CAR	30	3-12"	Brown clay occasional sand moist and stiff	CL/CH	4403750	372369	1177																				
	Carson Sink	CAR	31	3-12"	Brown clay occasional sand moist and stiff	CL/CH	4403750	372369	1177																				
	Carson Sink	CAR	32	3-12"	Brown clay occasional sand moist and stiff	CL/CH	4403750	372369	1177																				
	Carson Sink	CAR	33	3-12"	Brown clay occasional sand moist and stiff	CL/CH	4403750	372369	1177																				
	Carson Sink	CAR	34	3-12"	Brown clay occasional sand moist and stiff	CL/CH	4403750	372369	1177																				
	Carson Sink	CAR	35	3-12"	Brown clay occasional sand moist and stiff	CL/CH	4403750	372369	1177																				
	Carson Sink	CAR	36	3-12"	Brown clay occasional sand moist and stiff	CL/CH	4403750	372369	1177																				
	Carson Sink	CAR	37	3-12"	Brown clay occasional sand moist and stiff	CL/CH	4403750	372369	1177																				
	Carson Sink	CAR	38	3-12"	Brown clay occasional sand moist and stiff	CL/CH	4403750	372369	1177																				
	Carson Sink	CAR	39	3-12"	Brown clay occasional sand moist and stiff	CL/CH	4403750	372369	1177																				
	Carson Sink	CAR	40	3-12"	Brown clay occasional sand moist and stiff	CL/CH	4403750	372369	1177																				

Test Samples	Location	Sample	Depth	Description	Unified	WGS84 N	WGS84 E	Elevation	Location	Depth	34mm GeoVane Data	Depth	34mm GeoVane Data	UTM Northing	UTM Easting	Test #	Latitude (degrees only)	Longitude (degrees only)	Depth tested	Wet Density (lb/ft ³)	Water content (%) w%=Mwater / Msoil	Dry Density (lb/ft ³)	UTM Northing	UTM Easting	Depth Code			
(E) East (Sample)	Carson Sink	CAR	41	4-13"	Brown clayey fine sand trace silt moist to dry and med dense	SM	4403658	377268	1182	CAR Nuc	0-4"	52.58,84,70,50	4-8"	140+	4403660	377001	1	39.774	118.43308	Surface to 2"	65.2	2.7	65.2	4403656.068	377268.0456	0		
	Carson Sink	CAR	42	4-13"	Brown clayey fine sand trace silt moist to dry and med dense	SM	4403658	377268	1182								2	39.774	118.43308	3-4"	75.3	2.8	73.2	4403656.068	377268.0456	3		
	Carson Sink	CAR	43	4-13"	Brown clayey fine sand trace silt moist to dry and med dense	SM	4403658	377268	1182								3	39.774	118.43308	6"	83.6	2.2	81.2	4403656.068	377268.0456	6		
	Carson Sink	CAR	44	4-13"	Brown clayey fine sand trace silt moist to dry and med dense	SM	4403658	377268	1182								4	39.774	118.43308	12"	96.7	1.9	94.9	4403656.068	377268.0456	12		
	Carson Sink	CAR	45	4-13"	Brown clayey fine sand trace silt moist to dry and med dense	SM	4403658	377268	1182								5	39.774	118.43308	18"	90.5	19.6	75.7	4403656.068	377268.0456	18		
	Carson Sink	CAR	46	4-13"	Brown clayey fine sand trace silt moist to dry and med dense	SM	4403658	377268	1182																			
	Carson Sink	CAR	47	4-13"	Brown clayey fine sand trace silt moist to dry and med dense	SM	4403658	377268	1182																			
	Carson Sink	CAR	48	4-13"	Brown clayey fine sand trace silt moist to dry and med dense	SM	4403658	377268	1182																			
	Carson Sink	CAR	49	4-13"	Brown clayey fine sand trace silt moist to dry and med dense	SM	4403658	377268	1182																			
	Carson Sink	CAR	50	4-13"	Brown clayey fine sand trace silt moist to dry and med dense	SM	4403658	377268	1182																			
	Carson Sink	CAR	51	4-13"	Brown clayey fine sand trace silt moist to dry and med dense	SM	4403658	377268	1182																			
	Carson Sink	CAR	52	4-13"	Brown clayey fine sand trace silt moist to dry and med dense	SM	4403658	377268	1182																			
	Carson Sink	CAR	53	4-13"	Brown clayey fine sand trace silt moist to dry and med dense	SM	4403658	377268	1182																			
	Carson Sink	CAR	54	4-13"	Brown clayey fine sand trace silt moist to dry and med dense	SM	4403658	377268	1182																			
	Carson Sink	CAR	55	4-13"	Brown clayey fine sand trace silt moist to dry and med dense	SM	4403658	377268	1182																			
	Carson Sink	CAR	56	4-13"	Brown clayey fine sand trace silt moist to dry and med dense	SM	4403658	377268	1182																			
	Carson Sink	CAR	57	4-13"	Brown clayey fine sand trace silt moist to dry and med dense	SM	4403658	377268	1182																			
	Carson Sink	CAR	58	4-13"	Brown clayey fine sand trace silt moist to dry and med dense	SM	4403658	377268	1182																			
	Carson Sink	CAR	59	4-13"	Brown clayey fine sand trace silt moist to dry and med dense	SM	4403658	377268	1182																			
	Carson Sink	CAR	60	4-13"	Brown clayey fine sand trace silt moist to dry and med dense	SM	4403658	377268	1182																			
	Carson Sink	CAR	61	4-13"	Brown clayey fine sand trace silt moist to dry and med dense	SM	4403658	377268	1182																			
	Carson Sink	CAR	62	4-13"	Brown clayey fine sand trace silt moist to dry and med dense	SM	4403658	377268	1182																			
	Carson Sink	CAR	63	4-13"	Brown clayey fine sand trace silt moist to dry and med dense	SM	4403658	377268	1182																			
	Carson Sink	CAR	64	4-13"	Brown clayey fine sand trace silt moist to dry and med dense	SM	4403658	377268	1182																			
	Carson Sink	CAR	12	10-12"	brown fine sand with silt occasional gravel cobble moist and dense to very dense	ISM	4402000	376414																				

Data from Locations without an associated soil sample

General Density Sampling																		
Date	Test #	Latitude (degrees only)	Longitude (degrees only)	Depth tested at	Wet Density (lbs/ft ³)	Water content (% w% = Mw / Msol)	Dry Density (lbs/ft ³)	UTM Northing	UTM Easting	Depth Code	Location	Depth	34mm GeoVane Data	GeoVane Depth	34mm GeoVane Data	GeoVane Depth	UTM Northing	UTM Easting
10/30/2007	6	39.77418	118.45273	Surface to 2"	72.2	2.8	70.3	4403703.167	375585.437	0	CAR Nuc	2	0-4"	74,68.60	4-8"	140+	4403683	375579
10/30/2007	7	39.77418	118.45273	6"	78.8	2.2	77.1	4403703.167	375585.437	6								
10/30/2007	8	39.77418	118.45273	12"	84.0	2.9	81.6	4403703.167	375585.437	12								
10/30/2007	9	39.77418	118.45273	18"	82.8	20.0	69.0	4403703.167	375585.437	18								
10/30/2007	10	39.77438	118.47083	Surface to 2"	79.0	3.0	76.7	4403750.674	374035.621	0	CAR Nuc	3	0-4"	68,60,62,90	4-8"	140+	4403708	374037
10/30/2007	11	39.77438	118.47083	6"	86.1	2.8	83.7	4403750.674	374035.621	6								
10/30/2007	12	39.77438	118.47083	12"	92.0	2.7	89.6	4403750.674	374035.621	12								
10/30/2007	13	39.77438	118.47083	18"	84.9	14.9	73.9	4403750.674	374035.621	18								
10/30/2007	18	39.77453	118.50743	Surface to 2"	88.0	4.3	84.4	4403819.456	370901.2839	0								
10/30/2007	19	39.77453	118.50743	6"	93.1	3.6	89.9	4403819.456	370901.2839	6	CAR Nuc	6	0-4"	70,74,84	4-8"	none	4403761	370903
10/30/2007	20	39.77453	118.50743	12"	95.6	3.8	92.1	4403819.456	370901.2839	12								
10/30/2007	21	39.77428	118.53227	Surface to 2"	75.2	6.1	70.9	4403827.82	368773.3792	0	CAR Nuc	7	0-4"	60,57,50,52	4-8"	none	4403796	368796
10/30/2007	22	39.77428	118.53227	6"	80.3	6.8	75.1	4403827.82	368773.3792	6								
10/30/2007	23	39.77428	118.53227	12"	84.2	6.3	79.2	4403827.82	368773.3792	12								
10/31/2007	24	39.74032	118.45267	0"	61.4	6.2	57.7	4399944.89	375529.6245	0	CAR Nuc	9	0-4"	none	4-8"	none	4399910	375501
10/31/2007	25	39.74032	118.45267	6"	95.8	4.1	92.0	4399944.89	375529.6245	6								
10/31/2007	26	39.74032	118.45267	12"	102.2	3.8	98.4	4399944.89	375529.6245	12								
10/31/2007	27	39.74049	118.4528	0"	98.4	1.5	97.0	4399963.939	375518.7911	0	CAR Nuc	8	0-4"	66,48,90	4-8"	140+	4399910	375501
10/31/2007	28	39.74049	118.4528	6"	101.3	1.2	100.1	4399963.939	375518.7911	6								
10/31/2007	29	39.74049	118.4528	12"	101.6	1.0	100.5	4399963.939	375518.7911	12								
10/31/2007	30	39.7529	118.50867	0"	32.0	7.7	29.7	4401420.471	370754.6403	0	CAR Nuc	10	0-4"	51,63,65	4-8"	140+,130	4401432	370727
10/31/2007	31	39.7529	118.50867	6"	89.7	3.2	86.9	4401420.471	370754.6403	6								
10/31/2007	32	39.7529	118.50867	12"	93.8	3.8	90.4	4401420.471	370754.6403	12								
10/31/2007	38	39.75303	118.4893	2"	76.7	2.7	74.7	4401407.13	372414.3467	2	CAR Nuc	12	0-4"	too hard	4-8"	140+	4401407	372414
10/31/2007	39	39.75303	118.4893	6"	86.6	2.5	84.4	4401407.13	372414.3467	6								
10/31/2007	40	39.75303	118.4893	12"	94.3	2.6	92.0	4401407.13	372414.3467	12								
10/31/2007	41	39.79667	118.48881	0"	84.1	5.7	79.6	4406250.157	372536.8674	0	CAR Nuc	13	0-4"	54,48,70,72	4-8"	140+	4406220	372534
10/31/2007	42	39.79667	118.48881	6"	88.8	5.2	84.3	4406250.157	372536.8674	6								
10/31/2007	43	39.79667	118.48881	12"	98.0	4.6	93.7	4406250.157	372536.8674	12								
10/31/2007	48	39.8057	118.53253	0"	83.9	5.6	79.5	4407315.616	368810.8228	0	CAR Nuc	15	0-4"	110,90,81	4-8"	140+	4407316	368808
10/31/2007	49	39.8057	118.53253	6"	88.0	5.3	83.5	4407315.616	368810.8228	6								
10/31/2007	50	39.8057	118.53253	12"	95.7	4.9	91.2	4407315.616	368810.8228	12								
10/31/2007	54	39.73863	118.52512	0"	75.3	3.8	72.5	4399860.472	369318.3712	0								
10/31/2007	55	39.73863	118.52512	6"	83.4	3.2	80.9	4399860.472	369318.3712	6								
10/31/2007	56	39.73863	118.52512	12"	87.6	3.0	85.0	4399860.472	369318.3712	12								
10/31/2007	57	39.80693	118.45155	0"	74.5	3.2	72.2	4407336.54	375745.4475	0								
10/31/2007	58	39.80693	118.45155	6"	78.2	3.5	75.6	4407336.54	375745.4475	6								
10/31/2007	59	39.80693	118.45155	12"	91.6	3.0	89.0	4407336.54	375745.4475	12								
10/31/2007	60	39.75329	118.46956	0"	79.0	2.6	77.0	4401408.058	374105.9793	0								
10/31/2007	61	39.75329	118.46956	6"	82.4	2.4	80.5	4401408.058	374105.9793	6								
10/31/2007	62	39.75329	118.46956	12"	90.6	2.5	88.4	4401408.058	374105.9793	12								

Site	0 to 6"		6 to 12"		0 to 12"		Depths approximate
	CBR %	Bearing (psi)	CBR %	Bearing (psi)	CBR %	Bearing (psi)	
CD 1-1	8	14.2	8	14.4	8	14.3	
CD 1-2	5	11.4	11	17.1	8	14.1	
CD 2-1	6	12	9	15.2	8	13.8	
CD 2-2	5	11.2	11	17.2	8	14	
CD 3-1	0	0	12	18.6	-	-	*Sunk under own weight to ~7"
CD 3-2	5	10.5	27	32.8	13	19.8	
CD 4-1	10	16.6	28	33.8	19	25.6	
CD 4-2	7	12.9	21	27.7	13	19.6	
CD 5-1	14	21	20	26.9	17	23.9	
CD 5-2	6	11.7	20	26.4	13	19.4	
CD 6-1	5	11.3	8	14.3	7	12.7	
CD 6-2	5	11.2	7	12.7	6	11.9	
CDL 3-1	18	25	36	41.1	27	32.9	
CDL 3-2	26	32.3	35	40.2	31	36.3	* Heavy weight used

Estimates of CBR and Bearing based on Kessler DCP spreadsheet

$$CBR = 0.292 / DCP^{1.12} \quad \text{where, DCP} = \text{penetration rate in mm/blow for 8Kg hammer} \quad \text{consistent with general soil relationship in ASTM D6951-03}$$

$$Bearing (psf) = -.7051 * CBR^2 + 167.99 * CBR + 754.53$$

approximate interrelationships of CBR and Bearing values from "Design of Concrete Airport Pavement, Portland Cement Association, page 8, 1955."

Test 1: 4.6 Kg (10.1 lb) hammer		
Drops	Accumulative Penetration (mm)	Accumulative Penetration (in)
0	0	0
3	62	2.440944882
3	96	3.779527559
3	123	4.842519685
3	150	5.905511811
3	182	7.165354331
3	209	8.228346457
3	255	10.03937008
3	297	11.69291339
3	331	13.03149606

Test 2: 4.6 Kg (10.1 lb) hammer		
Drops	Accumulative Penetration (mm)	Accumulative Penetration (in)
0	0	0
3	86	3.385826772
3	125	4.921259843
3	159	6.25984252
3	190	7.480314961
3	220	8.661417323
3	253	9.960629921
3	281	11.06299213
3	303	11.92913386
3	323	12.71653543
3	342	13.46456693

Test 1: 4.6 Kg (10.1 lb) hammer

No. Drops	Accumulative Penetration (mm)	Accumulative Penetration (in)
0	0	0
3	85	3.346456693
3	111	4.37007874
3	145	5.708661417
3	185	7.283464567
3	220	8.661417323
3	250	9.842519685
3	283	11.14173228
3	314	12.36220472
3	344	13.54330709

Test 2: 4.6 Kg (10.1 lb) hammer

No. Drops	Accumulative Penetration (mm)	Accumulative Penetration (in)
0	0	0
3	83	3.267716535
3	120	4.724409449
3	164	6.456692913
3	207	8.149606299
3	234	9.212598425
3	255	10.03937008
3	277	10.90551181
3	307	12.08661417
3	330	12.99212598

Test 1: 4.6 Kg (10.1 lb) hammer

No. Drops	Accumulative Penetration (mm)	Accumulative Penetration (in)
0	180	7.086614173
3	260	10.23622047
3	285	11.22047244
3	302	11.88976378
3	314	12.36220472
3	325	12.79527559
3	335	13.18897638
3	343	13.50393701
3	350	13.77952756
3	354	13.93700787

Hammer sunk under own weight to ~180mm

Test 2: 4.6 Kg (10.1 lb) hammer

No. Drops	Accumulative Penetration (mm)	Accumulative Penetration (in)
0	0	0
3	64	2.519685039
3	118	4.645669291
3	184	7.244094488
3	215	8.464566929
3	228	8.976377953
3	238	9.37007874
3	247	9.724409449
3	255	10.03937008
3	264	10.39370079
3	274	10.78740157
3	284	11.18110236
3	297	11.69291339
3	309	12.16535433
3	323	12.71653543
3	337	13.26771654
3	352	13.85826772

Test 1: 4.6 Kg (10.1 lb) hammer

No. Drops	Accumulative Penetration (mm)	Accumulative Penetration (in)
0	0	0
3	56	2.204724409
3	90	3.543307087
3	115	4.527559055
3	134	5.275590551
3	150	5.905511811
3	163	6.417322835
3	177	6.968503937
3	191	7.519685039
3	204	8.031496063
3	217	8.543307087
3	231	9.094488189
3	241	9.488188976
3	253	9.960629921
3	263	10.35433071
3	273	10.7480315
3	286	11.25984252
3	297	11.69291339
3	310	12.20472441
3	325	12.79527559
3	337	13.26771654
3	351	13.81889764
3	365	14.37007874

Test 2: 4.6 Kg (10.1 lb) hammer

No. Drops	Accumulative Penetration (mm)	Accumulative Penetration (in)
0	0	0
3	49	1.929133858
3	90	3.543307087
3	130	5.118110236
3	173	6.811023622
3	199	7.834645669
3	215	8.464566929
3	231	9.094488189
3	245	9.645669291
3	260	10.23622047
3	273	10.7480315
3	287	11.2992126
3	300	11.81102362
3	314	12.36220472
3	327	12.87401575
3	340	13.38582677
3	354	13.93700787

Test 1: 4.6 Kg (10.1 lb) hammer

No. Drops	Accumulative Penetration (mm)	Accumulative Penetration (in)
0	0	0
3	47	1.850393701
3	82	3.228346457
3	100	3.937007874
3	115	4.527559055
3	127	5
3	142	5.590551181
3	154	6.062992126
3	170	6.692913386
3	184	7.244094488
3	198	7.795275591
3	211	8.307086614
3	228	8.976377953
3	244	9.606299213
3	260	10.23622047
3	281	11.06299213
3	300	11.81102362
3	317	12.48031496
3	335	13.18897638
3	355	13.97637795

Test 2: 4.6 Kg (10.1 lb) hammer

No. Drops	Accumulative Penetration (mm)	Accumulative Penetration (in)
0	0	0
3	110	4.330708661
3	133	5.236220472
3	151	5.94488189
3	170	6.692913386
3	188	7.401574803
3	206	8.11023622
3	220	8.661417323
3	230	9.05511811
3	241	9.488188976
3	257	10.11811024
3	275	10.82677165
3	295	11.61417323
3	317	12.48031496
3	333	13.11023622
3	350	13.77952756

Test 1: 4.6 Kg (10.1 lb) hammer

No. Drops	Accumulative Penetration (mm)	Accumulative Penetration (in)
0	0	0
3	72	2.834645669
3	109	4.291338583
3	161	6.338582677
3	208	8.188976378
3	247	9.724409449
3	280	11.02362205
3	310	12.20472441
3	337	13.26771654

Test 2: 4.6 Kg (10.1 lb) hammer

No. Drops	Accumulative Penetration (mm)	Accumulative Penetration (in)
0	0	0
3	95	3.74015748
3	126	4.960629921
3	164	6.456692913
3	207	8.149606299
3	254	10
3	297	11.69291339
3	337	13.26771654
3	373	14.68503937

Test 1: 4.6 Kg (10.1 lb) hammer

No. Drops	Accumulative Penetration (mm)	Accumulative Penetration (in)
0	0	0
3	35	1.377952756
3	60	2.362204724
3	75	2.952755906
3	92	3.622047244
3	102	4.015748031
3	118	4.645669291
3	132	5.196850394
3	145	5.708661417
3	160	6.299212598
3	168	6.614173228
3	178	7.007874016
3	189	7.440944882
3	198	7.795275591
3	211	8.307086614
3	222	8.74015748
3	231	9.094488189
3	241	9.488188976
3	250	9.842519685
3	260	10.23622047
3	269	10.59055118
3	278	10.94488189
3	287	11.2992126
3	295	11.61417323
3	305	12.00787402
3	315	12.4015748
3	324	12.75590551
3	333	13.11023622
3	342	13.46456693
3	351	13.81889764
3	360	14.17322835

Test 2: 8 Kg (17.6 lb) hammer

No. Drops	Accumulative Penetration (mm)	Accumulative Penetration (in)
0	0	0
3	42	1.653543307
3	67	2.637795276
3	90	3.543307087
3	111	4.37007874
3	131	5.157480315
3	156	6.141732283
3	176	6.929133858
3	197	7.755905512
3	216	8.503937008
3	234	9.212598425
3	254	10
3	275	10.82677165
3	294	11.57480315
3	315	12.4015748
3	336	13.22834646
3	354	13.93700787

Note heavy weight used

Site	0 to 6"		6 to 12"		0 to 12"		Depths approximate
	CBR %	Bearing (psi)	CBR %	Bearing (psi)	CBR %	Bearing (psi)	
South_1	3	9	0.6	5.9	1	6.9	
South_2	2	7.6	0.6	5.9	1	6.9	
North_1	5	10.7	4	9.8	4	10.3	
North_2	5	10.8	5	10.9	5	10.8	
East_1	3	8.7	1	6.7	2	7.8	
East_2	2	7.7	-	-	2	7.6	
Center_1	2	7.3	0.3	5.6	0.7	6.1	
Center_2	0.8	6.2	0.4	5.7	0.6	5.9	

Estimates of CBR and Bearing based on Kessler DCP spreadsheet

$CBR = 0.292 / DCP^{1.12}$ where, DCP = penetration rate in mm/blow for 8Kg hammer consistent with general soil relationship in ASTM D6951-03

$$Bearing(psf) = -.7051 * CBR^2 + 167.99 * CBR + 754.53$$

approximate interrelationships of CBR and Bearing values from "Design of Concrete Airport Pavement, Portland Cement Association, page 8, 1955."

Test 1: 4.6 Kg (10.1 lb) hammer		
Drops	Accumulative Penetration (mm)	Accumulative Penetration (in)
0	0	0
3	73	2.874015748
2	137	5.393700787
1	227	8.937007874
1	401	15.78740157

Test 2: 4.6 Kg (10.1 lb) hammer		
Drops	Accumulative Penetration (mm)	Accumulative Penetration (in)
0	0	0
1	48	1.88976378
1	73	2.874015748
1	108	4.251968504
1	168	6.614173228
1	293	11.53543307
1	403	15.86614173
1	471	18.54330709
1	561	22.08661417
1	656	25.82677165

Test 1: 4.6 Kg (10.1 lb) hammer

No. Drops	Accumulative Penetration (mm)	Accumulative Penetration (in)
0	0	0
1	71	2.795275591
1	93	3.661417323
1	325	12.79527559
1	408	16.06299213
1	581	22.87401575

Test 2: 4.6 Kg (10.1 lb) hammer

No. Drops	Accumulative Penetration (mm)	Accumulative Penetration (in)
0	0	0
1	75	2.952755906
1	186	7.322834646
1	381	15
1	510	20.07874016
1	618	24.33070866

Test 1: 4.6 Kg (10.1 lb) hammer

No. Drops	Accumulative Penetration (mm)	Accumulative Penetration (in)
0	0	0
1	30	1.181102362
1	55	2.165354331
1	73	2.874015748
1	96	3.779527559
1	114	4.488188976
1	129	5.078740157
2	157	6.181102362
2	188	7.401574803
2	234	9.212598425
2	296	11.65354331
2	385	15.15748031
1	449	17.67716535
1	555	21.8503937
1	642	25.27559055

Test 2: 4.6 Kg (10.1 lb) hammer

No. Drops	Accumulative Penetration (mm)	Accumulative Penetration (in)
0	0	0
1	42	1.653543307
1	62	2.440944882
1	81	3.188976378
1	100	3.937007874
1	114	4.488188976
1	127	5
2	154	6.062992126
2	180	7.086614173
2	209	8.228346457
2	249	9.803149606
2	307	12.08661417
1	341	13.42519685
1	382	15.03937008
1	430	16.92913386
1	504	19.84251969
1	582	22.91338583

Test 1: 4.6 Kg (10.1 lb) hammer

No. Drops Accumulative Penetration (mm) Accumulative Penetration (in)

0	0	0
3	70	2.755905512
3	180	7.086614173
1	285	11.22047244
1	310	12.20472441
3	340	13.38582677
3	367	14.4488189
3	393	15.47244094
3	421	16.57480315
3	457	17.99212598
3	490	19.29133858
3	513	20.19685039

Test 2: 4.6 Kg (10.1 lb) hammer

No. Drops Accumulative Penetration (mm) Accumulative Penetration (in)

0	0	0
3	68	2.677165354
3	241	9.488188976
1	298	11.73228346
3	338	13.30708661
3	365	14.37007874
3	388	15.27559055
3	413	16.25984252
3	443	17.44094488
3	470	18.50393701
3	493	19.40944882
3	522	20.5511811

Appendix C: Laboratory data

Because of the volume of laboratory data generated, all of the raw lab data could not be combined into this report without due encumbrance. The only attached test data is the Atterberg limits worksheet. The test log, individual triaxial tests, tabular values for all test plots, and other laboratory data can be made available on disk or as a separate file.

**ATTERBERG LIMITS
ASTM D4318-05**

SAMPLE ID:	CAR-53	SAMPLED DATE:	
TEST NUMBER:	1	LETTING DATE:	
SAMPLE STATUS:		CONTROLLING CSJ:	
COUNTY:		SPEC YEAR:	
SAMPLED BY:	Casey T'kindt	SPEC ITEM:	
SAMPLE LOCATION:	Carson Sink, NV	SPECIAL PROVISION:	
MATERIAL CODE:		GRADE:	
MATERIAL NAME:			
PRODUCER:			
AREA ENGINEER:		PROJECT MANAGER:	Mike Thomas

COURSE/LIFT:		STATION:		DIST. FROM CL:	
--------------	--	----------	--	----------------	--

Liquid Limit

	Dish No.	Mass of Wet Sample + Tare (g)	Mass of Dry Sample + Tare (g)	Tare Mass (g)	Moisture Content (%)	Number of Blows	Single-Point Liquid Limit (%)
1	CAR-53-LL1	34.69	31.13	17.6	26.3	21	26
2	CAR-53-LL2	37.16	32.56	16.8	29.2	10	26
3	CAR-53-LL3	40.51	34.47	10.06	24.7	31	25
4							

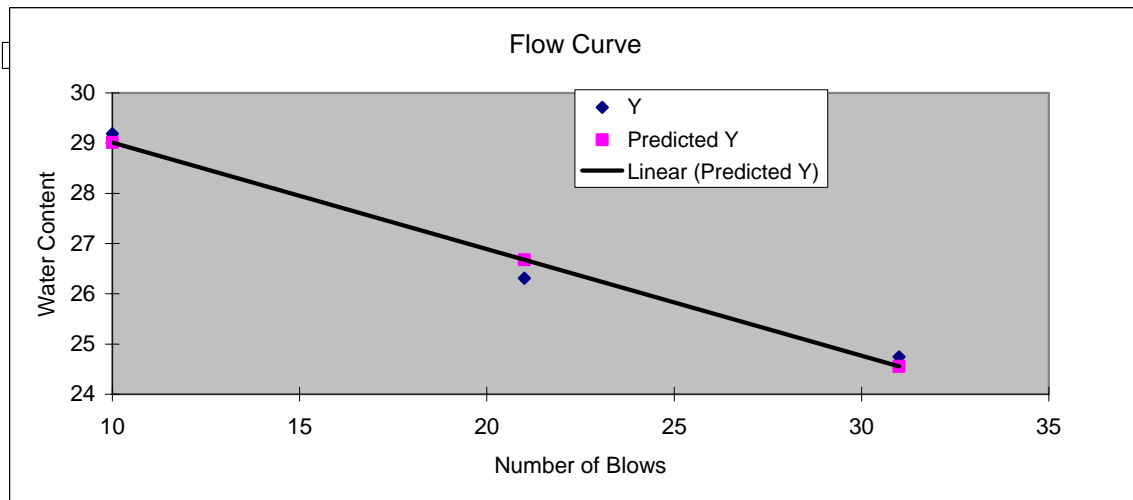
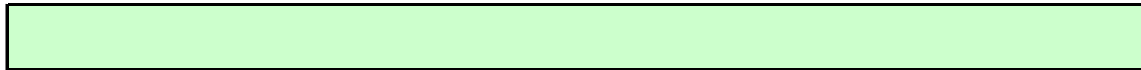
Multiple Point Liquid Limit	26
------------------------------------	-----------

Plastic Limit

	Dish No.	Mass of Wet Sample + Tare (g)	Mass of Dry Sample + Tare (g)	Tare Mass (g)	Mass of Water (g)	Plastic Limit (%)
1	CAR-53-PL1	15.12	14.38	10.08	0.74	17
2	CAR-53-PL2	13.4	12.96	10.06	0.44	15
3						
					Plastic Limit	16

Plasticity Index

Plasticity Index	10
-------------------------	-----------



SUMMARY OUTPUT

<i>Regression Statistics</i>	
Multiple R	0.990099
R Square	0.980295
Adjusted R Square	0.96059
Standard Error	0.447419
Observations	3

ANOVA

	<i>df</i>	<i>SS</i>	<i>MS</i>	<i>F</i>	<i>Significance F</i>
Residual	1	0.200184	0.200184		
Total	2	10.15908			

	<i>Coefficient</i>	<i>standard Error</i>	<i>t Stat</i>	<i>P-value</i>	<i>Lower 95%</i>	<i>Upper 95%</i>	<i>Lower 95.0%</i>	<i>Upper 95.0%</i>
Intercept	31.13833	0.673939	46.20346	0.013776	22.57511672	39.7015377	22.57511672	39.7015377
X Variable 1	-0.21244	0.030119	-7.053274	0.089661	-0.595143808	0.170262921	-0.595143808	0.170262921

RESIDUAL OUTPUT

<i>Observation</i>	<i>Predicted Y</i>	<i>Residuals</i>
1	26.67708	-0.365178
2	29.01392	0.173894
3	24.55267	0.191284

**ATTERBERG LIMITS
ASTM D4318-05**

SAMPLE ID:	CAR-32	SAMPLED DATE:	
TEST NUMBER:	1	LETTING DATE:	
SAMPLE STATUS:		CONTROLLING CSJ:	
COUNTY:		SPEC YEAR:	
SAMPLED BY:	Casey T'kindt	SPEC ITEM:	
SAMPLE LOCATION:	Carson Sink, NV	SPECIAL PROVISION:	
MATERIAL CODE:		GRADE:	
MATERIAL NAME:			
PRODUCER:			
AREA ENGINEER:		PROJECT MANAGER:	Mike Thomas

COURSE/LIFT:		STATION:		DIST. FROM CL:	
--------------	--	----------	--	----------------	--

Liquid Limit

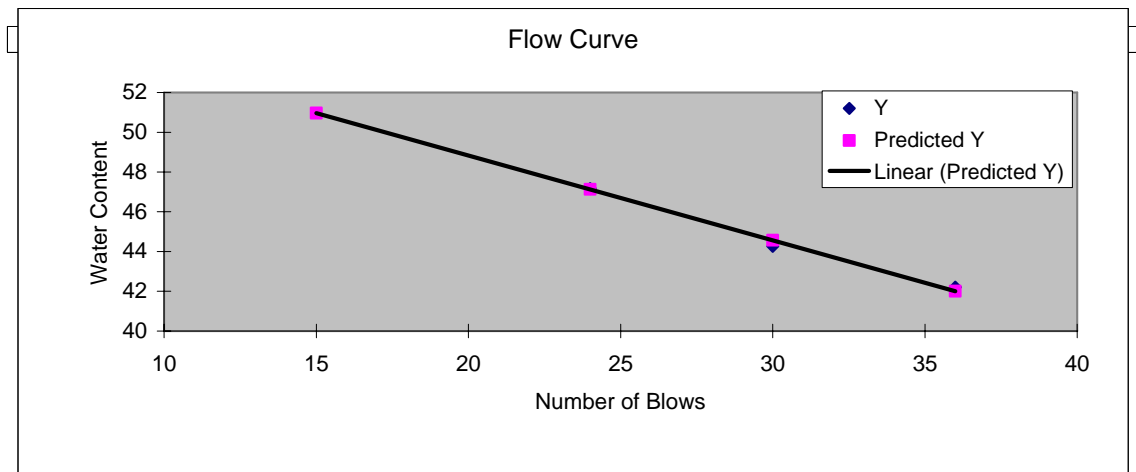
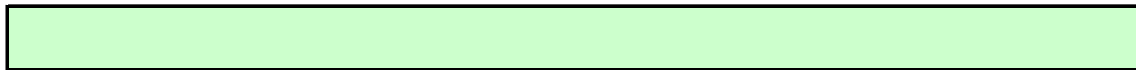
	Dish No.	Mass of Wet Sample + Tare (g)	Mass of Dry Sample + Tare (g)	Tare Mass (g)	Moisture Content (%)	Number of Blows	Single-Point Liquid Limit (%)
1	CAR-32-LL1	28.78	23.18	9.91	42.2	36	44
2	CAR-32-LL2	31.43	24.87	10.05	44.3	30	45
3	CAR-32-LL3	24.26	19.67	9.94	47.2	24	47
4	CAR-32-LL4	25.68	20.41	10.08	51.0	15	48
5							
Multiple Point Liquid Limit							47

Plastic Limit

	Dish No.	Mass of Wet Sample + Tare (g)	Mass of Dry Sample + Tare (g)	Tare Mass (g)	Mass of Water (g)	Plastic Limit (%)
1	CAR-32-PL1	21.48	19.78	9.89	1.7	17
2	CAR-32-PL2	21.23	19.35	9.83	1.88	20
3	CAR-32-PL3	21.82	20.09	9.85	1.73	17
Plastic Limit						18

Plasticity Index

Plasticity Index:	29
--------------------------	-----------



SUMMARY OUTPUT

<i>Regression Statistics</i>	
Multiple R	0.998478047
R Square	0.99695841
Adjusted R Square	0.995437615
Standard Error	0.258336908
Observations	4

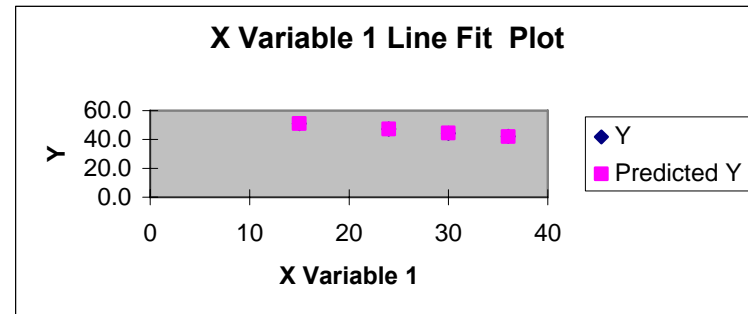
ANOVA

	<i>df</i>	<i>SS</i>	<i>MS</i>	<i>F</i>	<i>Significance F</i>
Regression	1	43.75012	43.75012	655.5508	0.001521953
Residual	2	0.133476	0.066738		
Total	3	43.88359			

	<i>Coefficients</i>	<i>Standard Error</i>	<i>t Stat</i>	<i>P-value</i>	<i>Lower 95%</i>	<i>Upper 95%</i>	<i>Lower 95.0%</i>	<i>Upper 95.0%</i>
Intercept	57.35392318	0.45574	125.848	6.31E-05	55.39303432	59.31481205	55.39303432	59.31481205
X Variable 1	-0.426291301	0.01665	-25.60373	0.001522	-0.497928666	-0.354653936	-0.497928666	-0.354653936

RESIDUAL OUTPUT

<i>Observation</i>	<i>Predicted Y</i>	<i>Residuals</i>
1	42.00743634	0.193016
2	44.56518415	-0.300677
3	47.12293196	0.050758
4	50.95955367	0.056903



**ATTERBERG LIMITS
ASTM D4318-05**

SAMPLE ID:	CDS-24	SAMPLED DATE:	
TEST NUMBER:	1	LETTING DATE:	
SAMPLE STATUS:		CONTROLLING CSJ:	
COUNTY:		SPEC YEAR:	
SAMPLED BY:	Casey T'kindt	SPEC ITEM:	
SAMPLE LOCATION:	Cuddeback, CA	SPECIAL PROVISION:	
MATERIAL CODE:		GRADE:	
MATERIAL NAME:			
PRODUCER:			
AREA ENGINEER:		PROJECT MANAGER:	Mike Thomas

COURSE/LIFT:		STATION:		DIST. FROM CL:	
--------------	--	----------	--	----------------	--

Liquid Limit

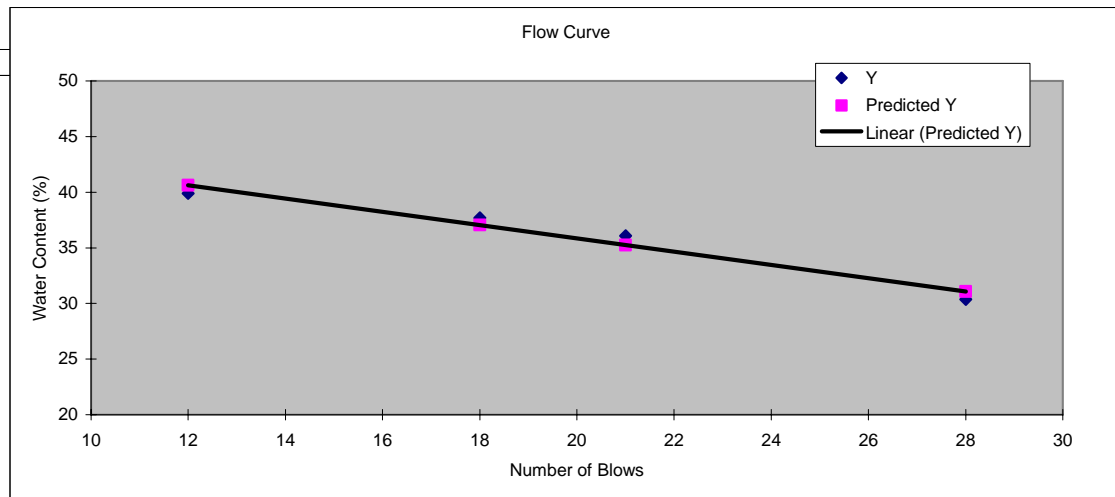
	Dish No.	Mass of Wet Sample + Tare (g)	Mass of Dry Sample + Tare (g)	Tare Mass (g)	Moisture Content (%)	Number of Blows	Single-Point Liquid Limit (%)
1	CDS-24-LL1	23.57	19.85	9.98	37.7	18	36
2	CDS-24-LL2	22.05	18.84	9.94	36.1	21	35
3	CDS-24-LL3	19.89	17.07	10	39.9	12	36
4	CDS-24-LL4	21.23	18.6	9.94	30.4	28	31
5							
Multiple Point Liquid Limit							33

Plastic Limit

	Dish No.	Mass of Wet Sample + Tare (g)	Mass of Dry Sample + Tare (g)	Tare Mass (g)	Mass of Water (g)	Plastic Limit (%)
1	CDS-24-PL1	13.75	12.99	9.91	0.76	25
2	CDS-24-PL2	19.22	17.41	9.86	1.81	24
3	CDS-24-PL3	21.94	19.67	9.86	2.27	23
Plastic Limit						24

Plasticity Index

Plasticity Index:	9
--------------------------	----------



SUMMARY OUTPUT

<i>Regression Statistics</i>	
Multiple R	0.978397
R Square	0.957262
Adjusted R Square	0.935892
Standard Error	1.030252
Observations	4

ANOVA

	<i>df</i>	<i>SS</i>	<i>MS</i>	<i>F</i>	<i>Significance F</i>
Regression	1	47.54759	47.54759	44.79624	0.021602573
Residual	2	2.122838	1.061419		
Total	3	49.67043			

	<i>Coefficient</i>	<i>Standard Error</i>	<i>t Stat</i>	<i>P-value</i>	<i>Lower 95%</i>	<i>Upper 95%</i>	<i>Lower 95.0%</i>	<i>Upper 95.0%</i>
Intercept	47.82334	1.839605	25.99652	0.001476	39.908161	55.73852731	39.908161	55.73852731
X Variable 1	-0.598476	0.089418	-6.692999	0.021603	-0.983212034	-0.213740636	-0.983212034	-0.213740636

RESIDUAL OUTPUT

<i>Observation</i>	<i>Predicted Y</i>	<i>Residuals</i>
1	37.05077	0.639199
2	35.25534	0.812075
3	40.64163	-0.754782
4	31.06601	-0.696492

**ATTERBERG LIMITS
ASTM D4318-05**

SAMPLE ID:	CDL-9	SAMPLED DATE:	
TEST NUMBER:		LETTING DATE:	
SAMPLE STATUS:		CONTROLLING CSJ:	
COUNTY:		SPEC YEAR:	
SAMPLED BY:	Casey T'kindt	SPEC ITEM:	
SAMPLE LOCATION:	Cuddeback, CA	SPECIAL PROVISION:	
MATERIAL CODE:		GRADE:	
MATERIAL NAME:			
PRODUCER:			
AREA ENGINEER:		PROJECT MANAGER:	Mike Thomas

COURSE/LIFT:		STATION:		DIST. FROM CL:	
--------------	--	----------	--	----------------	--

Liquid Limit

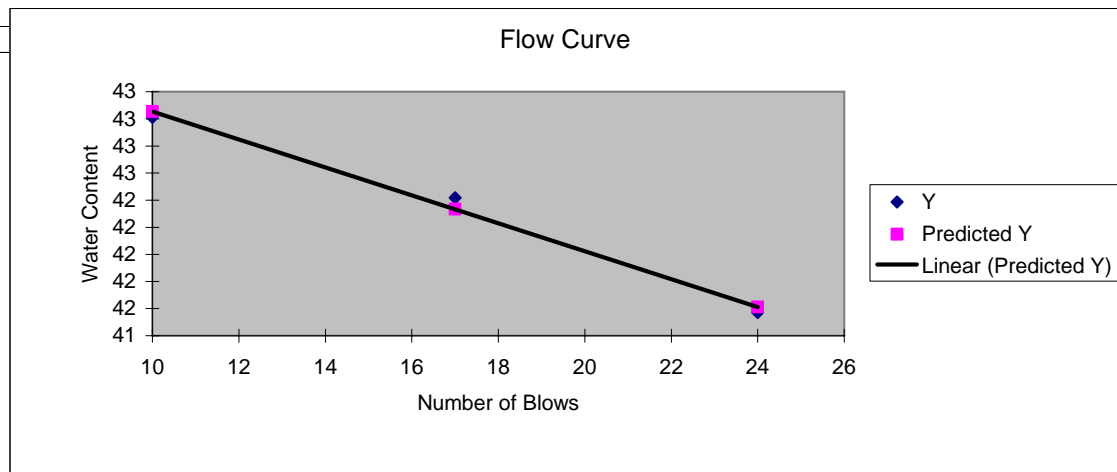
	Dish No.	Mass of Wet Sample + Tare (g)	Mass of Dry Sample + Tare (g)	Tare Mass (g)	Moisture Content (%)	Number of Blows	Single-Point Liquid Limit (%)
1	CDL-9-LL1	20.34	17.17	9.80	43.0	10	38
2	CDL-9-LL2	21.82	18.24	9.80	42.4	17	40
3	CDL-9-LL3	22.05	18.45	9.79	41.6	24	41
4							
5							
Multiple Point Liquid Limit							42

Plastic Limit

	Dish No.	Mass of Wet Sample + Tare (g)	Mass of Dry Sample + Tare (g)	Tare Mass (g)	Mass of Water (g)	Plastic Limit (%)
1	CDL-9-PL1	27.77	25.61	17.62	2.16	27
2	CDL-9-PL2	25.4	23.53	16.79	1.87	28
3	CDL-9-PL3	28.24	25.76	16.75	2.48	28
Plastic Limit						27

Plasticity Index

Plasticity Index:	15
--------------------------	-----------



SUMMARY OUTPUT

<i>Regression Statistics</i>	
Multiple R	0.994968
R Square	0.989961
Adjusted R Square	0.979922
Standard Error	0.102663
Observations	3

ANOVA

	<i>df</i>	<i>SS</i>	<i>MS</i>	<i>F</i>	<i>Significance F</i>
Regression	1	1.039355	1.039355	98.61275	0.063892809
Residual	1	0.01054	0.01054		
Total	2	1.049894			

	<i>Coefficient</i>	<i>Standard Error</i>	<i>t Stat</i>	<i>P-value</i>	<i>Lower 95%</i>	<i>Upper 95%</i>	<i>Lower 95.0%</i>	<i>Upper 95.0%</i>
Intercept	44.08396	0.185997	237.0147	0.002686	41.72064905	46.44727407	41.72064905	46.44727407
X Variable 1	-0.102984	0.010371	-9.930395	0.063893	-0.234754256	0.028786703	-0.234754256	0.028786703

RESIDUAL OUTPUT

<i>Observation</i>	<i>Predicted Y</i>	<i>Residuals</i>
1	43.05412	-0.041912
2	42.33324	0.083824
3	41.61235	-0.041912

Appendix D: Media library on DVD

A DVD containing photographic and video media of both Carson Sink and Cuddeback field visits is available from ARA.

REPORT DOCUMENTATION PAGE

*Form Approved
OMB No. 0704-0188*

The public reporting burden for this collection of information is estimated to average 1 hour per response, including the time for reviewing instructions, searching existing data sources, gathering and maintaining the data needed, and completing and reviewing the collection of information. Send comments regarding this burden estimate or any other aspect of this collection of information, including suggestions for reducing this burden, to Department of Defense, Washington Headquarters Services, Directorate for Information Operations and Reports (0704-0188), 1215 Jefferson Davis Highway, Suite 1204, Arlington, VA 22202-4302. Respondents should be aware that notwithstanding any other provision of law, no person shall be subject to any penalty for failing to comply with a collection of information if it does not display a currently valid OMB control number.
PLEASE DO NOT RETURN YOUR FORM TO THE ABOVE ADDRESS.

1. REPORT DATE (DD-MM-YYYY) 01-08 - 2008			2. REPORT TYPE Contractor Report		3. DATES COVERED (From - To)	
4. TITLE AND SUBTITLE Constitutive Soil Properties for Cuddeback Lake, California and Carson Sink, Nevada					5a. CONTRACT NUMBER NNL07AA00B	
					5b. GRANT NUMBER	
					5c. PROGRAM ELEMENT NUMBER	
6. AUTHOR(S) Thomas, Michael A.; Chitty, Daniel E.; Gildea, Martin L.; and T'Kindt, Casey M.					5d. PROJECT NUMBER	
					5e. TASK NUMBER	
					5f. WORK UNIT NUMBER 644423.04.31.04.40.42	
7. PERFORMING ORGANIZATION NAME(S) AND ADDRESS(ES) NASA Langley Research Center Hampton, VA 23681-2199					8. PERFORMING ORGANIZATION REPORT NUMBER	
9. SPONSORING/MONITORING AGENCY NAME(S) AND ADDRESS(ES) National Aeronautics and Space Administration Washington, DC 20546-0001					10. SPONSOR/MONITOR'S ACRONYM(S) NASA	
					11. SPONSOR/MONITOR'S REPORT NUMBER(S) NASA/CR-2008-215345	
12. DISTRIBUTION/AVAILABILITY STATEMENT Unclassified - Unlimited Subject Category 39 Availability: NASA CASI (301) 621-0390						
13. SUPPLEMENTARY NOTES Langley Technical Monitor: Ralph D. Buehrle						
14. ABSTRACT Accurate soil models are required for numerical simulations of land landings for the Orion Crew Exploration Vehicle. This report provides constitutive material modeling properties for four soil models from two dry lakebeds in the western United States. The four soil models are based on mechanical and compressive behavior observed during geotechnical laboratory testing of remolded soil samples from the lakebeds. The test specimens were reconstituted to measured in situ density and moisture content. Tests included: triaxial compression, hydrostatic compression, and uniaxial strain. A fit to the triaxial test results defines the strength envelope. Hydrostatic and uniaxial tests define the compressibility. The constitutive properties are presented in the format of LS-DYNA Material Model 5: Soil and Foam. However, the laboratory test data provided can be used to construct other material models. The four soil models are intended to be specific only to the two lakebeds discussed in the report. The Cuddeback A and B models represent the softest and hardest soils at Cuddeback Lake. The Carson Sink Wet and Dry models represent different seasonal conditions. It is possible to approximate other clay soils with these models, but the results would be unverified without geotechnical tests to confirm similar soil behavior.						
15. SUBJECT TERMS LS-DYNA; Compressive behavior; Constitutive properties; Geotechnical; Laboratory tests; Landing simulations; Material model; Mechanical behavior; Soil; Soil model						
16. SECURITY CLASSIFICATION OF:			17. LIMITATION OF ABSTRACT	18. NUMBER OF PAGES	19a. NAME OF RESPONSIBLE PERSON	
a. REPORT	b. ABSTRACT	c. THIS PAGE			19b. TELEPHONE NUMBER (Include area code)	
U	U	U	UU	148	STI Help Desk (email: help@sti.nasa.gov) (301) 621-0390	